UNIVERSITAT ROVIRA i VIRGILI

Climate Change analysis and its impacts on the agriculture sector in Madagascar

Luc Yannick Andréas Randriamarolaza

UNIVERSITAT ROVIRA i VIRGILI

Climate Change analysis and its impacts on the agriculture sector in Madagascar

Luc Yannick Andréas RANDRIAMAROLAZA

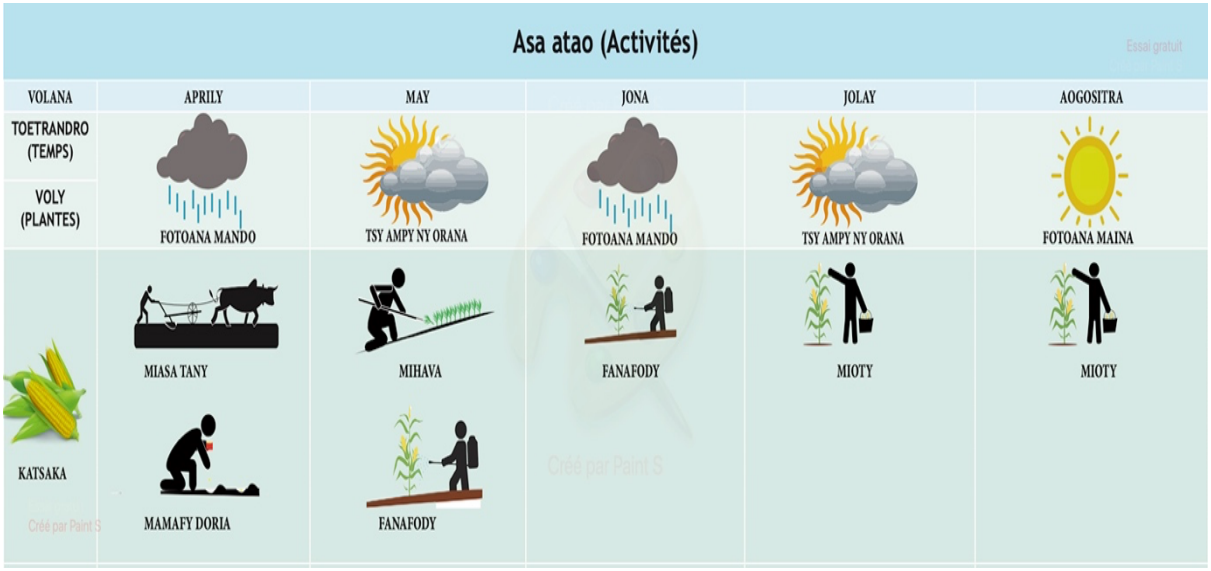

DOCTORAL THESIS
2024

Ph.D. Dissertation

Climate Change analysis and its impacts on the agriculture sector in Madagascar

Luc Yannick Andréas Randriamarolaza

December 2023

Ph.D. Program in City, Territory, and Sustainable Planning

Departament de Geografia

Universitat Rovira i Virgili

Director

Dr. Enric Aguilar Anfrons

Departament de Geografia

Centre for Climate Change

Institut Universitari de Recerca en Sostenibilitat, Canvi Climàtic i Transició Energètica

Universitat Rovira i Virgili

UNIVERSITAT ROVIRA i VIRGILI

FAIG CONSTAR que aquest treball, titulat "Climate Change analysis and its impacts on the agriculture sector in Madagascar", que presenta Luc Yannick Andréas Randriamarolaza per a l'obtenció del títol de Doctor, ha estat realitzat sota la meva direcció al Departament Geografia d'aquesta universitat.

HAGO CONSTAR que el presente trabajo, titulado "Climate Change analysis and its impacts on the agriculture sector in Madagascar", que presenta Luc Yannick Andréas Randriamarolaza para la obtención del título de Doctor, ha sido realizado bajo mi dirección en el Departamento Geografia de esta universidad.

I STATE that the present study, entitled "Climate Change analysis and its impacts on the agriculture sector in Madagascar", presented by Luc Yannick Andréas Randriamarolaza for the award of the degree of Doctor, has been carried out under my supervision at the Department of Geography of this university.

Tarragona, 22/02/2024

El/s director/s de la tesi doctoral
El/los director/es de la tesis doctoral
Doctoral Thesis Supervisor/s

Enric Aguilar

Firmado digitalmente por Enric Aguilar
Fecha: 2024.02.22 07:38:09 +01'00'

PREFACE

Climate change is one of the biggest challenges that everyone should be aware of. Scientists or researchers must produce scientifically-based information on climate change and its impacts that end-users use to find adaptation strategies. Mostly, knowledge transfer plays an important role in achieving this objective. Following this optic, this thesis capitalizes on scientific knowledge developed by project INDECIS (http://www.indecis.eu/) to tailor climate change information and its effects on the agriculture sector in Madagascar.

This dissertation is built by a compendium of three articles written during the Ph.D. course in the Program of City, Territory, and Sustainable Planning at the University Research Institute on Sustainability, Climate Change and Energy Transition (IU-RESCAT), Centre for Climate Change (C3) and the Department of Geography of the Universitat Rovira i Virgili. Therefore, this dissertation is planned as follows:

PART I presents the background of the thesis. Firstly, it presents the research introduction, the working hypotheses, and the objectives. Secondly, it describes the thesis structure. Finally, it explains the general theoretical framework of the dissertation.

PART II concerns the scientific publications. Three papers form the main core of the thesis, which are:

- **Randriamarolaza, L.Y.A.**, Aguilar, E., Skrynyk, O., Vicente- Serrano, S.M. & Domínguez-Castro, F. (2021) Indices for daily temperature and precipitation in Madagascar, based on quality- controlled and homogenized data, 1950–2018. International Journal of Climatology, 42 (1), 265–288. Available from: https://doi.org/10.1002/joc.7243 [JCR Q1, IF 3.651]
- **Randriamarolaza, L.Y.A.**, Aguilar, E. & Skrynyk, O. (2023) Extreme temperatures detection and attribution related to external forcing in Madagascar. International Journal of Climatology, 43 (8), 3907-3924. Available from: https://doi.org/10.1002/joc.8065 [JCR Q1, IF 3.651]
- **Randriamarolaza, L.Y.A.** & Aguilar, E. (2023) Rainy season and crop calendars comparison between past (1950-2018) and future (2030-2100) in Madagascar. Meteorological Applications, 30 (5), e2146. Available from https://doi.org/10.1002/met.2146 [JCR Q3, IF 2.451]

PART III consists of a discussion, a conclusion, a software tool, and future perspectives.

The INDECIS project supported this thesis. The project focused on an integrated approach for the development across Europe of user-oriented climate indicators for GFCS high-priority sectors: agriculture, disaster risk reduction, energy, health, water, and tourism. It was part of ERA4CS, an ERA-NET initiated by JPI Climate, and funded by FORMAS (SE), DLR (DE), BMWFW (AT), IFD (DK), MINECO (ES), ANR (FR) with co-funding by the European Union Grant 690462). Moreover, the collaboration between the World Meteorological Organization (WMO) and Universitat Rovira i Virgili (URV) brings additional funding.

I had also the opportunity to exchange experiences and knowledge with other experts on climate during my doctoral thesis development. Therefore, I was a co-author of one paper that contributed to INDECIS project activities. I would like to indicate that this paper does not form the doctoral thesis but supports it.

- Skrynyk, O., Aguilar, E., Guijarro, J., **Randriamarolaza, L.Y.A.,** and Bubin, S. (2021) Uncertainty evaluation of Climatol's adjustment algorithm applied to daily air temperature time series. International Journal of Climatology, 41(Suppl. 1), E2395– E2419.

Moreover, I presented a poster on “Climate Change Impacts on growing rice and maize seasons in the highland of Madagascar” during the International Conference on Regional Climate ICRC-CORDEX 2023 in Trieste (Italy), 25 – 29 September 2023. This conference gave me an overview of regional climate downscaling methods that can be implemented in my future research.

ACKNOWLEDGEMENT

Firstly, I would like to thank my supervisor Dr. Enric Aguilar, Director of the University Research Institute on Sustainability, Climate Change and Energy Transition, for accepting and allowing me to realize my PhD at URV with the support financially of the INDECIS project. Even if I had to go back home because of COVID-19, he was devoted to helping, encouraging, and involving me in finishing my thesis. Furthermore, he trusted me to contribute to some projects. In brief, he forges me to become a good scientist through his suggestions and comments which improve and enrich my scientific knowledge and behaviors.

Secondly, my thanks go to Dr. Manuela Brunet, director of the Center for Climate Change (C3), for her encouragement, especially about the accomplishment of collaborative projects with the World Meteorological Organization, World Bank, and Food Agriculture Organization.

Thirdly, I am very thankful to everyone who has contributed directly or indirectly to this thesis, especially Mrs. Marisol Puga for solving visa and administrative issues, all colleagues at C3, and staff at the secretariat of the Geography Department for their hospitality and friendly environment.

Finally, I am very grateful to my wife, Razafiarinivo Mamy Noely, and my children, Randriamarolaza Mamy Fenohasina, and Randriamarolaza Finoana Sarobidy, and my family for their sacrifice and support.

ABSTRACT

Climate change imposes a challenge for all countries. Agriculture is a highly impacted and climate-sensitive sector. Madagascar is among the most climate-vulnerable countries. Therefore, tailoring and monitoring climate change and agriculture information helps the decision-makers explore strategies to address the issues. This thesis contributes to improving the climate change and agriculture information in Madagascar based on proven and recent scientific approaches. Two important steps, quality control and homogenization of climate data are undertaken before creating the climate change and agriculture information. Assessing the quality and homogenizing the climate and weather observational datasets are crucial steps to ascertain the reliability and reduce the uncertainty of the information. Calculating the climate change indices and their trends allows us to appreciate and evaluate changes. Detecting and attributing the causes of climate change helps to cope and mitigate climate change. Finally, highlighting climate change's effects on agriculture involves decision-makers and stakeholders to establish adaptation strategies. In this thesis, Madagascar is taken as a case study. The quality control is based on 19 functions. Detected errors are flagged following 4 categories. Using the observational datasets on minimum and maximum temperatures, and precipitation from 28 synoptic weather stations of Madagascar over 1950-2018, most errors were detected in the maximum temperature. The correction has been done using online support materials. Therefore, most checked values were replaced by missing values. The homogenization approach is automatic, but the results were compared with a semi-automatic approach. On the one hand, this approach confirms the efficiency of automatic homogenization, and it has the advantage of completing the missing values. The quality-controlled and homogenized observational datasets are employed to derive climate indices and to analyze rainy season and crop calendars. Temperatures increase in Madagascar. Changes in nighttime temperature are higher than daytime temperature. Warm and cold events significantly increase and decrease respectively. In addition, these extreme temperature events are mainly due to anthropogenic forcing according to fingerprinting method. Changes in precipitation are mostly non-significant. In general, the total precipitation amount has decreased, and an intensified drying period has been detected in the last fifteen years. Changes effects pass mainly on the agriculture sector. Mostly, the rainy season onset and cessation are late and early respectively. Consequently, the length of the rainy season is shortened. Moreover, the crops' calendars are disrupted. The results recommend farmers grow short-length crop cycles of rice and maize crops in the future.

RESUM

El canvi climàtic imposa un repte per a tots els països. L'agricultura és un sector molt afectat i sensible al clima. Madagascar es troba entre els països més vulnerables al clima. Per tant, adaptar i supervisar la informació sobre el canvi climàtic i l'agricultura ajuda els qui prenen decisions a explorar les estratègies per abordar els problemes. Aquesta tesi contribueix a millorar la informació sobre el canvi climàtic i l'agricultura a Madagascar a partir d'enfocaments científics provats i recents. Es duen a terme dos passos importants, el control de qualitat i l'homogeneïtzació de les dades climàtiques abans de crear la informació sobre el canvi climàtic i l'agricultura. L'avaluació de la qualitat i l'homogeneïtzació dels conjunts de dades d'observació del clima i el temps són passos crucials per determinar la fiabilitat i reduir la incertesa de la informació. El càlcul dels índexs de canvi climàtic i les seves tendències ens permet apreciar i avaluar els canvis. Detectar i atribuir les causes del canvi climàtic ajuda a fer front i mitigar el canvi climàtic. Finalment, posar en relleu els efectes del canvi climàtic en l'agricultura implica els responsables de la presa de decisions i les parts interessades per establir estratègies d'adaptació. En aquesta tesi, Madagascar es pren com a cas d'estudi. El control de qualitat es basa en 19 funcions. Els errors detectats es marquen seguint 4 categories. Utilitzant els conjunts de dades d'observació sobre temperatures mínimes i màximes, i precipitacions de 28 estacions meteorològiques sinòptiques de Madagascar durant el període 1950-2018, la majoria dels errors es van detectar a la temperatura màxima. La correcció s'ha fet utilitzant materials de suport en línia. Per tant, la majoria dels valors marcats es van substituir per valors que faltaven. L'enfocament d'homogeneïtzació és automàtic, però els resultats es van comparar amb un enfocament semiautomàtic. D'una banda, aquest enfocament confirma l'eficiència de l'homogeneïtzació automàtica, i té l'avantatge de completar els valors que falten. Els conjunts de dades observacionals homogeneïtzades i controlades de qualitat s'utilitzen per derivar índexs climàtics i analitzar calendaris de l'època de pluges i els cultius. Les temperatures augmenten a Madagascar. Els canvis en la temperatura nocturna són superiors a la temperatura diürna. Els esdeveniments càlids i freds augmenten i disminueixen significativament respectivament. A més, aquests esdeveniments de temperatura extrema es deuen principalment al forçament antròpic segons el mètode d'empremta digital. Els canvis en les precipitacions són majoritàriament no significatius. En general, la quantitat total de precipitació ha disminuït i s'ha detectat un període d'assecat intensificat en els darrers quinze anys. Els efectes dels canvis passen principalment al sector agrícola. Majoritàriament, l'inici i la cessació de la temporada de pluges són tardans i primerencs, respectivament. En conseqüència, la durada de la temporada de pluges s'escurça. A més, els calendaris dels conreus es veuen alterats. Els

resultats recomanen als agricultors que creixin cicles de cultiu de curta durada d'arròs i blat de moro en el futur.

RESUMEN

El cambio climático impone un desafío para todos los países. La agricultura es un sector muy afectado y sensible al clima. Madagascar se encuentra entre los países más vulnerables al clima. Por lo tanto, adaptar y monitorear la información sobre el cambio climático y la agricultura ayuda a los tomadores de decisiones a explorar las estrategias para abordar los problemas. Esta tesis contribuye a mejorar la información sobre el cambio climático y la agricultura en Madagascar basándose en enfoques científicos recientes y probados. Se llevan a cabo dos pasos importantes, el control de calidad y la homogeneización de los datos climáticos antes de crear la información sobre cambio climático y agricultura. Evaluar la calidad y homogeneizar los conjuntos de datos de observación del clima y del tiempo son pasos cruciales para determinar la confiabilidad y reducir la incertidumbre de la información. Calcular los índices de cambio climático y sus tendencias nos permite apreciar y evaluar los cambios. Detectar y atribuir las causas del cambio climático ayuda a afrontar y mitigar el cambio climático. Finalmente, resaltar los efectos del cambio climático en la agricultura implica que los tomadores de decisiones y las partes interesadas establezcan estrategias de adaptación. En esta tesis, Madagascar se toma como estudio de caso. El control de calidad se basa en 19 funciones. Los errores detectados se marcan siguiendo 4 categorías. Utilizando los conjuntos de datos de observación sobre temperaturas mínimas y máximas y precipitaciones de 28 estaciones meteorológicas sinópticas de Madagascar durante el período 1950-2018, la mayoría de los errores se detectaron en la temperatura máxima. La corrección se ha realizado utilizando materiales de soporte en línea. Por lo tanto, la mayoría de los valores verificados fueron reemplazados por valores faltantes. El enfoque de homogeneización es automático, pero los resultados se compararon con un enfoque semiautomático. Por un lado, este enfoque confirma la eficiencia de la homogeneización automática y tiene la ventaja de completar los valores faltantes. Los conjuntos de datos de observación homogeneizados y con control de calidad se emplean para derivar índices climáticos y analizar la temporada de lluvias y los calendarios de cultivos. Las temperaturas aumentan en Madagascar. Los cambios en la temperatura nocturna son mayores que los de la temperatura diurna. Los eventos cálidos y fríos aumentan y disminuyen significativamente respectivamente. Además, estos fenómenos de temperaturas extremas se deben principalmente al forzamiento antropogénico según el método de toma de huellas dactilares. Los cambios en las precipitaciones en su mayoría no son significativos. En

general, la cantidad total de precipitación ha disminuido y en los últimos quince años se ha detectado una intensificación del período de sequía. Los efectos de los cambios se transmiten principalmente al sector agrícola. En su mayoría, el inicio y el final de la temporada de lluvias son tardíos y tempranos, respectivamente. En consecuencia, se acorta la duración de la temporada de lluvias. Además, los calendarios de los cultivos se ven alterados. Los resultados recomiendan que los agricultores cultiven ciclos cortos de arroz y maíz en el futuro.

CONTENTS

LIST OF TABLES BY CHAPTERS

LIST OF FIGURES BY CHAPTERS

Chapter 5 Rainy season and crop calendars comparison between past (1950-2018) and future (2030-2100) in Madagascar

LIST OF ACRONYMS

ALL	Anthropogenic-plus-natural forcing
ANT	Anthropogenic forcing
CMIP	Coupled Model Inter-comparison Project
COST	European Cooperation in Science & Technology
CREWS	Climate Risk and Early Warning Systems
DGM	Direction General of Meteorology of Madagascar
DJF	December-January-February
ECA&D	European Climate Assessment & Dataset
ECOF-V1	Environment Canada's Optimal Fingerprint
ENANDES	Enhancing Adaptive Capacity of Andean Communities through Climate Services
ENSO	El Niño Southern Oscillation Index
EOF	Empirical Orthogonal Function
ETCCDI	Expert Team on Climate Change Detection and Indices
GCM	Global Climate Model
GFCS	Global Framework for Climate Services
GHG	Greenhouse Gases forcing
IDW	Inverse Distance Weighted
IGAD	Intergovernmental Authority on Development
IOD	Indian Ocean Dipole
ITCZ	Inter-Tropical Convergence Zone
JJA	June-July-August
LOESS	Locally Estimated Scatterplot Smoothing
MAM	March-April-May
MCT	Mozambique Channel Trough
MIP	Model Intercomparison Project
NAT	Natural forcing
NMHS	National Meteorological and Hydrological Services
NOAA	National Oceanic and Atmospheric Administration
OBS	Observation
QC	Quality Control
RCC	Residual Consistency Check

ROF	Regularized Optimal Fingerprinting
SON	September-October-November
SSP	Shared Socioeconomic Pathways
STARDEX	STAtistical and Regional dynamical Downscaling of Extremes for the European region
TC	Tropical Cyclone
TLS	Total Least Square
TTT	Tropical Temperate Trough
URV	Universität Rovira i Virgili
WMO	World Meteorological Organization

PART I: THESIS BACKGROUND

CHAPTER 1 General introduction

Madagascar is the fourth biggest island in the world. It is in the Southwestern Indian Oceana and separated from the African coast by the Mozambique channel with a width of 400 km. Besides, it is home to endemic flora and fauna (Myers et al. 2000; Goodman et al. 2022). Myers et al. (2000) classified Madagascar among the 25 biodiversity hotspots with 3.2 and 2.6% of plant and vertebrate species in the world respectively. This beauty is due to the hospitality of its weather and climate. they indicated that Madagascar has mainly tropical weather. Its weather and climate are mainly influenced by geographical position, reliefs, winds, and Ocean (Battistini and Richard-Vindard 1974). Cornet (1974) explained the interaction between reliefs and winds during the austral summer (December to February) and the austral winter (June to August). He concluded that the austral summer (winter) was dominated by monsoon (trade) winds from the northwest (southeast), triggered mainly by equatorial lows (Mascarenes highs). Then three climate types appeared. Firstly, the regions without dry seasons are noticed in the eastern part and central highlands influenced by droplets and fogs. Secondly, the regions with well-established dry seasons are indicated in the western part. Finally, the sub-arid regions were established in the south of Madagascar. Cornet (1974) noted some climate varieties due to the influence of the latitudes. Updates analysis was done using contemporary data based on surface measurement blended with satellite observations and numerical modeling outputs (M. R. Jury et al. 1994 and 1995; Nassor and Jury 1997 and 1998; Mark R. Jury 2016). These studies focused mainly on the Austral summer where most high-impact weather and climate events occur such as tropical cyclones, floods, and drought. They remarked that the more well-established the Inter Tropical Convergence Zone (ITCZ), the more intense the tropical cyclones might trigger a flood. The opposite fostered high-impact drought events. Furthermore, Ash and Matyas (2012) and Matyas (2014) noted that climate predictors (El Nino Southern Oscillation, Indian Ocean Subtropical Dipole, Madden Julian Oscillation, Southern Annular Mode) played important roles in the formation and trajectory of tropical cyclones in Southwestern Indian Ocean and Mozambique channel. As it was difficult to attribute one individual weather event to climate change, it remains a challenge to associate an extreme event with climate change. Stott et al. (2016) showed that it was more evident to attribute the human influence to extremely warm and cold temperature seasonal than to extreme precipitation events, droughts, and storms. However, Fitchett and Grab (2014) pointed out that no

statistically significant trends were found for the frequency of tropical cyclone landfalls in Madagascar and Mozambique. However, their trajectories seemed to move to the South of Madagascar. Then Barimalala et al. (2021) noticed that the west and southwest rainfall might increase. In the future, Tadross et al. (2008) noticed that the frequency of cyclone formation did not change but its intensity might increase in the Southwest Indian Ocean. Moreover, on the one hand, Otto et al. (2022) found that rainfall associated with tropical cyclones increased due to climate change in Madagascar. On the other hand, Harrington et al. (2022) concluded that the low rainfall was not linked directly to climate change in the southern part of Madagascar.

Africa is the most vulnerable continent to the impacts of climate change. Agricultural, health, and water availability are the main affected as they are climate-sensitive sectors (African Development Bank 2011). Madagascar's Gross Domestic Product (GDP) is supported by agriculture, tourism, services, industries, and manufacturing according to the World Bank. Agriculture and services contribute to 25 and 50% of the country's GDP but they create 64 and 27% of employment respectively (available on https://globaledge.msu.edu/countries/madagascar/economy visited on 15 May 2023). More than 80% of Malagasy work in the agriculture and tourism sectors. With very little and limited management and infrastructure on irrigation, smallholder farmers are rainfall-dependent for growing staple crops such as rice and maize. Furthermore, climate change presents a threat to these fauna and flora (Ingram and Dawson 2005). Moreover, Willis and Bhagwat (2009) showed how climate change effects might extinct species through prediction modeling of climate change impacts on biodiversity. The cost of damages is higher as highlighted by Busch et al. (2012). Nhamo et al. (2019) remarked that Southern Africa is mostly vulnerable to drought as most sectors of development are drought-sensitive, especially the agricultural sector. For instance, Fayad (2023) pointed out that Madagascar's human development was hampered by food insecurity and climate shocks. She found that climate issues, especially drought events, were the first factor to increase food insecurity levels, especially in the South. Mostly, the unpredictability of rainfall had an impact on the seeding period.

In general, Islands are threatened by sea level rise, extratropical and tropical storms, increasing air and sea surface temperatures, and changing patterns of rainfall as stated by Nurse et al. (2015). Therefore, this thesis concentrates on the climate change issues and their impacts on the agriculture sector in Madagascar.

1.1 Problematics, hypothesis, and objectives of the thesis

1.1.1 Problematics of thesis

Climate change issues mainly threaten the achievement of the sustainable development goal in 2030. Among African countries, southern Africa is the hardest hit by climate change effects (Asafu-Adjaye 2014). Weiskopf et al. (2021) analyzed the impacts of climate change on seven sectors in Madagascar. They found that plans and projects were designed to minimize climate change effects, but scientific information was insufficient to implement those plans and projects. Moreover, understanding the basis of climate change and helping decision-makers manage climate-related risk needed reliable detection and attribution of climate change (G. C. Hegerl et al. 2010b). Therefore, the efficiency and reliability of scientific information are crucial, especially those related to climate change. Three questions have emerged in this thesis:

How do we proceed to have the efficiency and reliability of scientific information on climate change?

How does climate change influence Madagascar's climate?

Is Madagascar's climate change due to natural or anthropogenic forcing?

Sasson (2012) mentioned that food security has been a great challenge for Africa. It may be exacerbated by climate change. This fact was ascertained by Fayad (2023) for the Madagascar case. As the agricultural sector is the most climate-sensitive sector, it is also the most impacted. Drought is frequently the most devastating for this sector. For instance, Madagascar has faced to food crisis due to recurring drought events over the last 30 years. The latest event was in 2020-2021 (Rigden et al. 2022). United Nations involves all countries in making strategies for early climate action. Rice and maize are among the most staple foods of Malagasy. Accordingly, the last question treated in this thesis is:

Does climate change affect the rainy season and crop calendars of rice and maize in Madagascar?

1.1.2 Hypothesis of thesis

Climate change is real, the effects vary across Madagascar. Their causes are mainly due to anthropogenic forcing as far as extreme temperatures are concerned. Their impacts are palpable on the rainy season and crop calendars, especially for rice and maize crops.

1.1.3 Objectives of thesis

This thesis contributes to ascertaining and updating scientific knowledge using the latest state-of-the-art techniques on climate change consequences, causes, and impacts on the agriculture sector, especially on rice and maize cultivation in Madagascar.

Thus, it could be taken as a scientific reference for implementing adaptation plans in the agricultural sector. In this thesis, rice and maize crops pick up as a concrete example.

This thesis has six specific objectives:

1. Assess the quality control of observational datasets by using the INQC tool developed by the INDECIS project;
2. Homogenize the quality-controlled observational datasets by applying two different approaches;
3. Calculate climate change indices proposed by the ClimInd package also developed by the INDECIS project and appreciate their trends to deduce changes;
4. Apply fingerprinting method to detect and attribute changes in extreme temperatures by considering external forcing;
5. Analyze the impacts of climate change on rainy seasons and deduct its effects on rice and maize crops calendars;
6. Describe the future perspectives.

CHAPTER 2 Research design and methodology

2.1 Research design

This dissertation is built by a compendium of three articles. Its structure is established to improve science-based climate information as recommended by the WMO on GFSC, or the Global Framework for Climate Services (Hewitt et al. 2012). In addition, Vaughan et al. (2016) pointed out that climate services should be built on the best available science. Therefore, the concepts' science and tools used are the results of research by the INDECIS project. Figure 1 shows the logical order and relationship of chapters of eight chapters. Firstly, Chapter 1 deals with the background and context of the thesis. Then chapter 2 shows the research design and methodology. Chapters 3 to 5 form the body of the thesis. They group the three papers compiled in this thesis. After, Chapter 6 contains the general discussion and conclusion. Finally, the last chapter describes future perspectives.

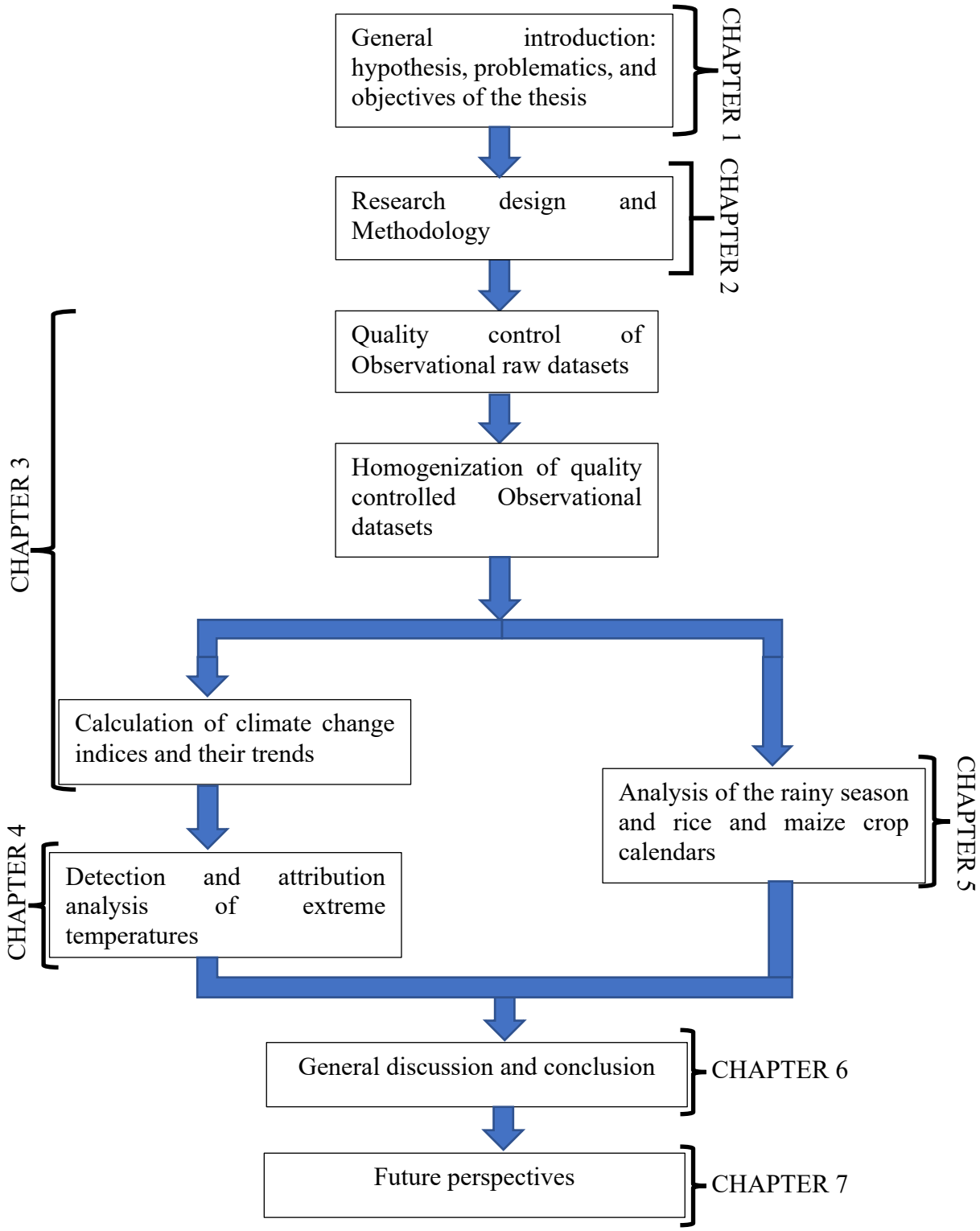

FIGURE 1 Thesis structure

2.2 Methodology

The methodology consists of ensuring the data reliability, assessing climate indices, detecting, and attributing causes of climate change through climate indices, and creating climate information for the agriculture sector. Details of methods are already included in every paper respectively. Therefore, this section gives a general overview and methods' relationship between papers.

2.2.1 Data reliability

Data reliability assessment is a crucial stage as it refers to data completeness, consistency, and accuracy. In this thesis, three steps are taken to achieve these objectives for the in-situ datasets. First, the basic control focuses on plotting the time series of observational datasets. It permits checking inconsistent values. Moreover, it helps to perform the next step, advanced control, by setting up threshold and window values. Second, the advanced control is based on a statistical test. INQC tool is used. Skrynyk et al. (2023) described the 19 different physical tests in INQC. After, error and suspect values were corrected using online materials. Finally, removing non-climatic factors or inhomogeneities and infilling the missing values from quality-controlled observational datasets increase the accuracy. Two complementary techniques of homogenization are adopted automatic and semi-automatic (i.e., human intervention on breakpoint acceptance). We employ Climatol and HOMER softwares respectively. Seasonal and annual trends are calculated to compare their results.

2.2.2 Climate change indices

The method is designed to update and compare the previous results done by Tadross et al. (2008) and Vincent et al. (2011). Therefore, annual indices calculated with STARDEX and Rclimdex are compared with ClimInd using quality-controlled and homogenized daily observational data. Their trends at 0.05 level are examined on station-by-station and regional. As updates, period length is increased, and new indices are added. These indices contributed to the next study.

2.2.3 Detection and attribution of extreme temperatures

The detection and attribution approaches are based on checking the influence of external forcings on extreme temperature indices (i.e., coldest and warmest night and day, cold and warm nights and days, very cold night, and very warm night). On the one hand, wavelet coherence is used to examine the linkage between indices and SSTs. On the other hand, the standard optimal fingerprinting method is used to establish the influence of human activities on climate as described by Ma et al. (2023). Then they explained that this is a regression method

of observation on the expected climate responses to external forcings. In this thesis, climate models' robustness is checked before applying these two methods. This is done by comparing regional annual indices from in-situ and multi-model ensemble mean data. The centred root-mean-square difference, correlation, and standard deviation were calculated to justify the relationship.

2.2.4 Climate information for the agriculture sector

The objective is to understand the climate change impacts on the rainy season and rainfed crops such as rice and maize crops. The method focuses on the comparison of the rainy season characteristics and crop calendars between the past period (1950-2018) and the future period (2030-2100). To achieve the goal, a multi-model ensemble is built to minimize uncertainty. Romanovska et al. (2023) adopted a similar approach in West Africa.

PART II: SCIENTIFIC PUBLICATIONS

CHAPTER 3 Indices for daily temperature and precipitation in Madagascar, based on quality-controlled and homogenized data, 1950-2018

Received: 2 October 2020 | Revised: 30 May 2021 | Accepted: 4 June 2021

DOI: 10.1002/joc.7243

RESEARCH ARTICLE

International Journal of Climatology RMetS

Indices for daily temperature and precipitation in Madagascar, based on quality-controlled and homogenized data, 1950–2018

Luc Yannick Andréas Randriamarolaza[1,2] | **Enric Aguilar**[1] | **Oleg Skrynyk**[1,3] | **Sergio M. Vicente-Serrano**[4] | **Fernando Domínguez-Castro**[5,6]

[1]Center for Climate Change (C3), Geography Department, Universitat Rovira i Virgili, Tarragona, Spain

[2]Direction de la Météorologie Appliquée, Direction Générale de la Météorologie, Antananarivo, Madagascar

[3]Division of Atmospheric Physics, Ukrainian Hydrometeorological Institute, Kyiv, Ukraine

[4]Instituto Pirenaico de Ecología, Spanish National Research Council (IPE-CSIC), Zaragoza, Spain

[5]Department of Geography, University of Zaragoza, Zaragoza, Spain

[6]ARAID Foundation, Zaragoza, Spain

Correspondence
Luc Yannick Andréas Randriamarolaza, 15 C. Joanot Martorell, Vila-seca, 43480, Spain.
Email: lucyannickandreas.randriamarolaza@urv.cat; luc.randriamarolaza@gmail.com

Funding information
FORMAS (SE), DLR (DE), BMWFW (AT), IFD (DK), MINECO (ES), ANR (FR), European Union, Grant/Award Number: 690462

Abstract

This study updates knowledge on climate evolution in Madagascar from 1950 to 2018. Changes were analyzed using annual and seasonal climate indices at regional and station level. The original daily series of minimum and maximum temperature and precipitation obtained from 28 meteorological stations were quality controlled and homogenized. Thirty-seven (37) climate indices were obtained from the daily series. The results show that changes in temperature had a higher degree of spatial coherence than changes in precipitation. Trends for temperature indices were mostly significant at 0.05 level and compatible with warming. Changes in minimum temperatures were greater than those for the maximum, leading to a significant decrease in the diurnal temperature range (DTR). Warm nights increased more than warm days, (0.70 days·decade^{-1}) and cold nights decreased more than cold days, (0.21 days·decade^{-1}). In addition, we found more stations with significant trends for very cold nights (92.60%) than for very warm days (51.80%) but they progressed differently (decrease and increase, respectively). Station-by-station precipitation index trends were mostly non-significant at 0.05 level, and most regional precipitation index showed decreasing trends. A shift in precipitation magnitude was observed around 2000–2018, a period of intensified drying (where 70.40% of stations recorded non-significant decreasing trends). An analysis of drought characteristics (i.e., intensity, magnitude and duration) highlighted the situation, especially in the south-east at an annual timescale.

KEYWORDS

climate change, climate indices, climate trends, Climatol, ClimInd, daily homogenization, HOMER, INQC, quality control

1 | INTRODUCTION

The expert team on climate change detection and indices (ETCCDI) developed different indices to assess and monitor trends on climate extremes. Some of these indices are globally comparable and mostly based on tails of the distribution of meteorological variables, (Zhang *et al*., 2011). Globally, changes in daily minimum temperature indices were faster than for daily maximum temperatures, and more heavy precipitation events were observed, as stated in Dunn *et al*. (2020).

In Africa, a first indices analysis indicated that cold and warm events decreased from 1960 to 1990 (Easterling *et al*., 2003). These first findings were improved by introducing climate data quality control and homogenization processes. Therefore, more recent papers showed that cold and warm events were decreasing and increasing respectively for Southern and West Africa (New *et al*., 2006), Western and Central Africa (Aguilar *et al*., 2009) and the Western Indian Ocean Region (Vincent *et al*., 2011). Also, Barry *et al*. (2018), using an updated data set, found that warm extremes were increasing and cold extremes decreasing in West Africa. In addition, homogenization improved coherency in the mean temperature trends among stations in South Africa (Kruger and Nxumalo, 2017).

In Madagascar, Tadross *et al*. (2008) and Vincent *et al*. (2011) agreed that annual temperature means increased from 1961 to 2005 and 1961 to 2008, respectively. However, certain inconsistencies were found for specific meteorological stations.

This study updates our understanding on how climate has changed in Madagascar. In comparison to the studies mentioned above, we extended the data period to 1950–2018 and used newly quality-controlled and homogenized data, including an assessment based on several climate indices. This assessment is highly relevant given climate change projections in the region. Nematchoua *et al*. (2018) suggested that warming could increase by more than 2°C, compared with 1960–2000, over the next decade in Madagascar based on A2 scenarios. According to Hoegh-Guldberg *et al*. (2018), 1.5°C above pre-industrial levels of global warming will be accompanied by larger temperature extremes and increased intensity and frequency of heavy precipitation and drought. For this reason, checking whether some of these projected changes could already be recorded in the observational data sets was a priority. For this purpose, we use a set of 28 quality controlled and homogenized stations (see Section 3 for details) and compute over them a set of 37 indices (see Domínguez-Castro *et al*. 2020), which extend the traditional set of ETCCDI indicators, to provide a complete assessment of the recent climate trends in Madagascar. Therefore, objectives of this study are to present trends in observational indices on daily temperature and precipitation and analyze drought intensity, magnitude and duration in Madagascar over 1950–2018.

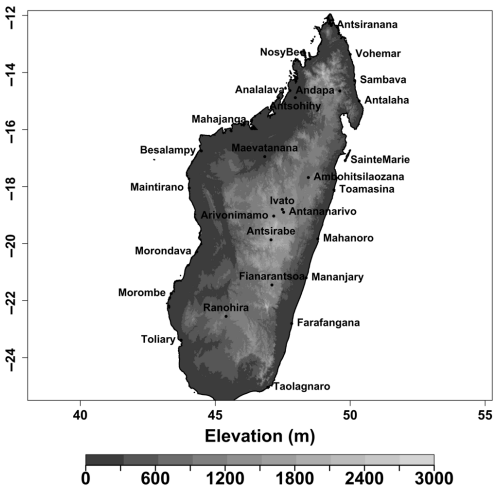

FIGURE 1 Relief and synoptic stations map of Madagascar. Elevation data are obtained from the SRTM digital elevation data in Jarvis *et al*. (Jarvis *et al*., 2008)

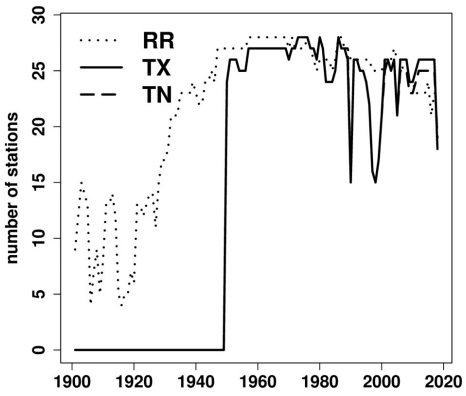

FIGURE 2 Number of synoptic weather stations per parameters. RR, precipitation; TX, maximum temperature; TN, minimum temperature

2 | STUDY AREA

Madagascar is located in the Western Indian Ocean, situated between latitudes 12°–25°S and longitudes

TABLE 1 Synoptic weather stations list

Stations	Longitude	Latitude	Elevation	WMO numbers	Start	End	Percentage of daily gaps		
							RR	TX	TN
Ambohitsilaozana	48.5	−17.7	786	67067	1928	2018	0.3	2.9	1.6
Analalava	47.8	−14.6	57	67019	1901	2017	26	15.5	32.6
Andapa[a]	49.6	−14.7	474	67022	1935	2008	52.7	51.4	51.6
Antalaha	50.3	−15.0	6	67025	1905	2018	0.2	18.9	18.7
Antananarivo	47.5	−18.9	1,310	67085	1943	2018	1.1	0.3	0.4
Antsirabe	47.1	−19.9	1,540	67107	1957	2018	2.8	9.2	8.7
Antsiranana	49.3	−12.4	105	67009	1901	2018	0.1	1.5	1.5
Antsohihy[b]	48.0	−14.9	28	67020	1923	2018	14.5	60.2	57.8
Arivonimamo[a]	47.2	−19.0	1,450	67109	1950	1981	100	54.2	54.2
Besalampy	44.5	−16.8	36	67037	1928	2018	2.2	17.1	15.9
Farafangana	47.8	−22.8	6	67157	1902	2018	0.7	7.1	8.4
Fianarantsoa	47.1	−21.5	1,106	67137	1902	2018	0	0.8	0.8
Ivato	47.5	−18.8	1,264	67083	1947	2018	0.4	0.5	0.5
Maevatanana[b]	46.8	−17.0	77	67045	1901	2017	17.3	40.5	40.5
Mahajanga	46.4	−15.7	22	67027	1897	2018	0	0.1	0.1
Mahanoro[b]	48.8	−19.8	5	67113	1903	2018	13.7	9.1	8.9
Maintirano	44.0	−18.1	25	67073	1903	2018	5.3	21.3	21.2
Mananjary	48.4	−21.2	6	67143	1901	2018	1.3	16.7	15.1
Morombe[b]	43.4	−21.8	4	67131	1928	2018	0.9	24.5	24.4
Morondava	44.3	−20.3	8	67117	1902	2018	3.3	4.8	4.2
NosyBe	48.3	−13.3	11	67012	1901	2018	6.7	7.8	7.7
Ranohira[b]	45.4	−22.6	823	67152	1935	2018	0.2	11.2	11.2
SainteMarie[b]	49.8	−17.1	9	67072	1947	2018	0.5	15.4	15.8
Sambava	50.2	−14.3	5	67023	1932	2018	1.8	14.5	15.2
Taolagnaro	47.0	−25.0	8	67197	1903	2018	0.5	0.6	0.7
Toamasina	49.4	−18.1	6	67095	1898	2018	0.7	7.3	6
Toliary	43.7	−23.4	9	67161	1901	2019	2	2.4	1.8
Vohemar[b]	50.0	−13.4	5	67017	1901	2017	19.5	15	14.7

Note: The longitude and latitude expressed in degrees and tenths of degree. Negative latitude corresponds to the southern, and longitude to the western, hemispheres. The percentages of valid values were calculated over period 1950–2018.
[a]Removed from analysis due to shorter records.
[b]Not used by HOMER.

TABLE 2 Station relocation records

WMO numbers	Name	Station relocation	Reasons
67085	Antananarivo	March 1, 1953	Moved to Betongolo
67143	Mananjary	March 12, 1953	Moved to airport
67117	Morondava	October 1, 1955	Moved to airport
67197	Taolagnaro	February 20, 1953	Moved to airport
67161	Toliary	August 1955	Moved to airport

43°–51°E, and a surface area covering ~590,000 km^2. The climate is conditioned by its geographical position, relief, the maritime influence and wind regime, which is mainly the easterly trade winds. Figure 1 shows the relief of Madagascar and the location of the available meteorological stations. The high mountains, running from north to

TABLE 3 Summary of QC process

	TX	TN	RR	Total
Checked values	892	205	85	1,182
Validated	35	11	4	50
Corrected	201	194	6	401
Set to missing	656	0	75	731
Total values passing QC	704,764	705,451	705,571	2,115,786
Total raw values	705,656	705,656	705,656	2,116,968

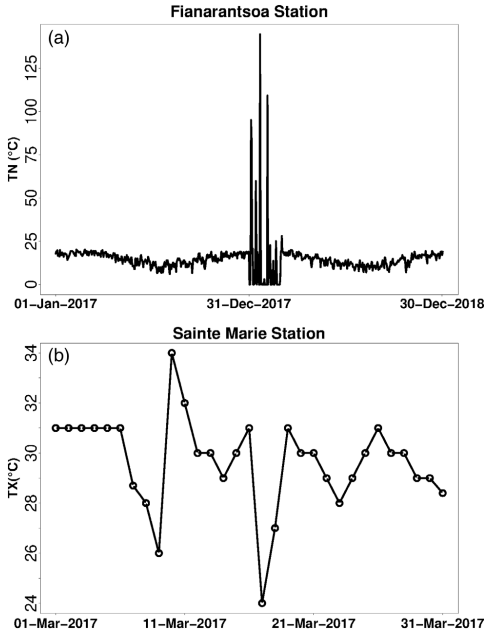

FIGURE 3 Examples of error types in raw data (a) erroneous and (b) suspects and collectively suspects

south, make the east and west as windward and leeward coasts respectively. Therefore, the west coast temperature is 1 to 3°C higher than on the east coast, but the east coast is wetter. The climate is clearly separated into two main seasons: wet and hot from November to April, and dry and cool from May to October. Mean annual temperature varies from 14 to 22°C in the highlands, and from 23 to 27°C in coastal areas. The lowest temperature occurs in July in the highlands, and the highest in November on the west coast. Their values are lower than 5°C and higher than 36°C respectively. The total annual rainfall varies from 350 mm on the south-west coast to 4,000 mm in the bay of Antongil (east coast).

During the hot, wet season, the easterly trade wind weakens but converges with the north-west monsoon wind to form the Inter-Tropical Convergence Zone (ITCZ), which covers the northern half of Madagascar. The analysis of annual zonal mean maximum precipitation and sea surface temperature done by Keshtgar *et al.* (2020) in Indian Ocean indicated that annual mean location of ITCZ was approximately 5.5°S. Moreover, Keshtgar *et al.* (2020) indicated also that the farthest south seasonal mean location of ITCZ was observed during December–January–February (DJF) and was approximately 7.5, 10.5 and 11.5°S according to analysis of seasonal zonal mean precipitation, mean wind speed near equator and zonal mean meridional wind respectively. Besides, Jury *et al.* (1994) found that ITCZ moved polewards to 15°S during DJF by analyzing outgoing longwave radiation. For instance, Randriamahefasoa and Reason (2017) noticed that this shift to southward of ITCZ associated to ENSO events influenced on the wet day frequency (daily rain exceeds 1 mm) in South and South-west regions. In addition, wet spells of these regions were also influenced by the development of tropical temperate trough (TTT) over Southern Africa and Mozambique channel from November to February as lined up by Macron *et al.* (2016). Ratna *et al.* (2013) showed that the TTT also modified the ITCZ structures. On the other hand, Donque (1972) remarked on the existence of a Mozambique Channel Trough (MCT) during this season. Then Barimalala *et al.* (2020) demonstrated that MCT appeared in December, intensified in February and weakened in May. Moreover, they concluded that a weak MCT activity caused dry conditions in Madagascar. Besides, the strong MCT activity promoted a cyclonic circulation over Mozambique channel (Barimalala *et al.*, 2020). Tropical cyclones (TCs) are frequent during this season. Madagascar is included in Southwest Indian Ocean basin (SWIO). It is boarded by Indian Ocean to the East and the Mozambique channel to the West. In SWIO, the frequency and tracks of (TCs) were related to ITCZ intensity and structure (Jury *et al.*, 1994). Jessica *et al.* (2016) ascertained that TCs period spanned from

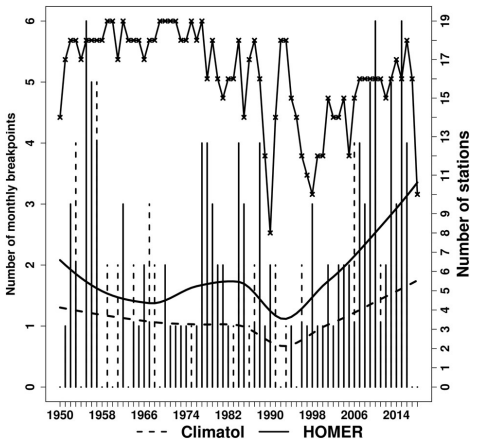

FIGURE 4 Comparison between number of monthly breakpoints for temperature for HOMER (line) and Climatol (dash) versus number of stations (cross). Number of stations was calculated from quality-controlled data such as data availability over the reference period 1961–1990 was 90% and no missing values more than 15 days in a year to calculate annual mean. The adjustment curves were done by LOESS function

November to April and its maximum activities were during DJF. On average, 9.7 tropical systems occurred of which around 97% (i.e., 9.4 up 9.7 on average) strengthened to tropical storms from which around 51% (i.e., 4.8 up 9.4 on average) became tropical cyclones (i.e., similar as hurricane or typhoon) each year during November to April as pointed out by Leroux *et al*. (2018). Besides, tropical activity and number of TC days were influenced by Indian Ocean Dipole (IOD) and El-Niño Southern Oscillation (ENSO) according to Jessica *et al*. (2016). Besides, Matyas (2015) showed that tropical cyclones formed in northern (southern) of Mozambique channel part if Indian Ocean Subtropical Dipole and Southern Annular Mode were negative (positive) phase. During the dry, cool season, the easterly trade wind dominates the island as noted by Donque (1972), who classified Madagascar into five climatic regions. Most regions receive rainfall during the hot, wet season, but the east coast continues to get rain even during the dry, cool season.

The eastern regions (reference stations: Vohemar, Sambava, Andapa, Antalaha, Sainte Marie, Ambohitsilaozana, Toamasina, Mahanoro, Mananjary, Farafangana, Taolaganro) are the most humid and threatened by tropical cyclones from the Indian Ocean. They receive around 2,500 mm per year and mean annual temparature is below 25°C. The central regions (reference stations: Ivato, Antananarivo, Arivonimamo, Antsirabe, Fianarantsoa, Ranohira) are dominated by altitude climate. The mean annual temperature is around 20°C, and total annual rainfall around 1,200 mm. The western regions (reference stations: Analalava, Antsohihy, Mahajanga, Maevatanana, Besalampy, Maintiarano, Morondava, Morombe) are dry due to the foehn effect, although these regions receive rainfall when the ITCZ and Mozambique channel depression are well established. Annual rainfall is ∼1,000 mm and mean annual temperature is above 25°C. The south and south-west regions (reference stations: Toliary) are dominated by a semi-arid climate. Annual rainfall is roughly 500 mm and mean annual temperature is around 23°C. The extreme north and north-west regions (reference stations: Antsiranana, Nosy-be) receive almost the same quantity of rainfall as in eastern regions, but the dry period is well-defined. The spatial pattern of rainfall is more discontinuous than temperature specifically in the south-western (dry area), where a single extreme rainfall can contribute a significant proportion of the annual rainfall (Tadross *et al*., 2008).

3 | DATA AND METHODOLOGY

3.1 | Data

Daily minimum and maximum temperature and daily precipitation data measured at 28 synoptic stations were taken from the Directorate General of Meteorology (DGM) of Madagascar. Most of the stations are in coastal areas (Figure 1). Although the DGM stores some data prior to 1950, 1950–2018 are taken as the study period due to the high proportion of non-missing values at all stations (see Figure 2, Table 1). Metadata information, in addition to basic locational aspects, is very limited and we are only aware of the different station relocations listed in Table 2.

3.1.1 | Data quality control

Quality control (QC) is necessary to improve the accuracy of observations by detecting and identifying errors in the process of recording, manipulating, formatting, transmitting and archiving data (Aguilar *et al*., 2003; WMO, 2020). For this purpose, we applied INQC, a new software developed by the authors within the framework of the INDECIS project (see https://cran.r-project.org/web/packages/INQC/index.html). INQC can be applied to quality control temperature, precipitation, relative humidity, wind speed, atmospheric pressure, snow depth, sunshine duration and cloud cover, and it was tested

TABLE 4 Annual and seasonal regional average trends and the confidence interval (in brackets) for temperature (°C/10 years) and precipitation (%/10 years) per method

Parameters	Methods	ANN	DJF	MAM
TX	Climatol	**0.21** (0.17;0.25)	**0.16** (0.11;0.22)	**0.21** (0.16;0.26)
	HOMER	**0.20** (0.12;0.28)	**0.13** (0.07;0.19)	**0.19** (0.14;0.25)
TN	Climatol	**0.24** (0.20;0.28)	**0.22** (0.17;0.28)	**0.26** (0.21;0.31)
	HOMER	**0.29** (0.24;0.34)	**0.23** (0.19;0.27)	**0.29** (0.23;0.34)
TM	Climatol	**0.22** (0.19;0.26)	**0.19** (0.13;0.24)	**0.24** (0.20;0.28)
	HOMER	**0.25** (0.20;0.31)	**0.18** (0.13;0.24)	**0.24** (0.20;0.27)
DTR	Climatol	**−0.04** (−0.07;-0.01)	**−0.04** (−0.07;0.00)	**−0.04** (−0.08;0.00)
	HOMER	**−0.07** (−0.13;0.00)	**−0.10** (−0.14;-0.05)	**−0.08** (−0.14;-0.01)
RR	Climatol	**−2.07** (−3.38;-0.90)	−0.96 (−2.76;0.95)	−2.35 (−5.19;0.32)
	HOMER	**−2.34** (−4.00;-1.15)	−1.24 (−3.32;1.00)	−2.56 (−5.54;0.60)

Parameters	Methods	JJA	SON
TX	Climatol	**0.20** (0.16;0.23)	**0.27** (0.21;0.33)
	HOMER	**0.18** (0.10;0.26)	**0.23** (0.10;0.35)
TN	Climatol	**0.23** (0.19;0.27)	**0.26** (0.21;0.30)
	HOMER	**0.28** (0.21;0.33)	**0.29** (0.22;0.35)
TM	Climatol	**0.21** (0.18;0.25)	**0.26** (0.21;0.31)
	HOMER	**0.23** (0.17;0.30)	**0.27** (0.17;0.36)
DTR	Climatol	0.00 (−0.06;0.00)	0.00 (−0.04;0.05)
	HOMER	**−0.07** (−0.13;-0.01)	**−0.11** (−0.20;-0.03)
RR	Climatol	−3.04 (−8.50;1.68)	**−4.52** (−6.61;-1.78)
	HOMER	−4.05 (−10.17;0.17)	**−5.34** (−7.77;-3.00)

Note: Boldface indicates significant trends at 0.05 level.
Abbreviations: ANN, Annual; DJF, December–January–February; DTR, Diurnal temperature range and RR, Precipitation; JJA, June–July–august; MAM, March–April–may; SON, September–October–November; TM, mean temperature; TN, minimum temperature; TX, maximum temperature.

within the framework of the project using a benchmark data set (Guijarro *et al*., 2019, Guijarro *et al*., 2018 and Pérez-Zanón *et al*., 2018).

INQC identifies erroneous (e.g., negative precipitation), suspect (e.g., outliers to the empirical distribution) and collectively suspect (e.g., runs of consecutive values) observations and, based on a flag system, provides information to the analysis for further inspection. The software is flexible and was parameterized to capture the climate of Madagascar by specifying different thresholds for temperatures and precipitation coherent with the study area section. The Extreme Value Approach was used to determine these thresholds. For instance, the highest and lowest temperatures were set at 40 and 0°C, respectively. INQC was applied station-by-station and flagged observations were grouped in Table 3. The application of INQC enabled obvious errors to be identified, such as those in the Fianarantsoa station (Figure 3a), introduced during the digitization and manipulation of the data set, when minimum temperature values were inadvertently replaced by rainfall values in early January 2018. The software also identified sequences of values that highlighted certain problems in the data set. This happened with the Ivato maximum temperature series, which were provided without the decimal point from 2006 to 2013. These values were compared with the Antananarivo maximum temperature series and SYNOP reports (http://www.ogimet.com/synops.phtml.en) for 2006–2013. Unfortunately, most values were validated because of the lack of decision support materials. Another case (Figure 3b) is the series of identical values found at Sainte Marie station in March 2017, combined with interdiurnal values that were too high. These values were errors and could be corrected by using SYNOP reports.

The quality control process also resulted in the validation of extreme values and unusually long spells. For example, a daily value of precipitation exceeding the 500 mm·day^{-1} pre-set threshold was found on January 21, 1977 (559.1 mm) at the Morondava station. This case

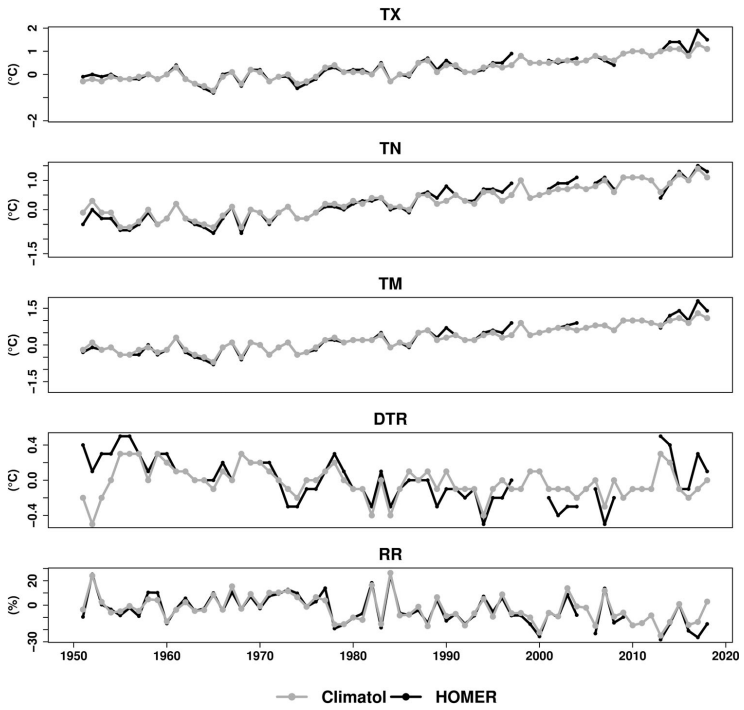

FIGURE 5 Annual regional anomalies of Climatol (grey) and HOMER (black) homogenized data

was caused by Tropical Storm Domitile, which lasted from January 18, to January 23, 1977. Therefore, the value was validated and saved. INQC also detected unusually long spells with no precipitation in Mahajanga (April–November 2014) and Ranohira (April–September 2013). Even though they are statistically suspect, they represent extremely dry seasons and were validated.

The approach adopted for validating flagged values was based on comparing the observations with neighbouring stations and consulting different archives. For the period 1950–1968, values were checked against the archives of the NOAA Central Library (https://library.noaa.gov/Collections/Digital-Docs/Foreign-Climate-Data/Madagascar-Climate-Data#o39758671) which stores scans of Malagasy daily climate data from 1935 to 1968. For 1969 to 2018, they were compared with SYNOP reports. Finally, the FIRINGA website (http://www.firinga.com/activite-cyclonique/ocean-indien.html), which archives tropical cyclone seasons in the South-West Indian Ocean Basin, was used for rainfall events associated with tropical cyclone seasons from 1969/1970 to 2018/2019. However, we were aware that precautions should be taken with synoptic messages as they might offset the absolute values of indices. Trends could be stable, as shown by the comparison of SYNOP and ECA&D data for temperature and precipitation (Besselaar *et al*., 2012). Moreover, the FIRINGA website highlighted the events without giving any observational values on precipitation, although it helped to make a decision between replacing the value by missing data or keeping the current value. Table 3 summarizes the QC process. A total of 1,182 values were checked, from which 50 were validated, 401 were corrected and 731 set to missing.

3.1.2 | Data homogenization

Non-climatic factors such as station relocations, changes in instruments, observation procedures and local environment can affect the homogeneity of long-term observational. Inhomogeneities could cause sudden and gradual biases in climate data and impact on climate analysis, specifically on climate trends (Peterson *et al*., 1998; Trewin, 2010). Thus, homogenization, or at least homogeneity assessment, is a mandatory preliminary step before tackling any sound climatological analysis. From the large number of different homogenization

TABLE 5 Selected CLIMIND climate indices and its ETCCDI equivalent

Elements	ClimInd	Description	ETCCDI	Unit
Temperature	CDD	Cold spell duration	CSDI*	Days
	WSD	Warm spell duration	WSDI*	Days
	CN	Percentage of days when TN < 10th percentile	TN10P	%
	CD	Percentage of days when TX < 10th percentile	TX10P	%
	GTN	Mean of TN	TNMean	°C
	GTX	Mean of TX	TXMean	°C
	NTN	Minimum of TN	TNn	°C
	NTX	Minimum of TX	TXn	°C
	XTN	Maximum of TN	TNx	°C
	XTX	Maximum of TX	TXx	°C
	TN	Tropical nights with TN > 20°C	TR20	Days
	D32	Days with TX > 32°C	-	Days
	CSD	Maximum consecutive summer days (MCSU25)	-	Days
	SUD	Summer days with TX > 25°C	SU25	Days
	VCD	Days when TN < 1st percentile (TN1P)	-	Days
	VWD	Days when TX > 99th percentile (TX99P)	-	Days
	WN	Percentage of days when TN > 90th percentile	TN90P	%
	WD	Percentage of days when TX > 90th percentile	TX90P	%
	DTR	Mean difference between TX and TN	DTR	°C
	ETR	Difference between the maximum TX and the minimum TN	-	°C
	VDTR	Mean absolute day-to-day difference in DTR	-	°C
Precipitation	D50mm	Heavy precipitation days with RR > 50 mm	RR50mm*	Days
	D95P	Very wet days with RR > 95p	-	Days
	DD	Dry days with RR < 1 mm	-	Days
	DR1mm	Wet days with RR > = 1 mm	RR1mm*	Days
	LDP	Maximum length of consecutive dry days (RR < 1 mm)	CDD	Days
	LWP	Maximum length of consecutive wet days (RR > =1 mm)	CWD	Days
	R10mm	Days precipitation > = 10 mm	RR10mm	Days
	R20mm	Days precipitation > = 20 mm	RR20mm	Days
	R95TOT	Precipitation exceeding 95p divided by total precipitation	R95P*	%
	R99TOT	Precipitation exceeding 99p divided by total precipitation	R99P*	%
	SDII	Precipitation in wet days divided by number of wet days	SDII	mm·days^{-1}
	RTI	Total precipitation	PRCPTOT	mm
	RTWD	Total precipitation in wet days (PRCWTOT)	-	mm
	RX	Highest amount of daily precipitation	RX1day	mm
	RX5D	Maximum consecutive 5-day precipitation	RX5day	mm
	SPEI	Standardized precipitation-evapotranspiration index calculated at 3- and 12-month timescale	-	z-units

Note: Dash (-) means climate indices are not included in ETCCDI. Asterisk (*) indicates that climate indices were not calculated in Vincent et al (2011).
Abbreviations: RR daily rainfall; TX, daily maximum temperature; TN, daily minimum temperature.

approaches, we selected Climatol (see Guijarro, 2018) and used the source code of the development version (see http://www.climatol.eu/), extensively tested via benchmarking in the MULTITEST and INDECIS projects. We chose to detect inhomogeneities over monthly data and then adjust to the daily scale instead of direct detection from daily values. This improved the signal to noise ratio and the performance of the method (Guijarro, 2018). Climatol detects breakpoints (potential inhomogeneities) using a modified version of SNHT (see Alexandersson, 1986; Alexandersson and Moberg, 1997; Moberg and Alexandersson, 1997). The monthly adjustments are calculated by orthogonal regression or Reduced Major Axis in which all scatter points are adjusted to a regression line by minimizing the perpendicular distance.

The data set was also homogenized with HOMER for comparison purposes. HOMER is the result of the European COST Action ES0601(2006–2011) (Venema *et al*., 2012) and uses completely different detection and adjustment methods (see Mestre *et al*., 2013). As HOMER only adjusts annual and monthly climate data (Mestre

TABLE 6 Regional trends with the confidence intervals (in brackets)

Index (Climind/ Rclimdex)	Trends (confidence interval)	Unit/ decade
CDD/CSDI	**−2.28** (−3.20; −1.48)	Days
WSD/WSDI	**3.81** (1.98; 6.01)	Days
CN/TN10P	**−1.52** (−1.90; −1.18)	%
CD/TX10P	**−1.31** (−1.72; −0.86)	%
GTN/TNMean	**0.24** (0.20; 0.28)	°C
GTX/TXMean	**0.21** (0.17; 0.25)	°C
NTN/TNn	**0.29** (0.19; 0.39)	°C
NTX/TXn	**0.11** (0.00; 0.22)	°C
XTN/TNx	**0.24** (0.11; 0.36)	°C
XTX/TXx	**0.23** (0.07; 0.36)	°C
TN/TR20	**7.72** (6.29; 9.22)	Days
D32	**0.43** (0.18; 0.66)	Days
CSD/MCSU25	**4.41** (1.76; 6.90)	Days
SUD/SU25	**5.40** (4.39; 6.48)	Days
VCD/TN1P	**−0.79** (−1.12; −0.49)	Days
VWD/TX99P	**0.82** (0.17; 1.54)	Days
WN/TN90P	**3.01** (1.84; 4.28)	%
WD/TX90P	**2.38** (1.27; 3.49)	%
DTR/DTR	**−0.04** (−0.07; −0.01)	°C
ETR	−0.05 (−0.26; 0.15)	°C
VDTR	0.01 (−0.03; 0.04)	°C

Note: Boldface indicates significant at 0.05 level.

et al., 2013), it was complemented by the approach described in Vincent *et al*. (2002) for temperature. For precipitation, annual factors were directly applied to the daily data. HOMER needs a limited amount of data, so the data set was reduced to 19 stations.

HOMER was run in a semi-automatic mode (i.e., assessing whether to accept or reject the breakpoints suggested by the test; metadata was used to validate breakpoints) meanwhile Climatol was run in a fully automatic mode. Despite the fact that a larger number of breakpoints were detected in HOMER (see Figure 4 for illustration), the regional trends were fairly similar, as suggested by Table 4 and Figure 5, which shows regional time series. Both homogenized data sets, produced independently and using completely different approaches, suggest a strong warming across the island, uniformly distributed throughout the year and slightly higher for night-time temperatures, which results in a small reduction in the DTR. These warming trends were coupled with uniform drying trends.

Once we remarked that both approaches return similar results, we used the data set homogenized with Climatol, since it includes a larger number of stations and the fact that it can be run safely in fully automated mode, which will enable our analysis to be seamlessly updated when additional data records become available. In addition, Climatol uses an iterative process to fill gaps in mean and standard deviation calculation, a task not performed by HOMER (Figure 5).

3.2 | Methods

3.2.1 | Climate indices calculation

Annual and seasonal climate indices were obtained using the quality-controlled and homogenized data set described in the previous sections. They were calculated using the CLIMIND package, developed by the INDECIS project (see Domínguez-Castro *et al*., 2020), which includes 125 sector-oriented indicators computed from surface air temperature, precipitation, relative humidity, wind speed, cloudiness, solar radiation and snow cover. Due to the characteristics of our data set, we calculated a subset of 37 climate indices which rely solely on temperature or/and precipitation. The Standardized Precipitation Evapotranspiration Index (SPEI, Vicente-Serrano *et al*., 2010) factors in the climatic water balance, determined from the difference between precipitation and reference evapotranspiration (ET0). Hargreaves formula (Hargreaves, 1994) was used to calculate ET0 because there was not sufficient data available to apply more robust procedures (e.g., the Penman-Monteith, which needs data on wind speed, solar radiation and relative humidity). CLIMIND expands the set of ETCCDI indicators that were used in a previous paper by Vincent *et al*. (2011) covering the Western Indian Ocean countries. Table 5 shows the set of 37 climate indices used, and a brief description of the indicator (see Domínguez-Castro *et al*., 2020 for a full description). For the sake of comparison with Vincent *et al*. (2011) and with other regional or global papers, we added a column with the ETCCDI names.

3.2.2 | Area averaging and trend calculation

To extract regional time series, we adopted the approach by Vincent *et al*. (2011) and calculated the average departures to the WMO reference 1961–1990 period for temperature and precipitation. However, the departures were divided by the 1961–1990 mean for total precipitation (RTI or PRCPTOT), total precipitation wet days (RTWD), maximum precipitation (RX or RX1day) and maximum 5-day precipitation (RX5D or RX5day). Thereafter,

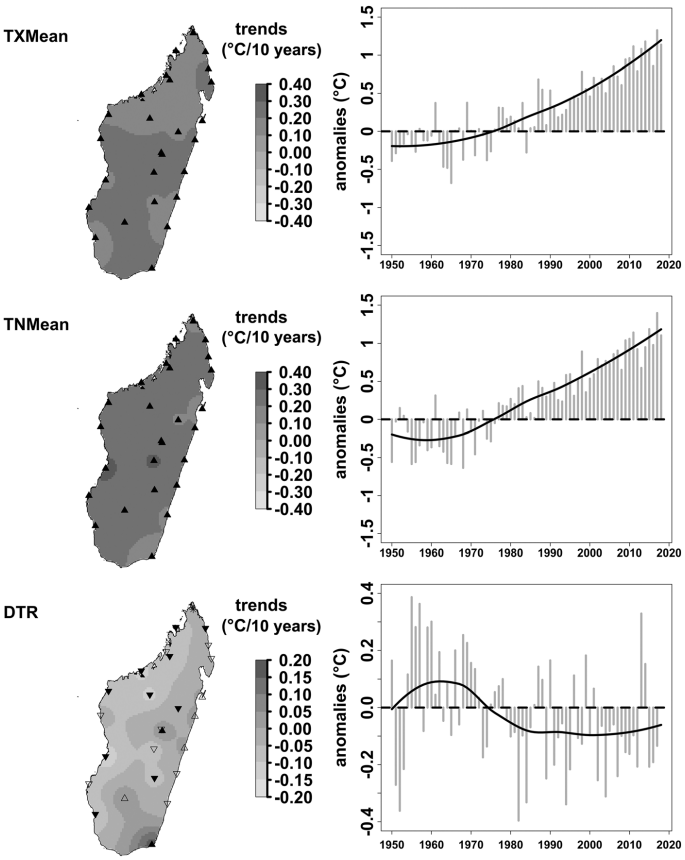

FIGURE 6 Station-by-station decadal trends and annual regional anomalies (fitted curve calculated using a LOESS function) of TXMean, TNMean and DTR. Solid point-up and point-down triangles indicate significant positive and negative trends at 0.05 level. Asterisk means no trend. Shaded colours are interpolation from the inverse distance weighted (IDW) function

regional time series were obtained by averaging all stations.

We calculated the drought characteristics (i.e., intensity, magnitude and duration) based on 3- and 12-month SPEI series. Drought events occur if 3- and 12-month SPEI values are lower than zero, similar to Domínguez-Castro *et al.* (2019). Drought duration is the period of consecutive years with SPEI <0. Drought magnitude and maximum intensity correspond to the sum and maximum severity of absolute values in drought duration, respectively. We adopted the z-score transformation as it is commonly used for drought monitoring (e.g., Morid *et al.*, 2006; Abrha and Hagos, 2019; Byrd *et al.*, 2020). Therefore, drought characteristics were transformed to z-score using the Equation (1) before calculating trends:

$$Z_i = \frac{X_i - \bar{X}}{\sigma} \quad (1)$$

Where i is the year from 1950 to 2018; Z_i is the z-score at year i; X_i is the drought characteristic at year i; $\bar{X}$ is the mean of the drought characteristic; σ is the standard deviation of the drought characteristic.

Trends and their significance at 0.05 level are calculated for each index, station and regional time series on an annual scale, using the Sen slope method (Sen, 1968) as implemented by Zhang (Zhang *et al.*, 2000). Calculations were made with the 'zyp' R package (Bronaugh and Werner, 2019). This package implements the method and was used in many papers, such as Barry *et al.* (2018) and Yosef *et al.* (Yosef *et al.*, 2019; Yosef *et al.*, 2021). The lower and upper limits of trend confidence interval are at 0.025 and 0.975, respectively. Both approaches—area averaging and trend calculation – have been used in similar papers (e.g., Aguilar *et al.*, 2005; Aguilar *et al.*, 2009; Vincent *et al.*, 2011; Barry *et al.*, 2018).

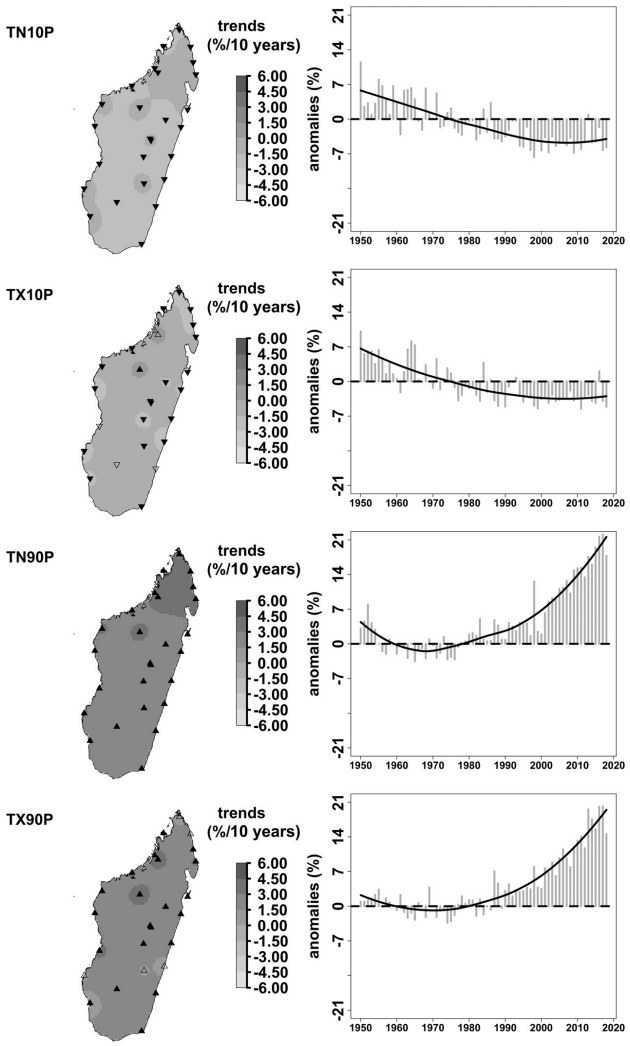

FIGURE 7 Station-by-station decadal trends and annual regional anomalies (fitted curve calculated using a LOESS function) of TN10P, TX10P, TN90P and TX90P. Solid point-up and point-down triangles indicate significant positive and negative trends at 0.05 level. Shaded colours are interpolation from the inverse distance weighted (IDW) function

4 | RESULTS

4.1 | Temperature indices

Regional temperature indices present a temporal evolution in agreement with warming (Table 6 and Figures 6 and 7). All trends are significant at the 0.05 level, except for ETR and VDTR, which both show the evolution of differences within daytime and night-time temperature and suggest a significant general decrease of −0.04°C /decade, as confirmed by the DTR. Also, trends in night-time indices, that is, those computed over minimum temperatures, are higher than for daytime (maximum temperature) indices. For example, warm nights indicate increasing trend of 3.01%/decade, whereas warm days show a positive trend of 2.38%/decade. We observe the same pattern when comparing the decrease in cold nights (−1.52%/decade) versus the decrease in cold days (−1.32%/decade). These four indices illustrate another feature of warming in Madagascar: it is due to both the occurrence of warmer weather and the suppression of cold weather, but the former mostly dominates. These

TABLE 7 Percentage of stations with positive significant, positive non-significant, negative significant and negative non-significant trends

Index (Climind/Rclimdex)	Positive trends (%)		Negative trends (%)	
	Significant	Non-significant	Significant	Non-significant
CDD/CSDI	0	0	66.7	14.8
WSD/WSDI	59.3	11.1	0	0
CN/TN10P	0	0	100	0
CD/TX10P	3.7	7.4	77.8	11.1
GTN/TNMean	100	0	0	0
GTX/TXMean	100	0	0	0
NTN/TNn	66.7	29.6	0	3.7
NTX/TXn	44.4	37	18.5	0
XTN/TNx	70.4	29.6	0	0
XTX/TXx	51.9	37	0	7.4
TN/TR20	88.9	0	0	0
D32	14.8	7.4	0	7.4
CSD/MCSU25	63	7.4	3.7	0
SUD/SU25	55.6	14.8	0	0
VCD/TN1P	0	0	55.6	37
VWD/TX99P	33.3	18.5	0	3.7
WN/TN90P	100	0	0	0
WD/TX90P	77.8	22.2	0	0
DTR	7.4	14.8	37	37
ETR	11.1	44.4	22.2	22.2
VDTR	11.1	37	14.8	22.2

TABLE 8 Regional trends with the confidence intervals (in brackets)

Index (Climind/Rclimdex)	Trends (confidence interval)		Unit/decade
	1950–2018	2000–2018	
D50MM/RR50mm	**−0.20** (−0.32; −0.07)	−0.11 (−0.29; 0.07)	Days
D95P	**−0.54** (−0.88; −0.25)	−0.21 (−0.56; 0.06)	Days
DD	0.59 (−0.29; 1.49)	−0.36 (−0.88; 0.29)	Days
DR1mm/RR1mm	−0.60 (−1.45; 0.26)	0.30 (−0.29; 0.79)	Days
LDP/CDD	1.09 (−0.46; 2.71)	−0.41 (−1.18; 0.25)	Days
LWP/CWD	0.02 (−0.12; 0.16)	−0.04 (−0.16; 0.04)	Days
R10mm/RR10mm	**−0.87** (−1.35; −0.39)	−0.08 (−0.58; 0.33)	Days
R20mm/RR20mm	**−0.67** (−1.01; −0.35)	−0.25 (−0.65; 0.25)	Days
R95TOT/R95P	−0.51(−1.07;0.14)	**−0.65** (−1.05; −0.11)	%
R99TOT/R90P	**−0.39** (−0.71; −0.07)	−0.24 (−0.58; 0.01)	%
SDII	**−0.18** (−0.31; −0.02)	−0.12 (−0.30; 0.06)	$mm \cdot days^{-1}$
RTI/PRCPTOT	**−2.07** (−3.38; −0.90)	−0.51 (−1.61; 0.46)	%
RTWD/PRCWTOT	**−2.10** (−3.35; −0.91)	−0.51 (−1.63; 0.41)	%
RX/RX1day	**−1.52** (−2.85; −0.19)	−1.24 (−2.16; 0.13)	%
RX5D/RX5day	**−1.85** (−3.43; −0.29)	−1.10 (−2.76; 0.04)	%

Note: Boldface indicates significant at 0.05 level.

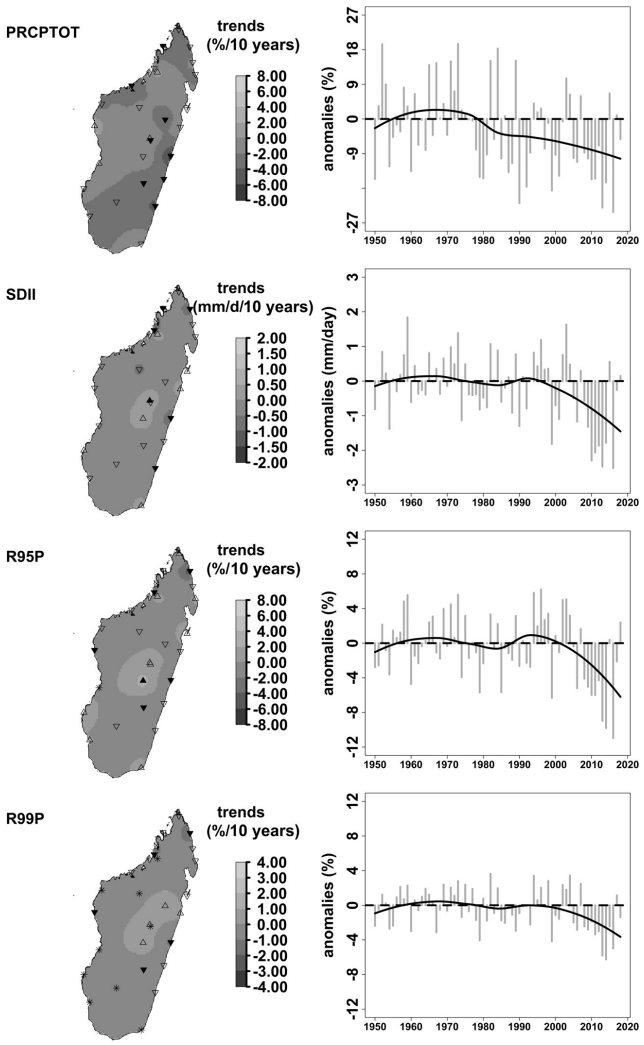

FIGURE 8 Station-by-station decadal trends and annual regional anomalies (fitted curve calculated using a LOESS function) of PRCPTOT, SDII, R95P and R99P. Solid point-up and point-down triangles indicate significant positive and negative trends at 0.05 level. Asterisk means no trend. Shaded colours are interpolation from the inverse distance weighted (IDW) function

two features are also evident from other indices, for example, the annual average of daily minimum temperatures (GTN) and the annual mean of daily maximum temperature (GTX). The seasonal analysis shows that warming occurs across the four seasons and is strongest in spring (Table 4). Finally, looking at trends at station level, even though noticeable differences in values are evident from Figures 6 and 7, they do not present a clear spatial pattern and uniform warming across the island. Table 7 shows the percentage of stations with significant positive/negative trends for each index.

4.2 | Precipitation indices

The analysis of the regional time series of precipitation indices and their trends in Madagascar displays an evolution towards drier conditions. The first five decades of the study period show values fluctuating around the long-term mean. At the turn of the century, precipitation decreases, and we observe the same pattern for the different climate indices. Not only PRCPTOT decays (-2.07 mm·decade^{-1}, significant at the 0.05 level), but also the number of rainfall

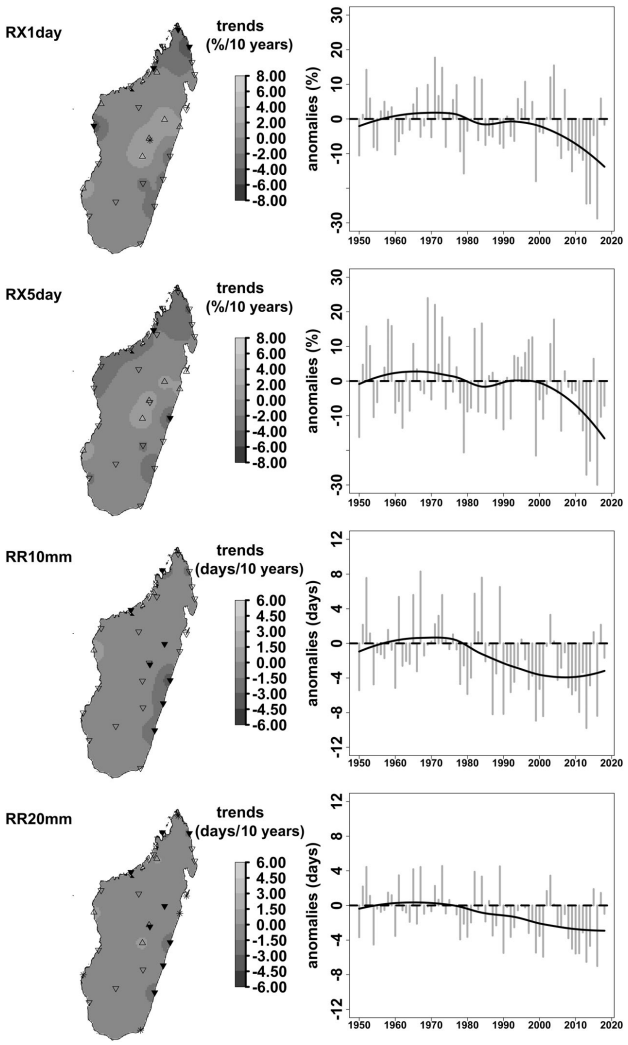

FIGURE 9 Station-by-station decadal trends and annual regional anomalies (fitted curve calculated using a LOESS function) of Rx1day, Rx5day, RR10 mm and RR20 mm. Solid point-up and point-down triangles indicate significant positive and negative trends at 0.05 level. Asterisk means no trend. Shaded colours are interpolation from the inverse distance weighted (IDW) function

days per year falls (−0.60 days·decade^{-1}) in the same proportion as dry days raise (0.59 days·decade^{-1}). The indices based on the upper tail of the distribution also display negative trends (e.g., the heavy precipitation fraction, R95TOT, −0.51 mm·decade^{-1}; SDII, −0.18 mm·decade^{-1}). The longest dry period (LDP) displays increasing trend of 1.09 days·decade^{-1}. These trends suggest a shift in the magnitude of precipitation, driven by fewer precipitation events leading towards smaller accumulations. Table 8 shows the trends for the 1950–2018, also trends for the 2000–2018 period of intensified drying.

As expected, observed trends in precipitation indices show more spatial diversity than those observed in temperature indices. Most significant drying trends occur in the east coast area (Figures 8 and 9). Moreover, we remark a large percentage of stations with negative trends (mostly non-significant) for all indices except for dry days (DD) and the longest dry period (LDP) for the 2000–2018 period of intensified drying (Table 9).

TABLE 9 Percentage of stations with positive significant, positive non-significant, negative significant and negative non-significant trends

Index	Positive trends (%)				Negative trends (%)			
	Significant		Non-significant		Significant		Non-significant	
(Climind/Rclimdex)	1950–2018	2000–2018	1950–2018	2000–2018	1950–2018	2000–2018	1950–2018	2000–2018
D50mm/RR50mm	3.7	0.0	11.1	29.8	25.9	7.4	29.6	40.7
D95P	0.0	3.7	14.8	14.8	37.0	11.1	37.0	55.6
DD	25.9	14.8	55.6	33.3	7.4	14.8	11.1	22.2
DR1mm/RR1mm	7.4	14.8	11.1	22.2	29.6	11.1	51.9	40.7
LDP/CDD	25.9	0.0	40.7	44.4	3.7	11.1	25.9	37.0
LWP/CWD	7.4	7.4	14.8	22.2	7.4	11.1	33.3	44.4
R10mm/RR10mm	0.0	3.7	11.1	25.9	25.9	3.7	63.0	51.9
R20mm/RR20mm	0.0	0.0	14.8	18.5	29.6	3.7	37.0	63.0
R95TOT/R95P	3.7	3.7	33.3	29.6	22.2	11.1	37.0	55.6
R99TOT/R90P	0.0	0.0	14.8	18.5	18.5	3.7	33.3	37.0
SDII	3.7	0.0	22.2	37.0	18.5	7.4	55.6	55.6
RTI/PRCPTOT	0.0	0.0	14.8	29.6	29.6	7.4	55.6	63.0
RTWD/PRCWTOT	0.0	0.0	11.1	25.9	29.6	7.4	59.3	63.0
RX/Rx1day	0.0	0.0	25.9	22.2	18.5	11.1	51.9	66.7
RX5D/Rx5day	0.0	3.7	22.2	18.5	7.4	7.4	70.4	70.4

4.3 | Drought indices

Figure 10 shows the regional drought events (black bars) from 1950 to 2018. Maximum and minimum drought events (49 and 34) appear at the beginning (September–October–November) and end (March–April–May) of the wet season, respectively, a situation that makes difficult to establish a cultural calendar in Madagascar. More severe drought events occur after the 1980s, which are more consecutive during the 2000–2018 period of intensified drying detected in the precipitation section (see Section 4.2). Figure 11 and Figure 12 present station-by-station decadal trends of drought magnitude and duration respectively. They point to drought being a local phenomenon in Madagascar. For instance, south-eastern stations (e.g., Farafangana and Ranohira) indicate large increasing trends in the magnitude and duration of drought annually. More than 70% of stations record positive non-significant drought characteristic trends at 0.05 level at annual and seasonal scales (except for December–January–February). Table 10 shows the percentage of stations with positive significant, positive non-significant, negative significant and negative non-significant trends at annual and seasonal scales.

5 | DISCUSSION

This paper generated very robust daily records by adopting the latest methods and tools on daily data quality control (QC) and homogenization. These steps were essential for a robust assessment of climate trends. According to Hunziker *et al.* (2017), QC procedures might improve a part of the data homogeneity specifically for the sparse network. We scrupulously checked 1,182 values detected as errors by INQC developed within the framework of the INDECIS project. Homogenization was a crucial step in climate analysis, as pointed out by Squintu *et al.* (2020). We performed daily homogenization with Climatol and HOMER, complemented by the approach described in Vincent *et al.* (2002). They were in good agreement as far as timing of breakpoints were concerned and showed a good overlap of annual regional anomalies. Moreover, annual and seasonal regional trends were almost consistent and significant at the 0.05 level. Climatol homogenization improved the accuracy and reliability of indices' trends, as Skrynyk *et al.* (2021) concluded. Therefore, climate indices were calculated using the daily homogenized series with Climatol.

This paper attempted use climate indices to increase knowledge on how climate changed in Madagascar from 1950 to 2018. As expected, due to the nature of both

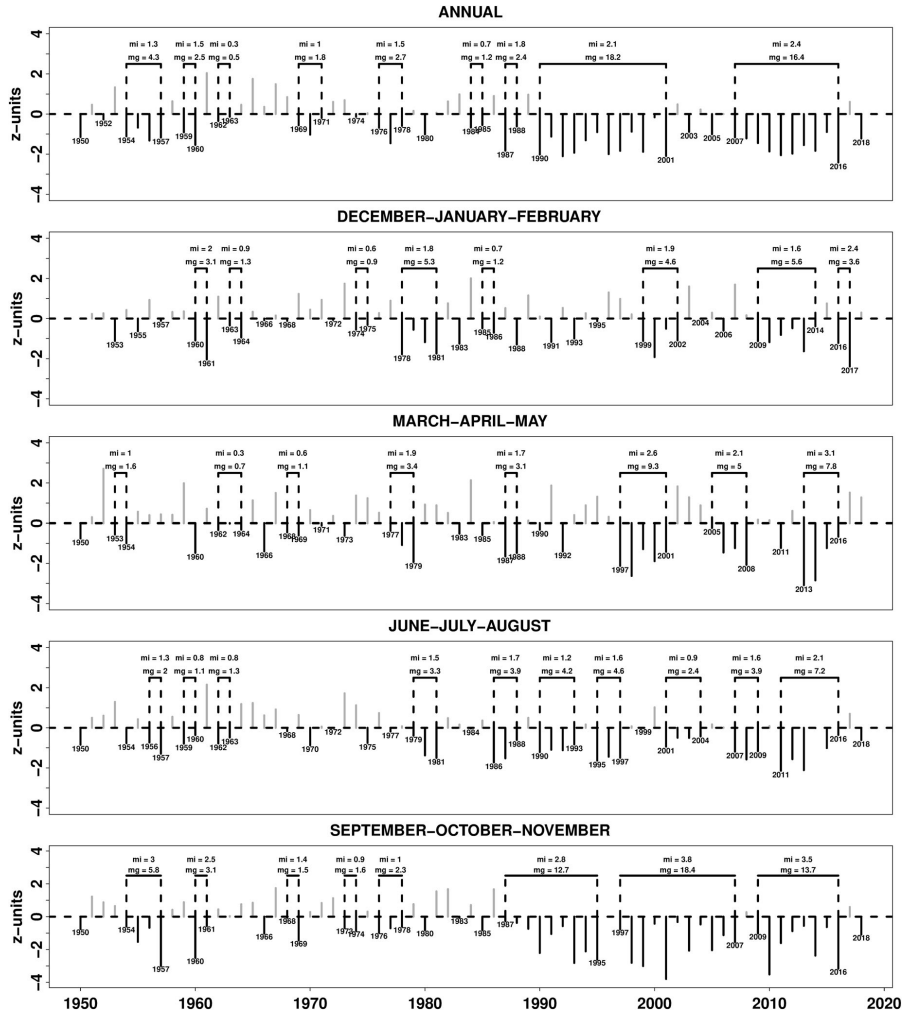

FIGURE 10 Regional drought characteristics from 3- and 12- month SPEI series. 'mi' and 'mg' indicate maximum intensity and magnitude values during consecutive drought periods (black bars), respectively

meteorological elements (i.e., temperature and precipitation), our analysis demonstrated that the changes in temperature had a higher degree of spatial coherence than in precipitation. Moreover, changes in both were noticeable, as suggested by the regional and station-by-station trends, most of which were significant at the 0.05 level for all indices during the last seven decades. Changes in temperature corroborated with warming. Changes in precipitation were moving towards drier conditions. Changes in drought characteristics indicated more consecutive drought events.

In agreement with Tadross *et al*. (2008), we found that warming occurred across all seasons and the highest warming appeared in spring. The web portal on climate change in the Southwest Indian Ocean (http://regionalclimate-change.sc/) provides a climate profile for member countries and we found that annual mean temperature increased in the region. However, our regional average of annual mean temperature was 0.02 and 0.08°C·decade^{-1} higher than for Comoros and Seychelles, respectively. Tara James *et al*. (Tara James and

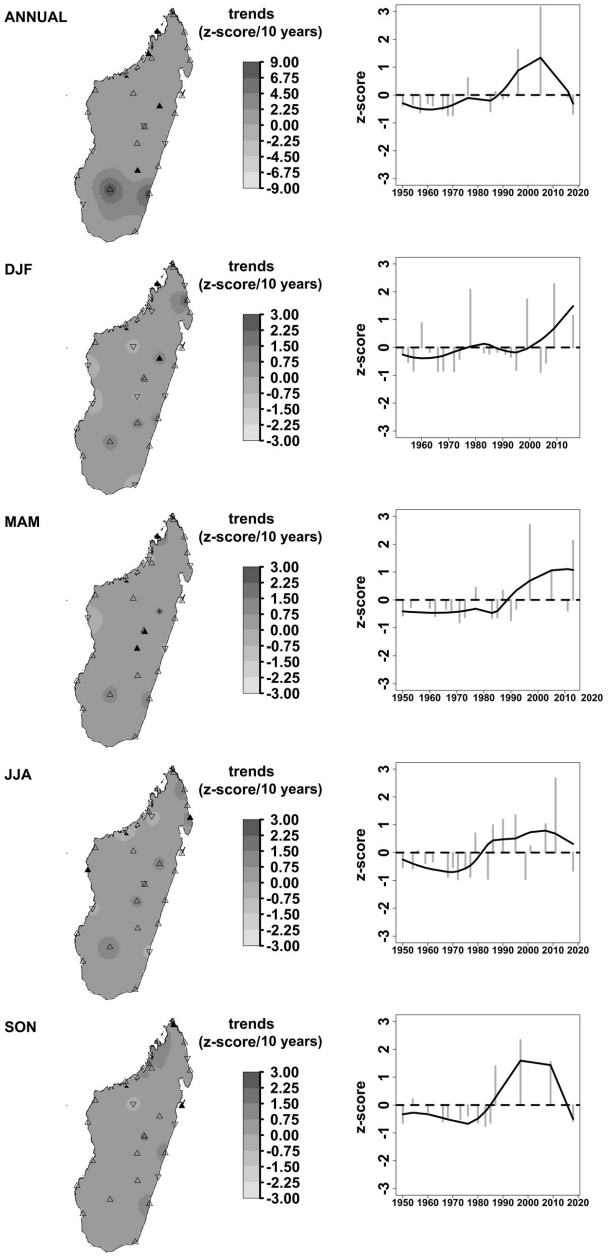

FIGURE 11 Station-by-station decadal trends and annual regional anomalies (fitted curve calculated using a LOESS function) of drought magnitude. Solid point-up and point-down triangles indicate significant positive and negative trends at 0.05 level. Asterisk means no trend. Shaded colours are interpolation from the inverse distance weighted (IDW) function. DJF, December–January–February; MAM, March–April–May; JJA, June–July–August; SON, September–October–November

Stacia, 2014) wrote that mean annual temperature had increased 0.15°C·decade^{-1} in Mauritius, which was 0.07°C·decade^{-1} lower than our trend. Our regional mean of annual maximum temperature trend was about 0.02 and 0.05°C·decade^{-1} higher than in Vincent *et al*. (2011) and Barry *et al*. (2018). The regional mean of annual

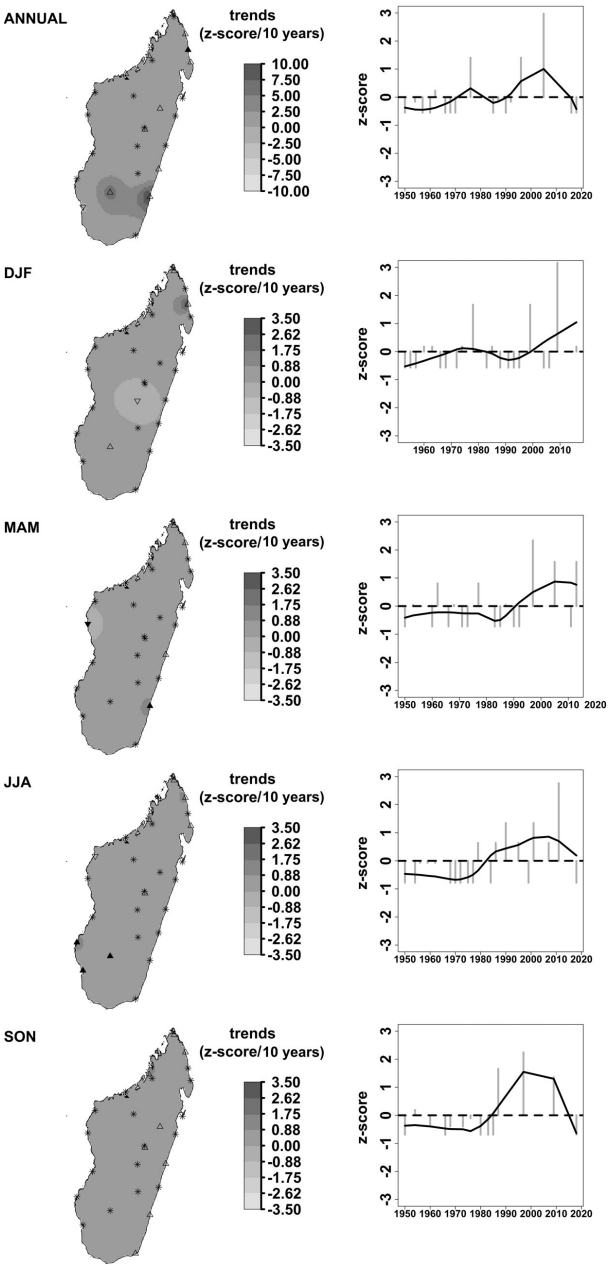

FIGURE 12 Station-by-station decadal trends and annual regional anomalies (fitted curve calculated using a LOESS function) of drought duration. Solid point-up and point-down triangles indicate significant positive and negative trends at 0.05 level. Asterisk means no trend. Shaded colours are interpolation from the inverse distance weighted (IDW) function. DJF, December–January–February; MAM, March-AprilMay; JJA, June–July–August; SON, September–October–November

minimum temperature was also about 0.04°C·decade^{-1} smaller than in Barry *et al*. (2018). The weakest and strongest regional trends were observed in summer (DJF) and spring (SON) for mean temperature. The opposite was observed in South Africa according to Kruger and Nxumalo (2017)). As also pointed out by Alexander

TABLE 10 Percentage of stations with positive significant, positive non-significant, negative significant and negative non-significant trends at the annual and seasonal scales

Index	Timescale	Positive trends (%)		Negative trends (%)	
		Significant	Non-significant	Significant	Non-significant
Magnitude	ANNUAL	14.8	70.4	0	14.8
	DJF	11.1	59.3	0	29.6
	MAM	11.1	70.4	0	14.8
	JJA	7.4	74.1	0	18.5
	SON	7.4	74.1	0	18.5
Duration	ANNUAL	7.4	37	0	3.7
	DJF	3.7	18.5	0	3.7
	MAM	7.4	14.8	3.7	0
	JJA	11.1	18.5	0	3.7
	SON	0	33.3	0	0

et al. (2006), Xu *et al*. (2013) and Barry *et al*. (2018), we observed a significant decrease in regional trends of the diurnal temperature range (DTR). This change was observed in 37% of our stations versus 49% of Chinese stations by Xu *et al*. (2013). Vincent *et al*. (2011), using a shorter and less complete version of the Malagasy climate data presented here, also pointed out the negative trend in DTR, although it was non-significant. Our findings also aligned with Niang *et al*. (2015), presented for the whole of Africa, including Madagascar. We noticed that extreme temperature indices were highly significant at 0.05 level, but those for the daily minimum temperature were most meaningful, similar to those in Israel indicated by Yosef *et al*. (2019). As pointed out by Aguilar *et al*. (2005), Alexander *et al*. (2006), New *et al*. (2006), Aguilar *et al*. (2009), Vincent *et al*. (2011), Xu *et al*. (2013), Whan *et al*. (2014), Abatan *et al*. (2016), Kruger and Nxumalo (2017), Barry *et al*. (2018) and Dunn *et al*. (2020), we observed a significant increase in warm nights and days, and a decrease in cold ones. The majority of stations (100% for night-time indices and 77.8% for daytime indices) indicated these warming trends, although Xu *et al*. (2013) observed a lower percentage for China. In addition, changes were more noticeable for high extremes (TX90P and TN90P) than low extremes (TX10P and TN10P) and their regional trend values were smaller and larger respectively compared with Vincent *et al*. (2011). Moreover, very high extremes (TX99P) and very low extremes (TN1P) had significant positive trends (observed in 33.3% of stations) and significant negative trends (observed in 55.6% of stations) respectively. Finally, our tropical nights (TR20) and summer days (SU25) regional trend values were also about 2.58 and 0.68 day·decade^{-1} higher than in Vincent *et al*. (2011).

Precipitation changes were less significant and non-coherent spatially than in temperature, as highlighted by New *et al*. (2006), Tadross *et al*. (2008), Vincent *et al*. (2011), Barry *et al*. (2018), Yosef *et al*. (2019) and Dunn *et al*. (2020). However, a significant decreasing regional trends was mostly explored for all indices except for dry days (DD), longest dry period (LDP) and the longest wet period (LWP). The reduction in total precipitation (PRCPTOT) was then associated with the reduction in heavy precipitation indices (e.g., RR50mm, RR20mm, RR10mm, R95TOT and R99TOT), the intensity of precipitation (SDII), amount of daily and maximum 5-day precipitation (RX1day and RX5day) similar to Vincent *et al*. (2011) for the Western Indian Ocean and Aguilar *et al*. (2009) for Guinea and Central Africa. This reduction was most obvious in the east coast area and agreed with Tadross *et al*. (2008). The regional trend of PRCPTOT was about 0.56%/decade smaller from 1950 to 2018 than in Vincent *et al*. (2011). On the contrary, some authors observed an increase in total precipitation accompanied by an increased simple daily precipitation index, heavy precipitation, daily precipitation and maximum 5-day precipitation for Global (Alexander *et al*., 2006 and Dunn *et al*., 2020), Central America and northern South America (Aguilar *et al*., 2005), Zimbabwe (Aguilar *et al*., 2009) and West Africa (Barry *et al*. 2018). Moreover, New *et al*. (2006) found a reduction in total precipitation, but daily rainfall intensity significantly increased for South and West Africa. Our study detected a shift in the magnitude of precipitation (i.e., a decrease in the number of precipitation events causes a reduction in the amount of rainfall) which was more tangible in the 2000–2018 period of intensified drying (in agreement with more than 60% of stations). This period was prone to extreme drought events (i.e., intensity greater than 2). Their magnitude and duration increased from 1950 to 2018. This result was ascertained by Kogan and Guo (2016), and Masih *et al*. (2014) noted severe and extreme drought events in the 21st century globally and in Africa, respectively. A

fact that may be related to the long drought in Australia called the 'Big dry' (Ummenhofer *et al*., 2009 and Heberger, 2012) which ran from 1997 to 2010.

Madagascar houses endemic fauna and flora (Goodman and Benstead, 2005; Raven *et al*., 2020), and such changes in temperature and precipitation threaten this biodiversity. For instance, Raxworthy *et al*. (2008) observed an upslope displacement of 30 species in the Tsaratanana Massif in northern Madagascar due to warming trends. Moreover, we showed that, if drought magnitude and duration increased, then the effects of drought could be seen in the environmental system, as pointed out by Vicente-Serrano *et al*. (2020). For instance, Sato *et al*. (2014) observed that lemurs altered their diets to cope with environmental stress due to changes in temperature and rainfall patterns. In addition, these changes affect socioeconomic sectors in Madagascar. Harvey *et al*. (2014) indicated the effects of climate change for smallholder farmers and Nematchoua (2019) outlined the increasing demand for cooling energy. Our findings contribute to implementing adaptation and mitigation strategies to cope with such threats in Madagascar. For instance, articles on climate change adaptation (e.g., Hannah *et al*., 2008; Busch *et al*., 2012) and on climate change mitigation (e.g., Nogueira *et al*., 2020) may be updated.

This paper reveals new features in changes (e.g., appearance of very extreme cold nights and warm days, a shift in precipitation magnitude and ever-increasing consecutive drought events) in the climate of Madagascar. The next step in this research is to delve further into an analysis of the findings by continuous improvement in the data set through Data Rescue (DARE) and homogenization, in order to reduce uncertainty (Skrynyk *et al*., 2021). For example, elements (e.g., solar radiation, wind speed, etc.) should be added to use a more robust estimation of reference evapotranspiration (Beguería *et al*., 2014). Future key questions are: are model outputs from CMIP5, CMIP6 or CORDEX consistent with our observational trends? And do our observational trends relate to certain atmospheric mechanisms?

6 | CONCLUSION

This paper used state-of-the-art daily data quality control and homogenization processes to guarantee robustness in climate data records before assessing climate trends. It also gave a broader range of climate indices to update knowledge on climate change in Madagascar. Our findings were most significant at 0.05 level for temperature indices at regional and station level. The temporal evolution of our regional temperature indices followed the warming. At station level, all stations (100%) indicated significant positive trends for means of annual temperatures and 74% presented negative DTR trends. For temperature extremes, night-time indices were higher than daytime indicators. Most precipitation indices had negative trends, and total precipitation (PRCPTOT) decreased (significant at 0.05 level) for regions, but at station level significant negative trends were 29.6 and 7.4%, and non-significant ones were 55.6 and 63.0% from 1950 to 2018 and 2000 to 2018, respectively. Regional time series also showed a shift in precipitation magnitude, which caused intensified drying after 2000 for all indicators. Drought indices highlighted an increased number of drought events after the 1980s.

ACKNOWLEDGEMENTS

This study could not have been carried out without financial support from the INDECIS project, which is a part of ERA4CS, an ERA-NET initiated by JPI Climate, and funded by FORMAS (SE), DLR (DE), BMWFW (AT), IFD (DK), MINECO (ES), ANR (FR) with co-funding by the European Union (Grant 690462), and without the climate data from the Directorate General of Meteorology (DGM) of Madagascar. The authors thank anonymous reviewers for their in-depth reading of the manuscript and the valuable comments and suggestions they have made.

AUTHOR CONTRIBUTIONS

Enric Aguilar: Conceptualization; formal analysis; funding acquisition; methodology; project administration; resources; software; supervision; validation; writing-original draft; writing-review & editing. **Oleg Skrynyk:** Data curation; methodology; resources; software; validation; writing-review & editing. **Sergio Vicente-Serrano:** Methodology; resources; software; validation; writing-review & editing. **F Dominguez-Castro:** Resources; software; validation; writing-review & editing.

ORCID

Luc Yannick Andréas Randriamarolaza https://orcid.org/0000-0002-2939-2250
Enric Aguilar https://orcid.org/0000-0002-8384-377X
Oleg Skrynyk https://orcid.org/0000-0001-8827-0280
Sergio M. Vicente-Serrano https://orcid.org/0000-0003-2892-518X
Fernando Domínguez-Castro https://orcid.org/0000-0003-3085-7040

REFERENCES

Abatan, A.A., Abiodun, B.J., Lawal, K.A. and Gutowski, W.J. (2016) Trends in extreme temperature over Nigeria from percentile-based threshold indices. *International Journal of Climatology*, 36(6), 2527–2540. https://doi.org/10.1002/joc.4510.

Abrha, H. and Hagos, H. (2019) Future drought and aridity monitoring using multi-model approach under climate change in Hintalo Wejerat district, Ethiopia. *Sustainable Water Resources Management*, 5(4), 1963–1972. https://doi.org/10.1007/s40899-019-00350-1.

Aguilar, E., Auer, I., Brunet, M., Peterson, T.C. and Wieringa, J. (2003) *WMO Guidelines on Climate Metadata and Homogenization. WCDMP no.53, WMO-TD No. 1186*. Geneva, Switzerland: WMO.

Aguilar, E., Aziz Barry, A., Brunet, M., Ekang, L., Fernandes, A., Massoukina, M., Mbah, J., Mhanda, A., do Nascimento, D.J., Peterson, T.C., Thamba Umba, O., Tomou, M. and Zhang, X. (2009) Changes in temperature and precipitation extremes in western Central Africa, Guinea Conakry, and Zimbabwe, 1955-2006. *Journal of Geophysical Research-Atmospheres*, 114 (2), D02115. https://doi.org/10.1029/2008JD011010.

Aguilar, E., Peterson, T.C., Ramírez Obando, P., Frutos, R., Retana, J.A., Solera, M., Soley, J., González García, I., Araujo, R.M., Rosa Santos, A., Valle, V.E., Brunet, M., Aguilar, L., Álvarez, L., Bautista, M., Castañón, C., Herrera, L., Ruano, E., Sinay, J.J., Sánchez, E., Hernández Oviedo, G.I., Obed, F., Salgado, J.E., Vázquez, J.L., Baca, M., Gutiérrez, M., Centella, C., Espinosa, J., Martínez, D., Olmedo, B., Ojeda Espinoza, C.E., Núñez, R., Haylock, M., Benavides, H. and Mayorga, R. (2005) Changes in precipitation and temperature extremes in Central America and northern South America, 1961-2003. *Journal of Geophysical Research-Atmospheres*, 110 (23), D23107. https://doi.org/10.1029/2005JD006119.

Alexander, L.V., Zhang, X., Peterson, T.C., Caesar, J., Gleason, B., Klein Tank, A.M.G., Haylock, M., Collins, D., Trewin, B., Rahimzadeh, F., Tagipour, A., Rupa Kumar, K., Revadekar, J., Griffiths, G., Vincent, L., Stephenson, D.B., Burn, J., Aguilar, E., Brunet, M., Taylor, M., New, M., Zhai, P., Rusticucci, M. and Vazquez-Aguirre, L. (2006) Global observed changes in daily climate extremes of temperature and precipitation. *Journal of Geophysical Research-Atmospheres*, 111(5), D05109. https://doi.org/10.1029/2005JD006290.

Alexandersson, H. (1986) A homogeneity test applied to precipitation data. *Journal of Climatology*, 6(6), 661–675. https://doi.org/10.1002/joc.3370060607.

Alexandersson, H. and Moberg, A. (1997) Homogenization of Swedish temperature data. Part I: homogeneity test for linear trends. *International Journal of Climatology*, 17(1), 25–34. https://doi.org/10.1002/(SICI)1097-0088(199701)17:1<25::AID-JOC103>3.0.CO;2-J.

Barimalala, R., Blamey, R.C., Desbiolles, F. and Reason, C.J.C. (2020) Variability in the Mozambique Channel trough and impacts on southeast African rainfall. *Journal of Climate*, 33(2), 749–765. https://doi.org/10.1175/JCLI-D-19-0267.1.

Barry, A.A., Caesar, J., Klein Tank, A.M.G., Aguilar, E., McSweeney, C., Cyrille, A.M., Nikiema, M.P., Narcisse, K.B., Sima, F., Stafford, G., Touray, L.M., Ayilari-Naa, J.A., Mendes, C.L., Tounkara, M., Gar-Glahn, E.V.S., Coulibaly, M. S., Dieh, M.F., Mouhaimouni, M., Oyegade, J., Sambou, E. and Laogbessi, E.T. (2018) West Africa climate extremes and climate change indices. *International Journal of Climatology*, 38, e921–e938. https://doi.org/10.1002/joc.5420.

Beguería, S., Vicente-Serrano, S.M., Reig, F. and Latorre, B. (2014) Standardized precipitation evapotranspiration index (SPEI) revisited: parameter fitting, evapotranspiration models, tools, datasets and drought monitoring. *International Journal of Climatology*, 34(10), 3001–3023. https://doi.org/10.1002/joc.3887.

Besselaar, E.J.M., Klein Tank, A.M.G., Schrier, G. and Jones, P.D. (2012) Synoptic messages to extend climate data records. *Journal of Geophysical Research. Atmospheres*, 117(7), D07101. https://doi.org/10.1029/2011JD016687.

Bronaugh, D. and Werner, A. (2019) zyp: Zhang+Yue-Pilon Trends Package. R package version 0.10–1.1 Available at: https://cran.r-project.org/web/packages/zyp/index.html [Accessed 25th January 2019]

Busch, J., Dave, R., Hannah, L., Cameron, A., Rasolohery, A., Roehrdanz, P. and Schatz, G. (2012) Climate change and the cost of conserving species in Madagascar. *Conservation Biology*, 26(3), 1–48. https://doi.org/10.1111/j.1523-1739.2012.01838.x.

Byrd, K.B., Lorenz, A.A., Anderson, J.A., Wallace, C.S.A., Moore-O'Leary, K.A., Isola, J., Ortega, R. and Reiter, M.E. (2020) Quantifying drought's influence on moist soil seed vegetation in California's Central Valley through remote sensing. *Ecological Applications*, 30, e02153. https://doi.org/10.1002/eap.2153.

Domínguez-Castro, F., Reig, F., Vicente-Serrano, S.M., Aguilar, E., Peña-Angulo, D., Noguera, I., Revuelto, J., van der Schrier, G. and El Kenawy, A.M. (2020) A multidecadal assessment of climate indices over Europe. *Scientific Data*, 7(1), 125. https://doi.org/10.1038/s41597-020-0464-0.

Domínguez-Castro, F., Vicente-Serrano, S.M., Tomás-Burguera, M., Peña-Gallardo, M., Beguería, S., El Kenawy, A., Luna, Y. and Morata, A. (2019) High-spatial-resolution probability maps of drought duration and magnitude across Spain. *Natural Hazards and Earth System Sciences*, 19(3), 611–628. https://doi.org/10.5194/nhess-19-611-2019.

Donque, G. (1972) The climatology of Madagascar. In: Battistini, R. and Richard-Vindard, G. (Eds.) *Biogeography and Ecology in Madagascar. Monographiae Biologicae*, Vol. 21. Dordrecht: Springer. https://doi.org/10.1007/978-94-015-7159-3_3.

Dunn, R.J.H., Alexander, L.V., Donat, M.G., Zhang, X., Bador, M., Herold, N., Lippmann, T., Allan, R., Aguilar, E., Barry, A.A., Brunet, M., Caesar, J., Chagnaud, G., Cheng, V., Cinco, T., Durre, I., de Guzman, R., Htay, T.M., Ibadullah, W.M.W., Ibrahim, M.K.I.B., Khoshkam, M., Kruger, A., Kubota, H., Leng, T.W., Lim, G., Li-Sha, L., Marengo, J., Mbatha, S., McGree, S., Menne, M., de los Milagros Skansi, M., Ngwenya, S., Nkrumah, F., Oonariya, C., Pabon-Caicedo, J.D., Panthou, G., Pham, C., Rahimzadeh, F., Ramos, A., Salgado, E., Salinger, J., Sané, Y., Sopaheluwakan, A., Srivastava, A., Sun, Y., Timbal, B., Trachow, N., Trewin, B., van der Schrier, G., Vazquez-Aguirre, J., Vasquez, R., Villarroel, C., Vincent, L., Vischel, T., Vose, R. and Yussof, M.N.A.B.H. (2020) Development of an updated global land in-situ-based dataset of temperature and precipitation extremes: HadEX3. *Journal of Geophysical Research. Atmospheres*, 125, e2019JD032263. https://doi.org/10.1029/2019JD032263.

Easterling, D.R., Alexander, L.V., Mokssit, A. and Detemmerman, V. (2003) CCI/CLIVAR workshop to develop priority climate indices. *Bulletin of the American Meteorological Society*, 84(10), 1403–1407. https://doi.org/10.1175/BAMS-84-10-1403.

Goodman, S.M. and Benstead, J.P. (2005) Updated estimates of biotic diversity and endemism for Madagascar. *Oryx*, 39(1), 73–77. https://doi.org/10.1017/S0030605305000128.

Guijarro, J.A. (2018) Homogenization of climatic series with Climatol. Version 3.1.1. Guide.

Guijarro, J.A, Aguilar, E., Caloiero, T., Coscarelli, R., Curley, M. and Pérez-Zanón N (2018): Homogenization of daily Essential Climatic Variables with Climatol 3.1 within the INDECIS project. EMS Annual Meeting (Budapest, 3–7 September)

Guijarro, J.A, Aguilar, E., Sigró, J., Stépanek, P., Venema, V. and Zahradnícek, P. (2019): Benchmarking results of the homogenization of daily Essential Climatic Variables within the INDECIS project. Oral at EGU General Assembly (Viena, 7–12 April)

Hannah, L., Dave, R., Lowry, P.P., Andelman, S., Andrianarisata, M., Andriamaro, L., Cameron, A., Hijmans, R., Kremen, C., MacKinnon, J., Randrianasolo, H.H., Andriambololonera, S., Razafimpahanana, A., Randriamahazo, H., Randrianarisoa, J., Razafinjatovo, P., Raxworthy, C., Schatz, G.E., Tadross, M. and Wilmé, L. (2008) Climate change adaptation for conservation in Madagascar. *Biology Letters*, 4(5), 590–594. https://doi.org/10.1098/rsbl.2008.0270.

Hargreaves, G.H. (1994) Defining and using reference evapotranspiration. *Journal of Irrigation and Drainage Engineering*, 120(6), 1132–1139. http://doi.org/10.1061/(ASCE)0733-9437(1994)120:6(1132).

Harvey, C.A., Rakotobe, Z.L., Rao, N.S., Dave, R., Razafimahatratra, H., Rabarijohn, R.H., Rajaofara, H. and MacKinnon, J.L. (2014) Extreme vulnerability of smallholder farmers to agricultural risks and climate change in Madagascar. *Philosophical Transactions of the Royal Society, B: Biological Sciences*, 369(1639), 20130089. https://doi.org/10.1098/rstb.2013.0089.

Heberger, M. (2012) Australia's millennium drought: impacts and responses. In: Gleick, P.H. (Ed.) *The World's Water Volume 7: The Biennial Report on Freshwater 97 © 2012 Pacific Institute for Studies in Development, Environment, and Security Resources*. Island Press, Washington, DC: The World's Water. https://doi.org/10.5822/978-1-59726-228-6_5.

Hoegh-Guldberg, O., Jacob, D., Taylor, M., Bindi, M., Brown, S., Camilloni, I., Diedhiou, A., Djalante, R., Ebi, K.L., Engelbrecht, F., Guiot, J., Hijioka, Y., Mehrotra, S., Payne, A., Seneviratne, S.I., Thomas, A., Warren, R. and Zhou, G. (2018) Impacts of 1.5°C global warming on natural and human systems. In: Masson-Delmotte, V., Zhai, P., Pörtner, H.-O., Roberts, D., Skea, J., Shukla, P.R., Pirani, A., Moufouma-Okia, W., Péan, C., Pidcock, R., Connors, S., Matthews, J.B.R., Chen, Y., Zhou, X., Gomis, M.I., Lonnoy, E., Maycock, T., Tignor, M. and Waterfield, T. (Eds.) Available at*Global Warming of 1.5°C. An IPCC Special Report on the Impacts of Global Warming of 1.5°C above Pre-Industrial Levels and Related Global Greenhouse Gas Emission Pathways, in the Context of Strengthening the Global Response to the Threat of Climate Change, Sustainable Development, and Efforts to Eradicate Poverty*. Geneva, Switzerland: World Meteorological Organization Technical Document, https://www.ipcc.ch/sr15 [Accessed May 25, 2020].

Hunziker, S., Gubler, S., Calle, J., Moreno, I., Andrade, M., Velarde, F., Ticona, L., Carrasco, G., Castellón, Y., Oria, C., Croci-Maspoli, M., Konzelmann, T., Rohrer, M. and Brönnimann, S. (2017) Identifying, attributing, and overcoming common data quality issues of manned station observations. *International Journal of Climatology*, 37(11), 4131–4145. https://doi.org/10.1002/joc.5037.

Jarvis, A, Reuter, H.I. Nelson, A. and Guevara, E. (2008) Hole-filled SRTM for the Globe Version 4, from the CGIAR-CSI SRTM 90m Database. Available at: http://srtm.csi.cgiar.org. [Accessed April 20, 2020].

Jessica, M.B., Subrahmanyam, B., Nyadjro, E.S. and Murty, V.S.N. (2016) Tropical cyclone activity over the southwest tropical Indian Ocean. *Journal of Geophysical Research, Oceans*, 121(9), 6762–6778. https://doi.org/10.1002/2016JC011992.

Jury, M.R., Parker, B. and Waliser, D. (1994) Evolution and variability of the ITCZ in the SW Indian Ocean: 1988-90. *Theoretical and Applied Climatology*, 48(4), 187–194. https://doi.org/10.1007/BF00867048.

Keshtgar, B., Alizadeh-Choobari, O. and Irannejad, P. (2020) Seasonal and interannual variations of the Intertropical convergence zone over the Indian Ocean based on an energetic perspective. *Climate Dynamics*, 54(7–8), 3627–3639. https://doi.org/10.1007/s00382-020-05195-5.

Kogan, F. and Guo, W. (2016) Early twenty-first-century droughts during the warmest climate. *Geomatics, Natural Hazards and Risk*, 7(1), 127–137. https://doi.org/10.1080/19475705.2013.878399.

Kruger, A.C. and Nxumalo, M. (2017) Surface temperature trends from homogenized time series in South Africa: 1931–2015. *International Journal of Climatology*, 37(5), 2364–2377. https://doi.org/10.1002/joc.4851.

Leroux, M.D., Meister, J., Mekies, D., Dorla, A.L. and Caroff, P. (2018) A climatology of Southwest Indian Ocean tropical systems: their number, tracks, impacts, sizes, empirical maximum potential intensity, and intensity changes. *Journal of Applied Meteorology and Climatology*, 57(4), 1021–1041. https://doi.org/10.1175/JAMC-D-17-0094.1.

Macron, C., Richard, Y., Garot, T., Bessafi, M., Pohl, B., Ratiarison, A. and Razafindrabe, A. (2016) Intraseasonal rainfall variability over Madagascar. *Monthly Weather Review*, 144(5), 1877–1885. https://doi.org/10.1175/MWR-D-15-0077.1.

Masih, I., Maskey, S., Mussá, F.E.F. and Trambauer, P. (2014) A review of droughts on the African continent: a geospatial and long-term perspective. *Hydrology and Earth System Sciences*, 18(9), 3635–3649. https://doi.org/10.5194/hess-18-3635-2014.

Matyas, C.J. (2015) Tropical cyclone formation and motion in the Mozambique Channel. *International Journal of Climatology*, 35(3), 375–390. https://doi.org/10.1002/joc.3985.

Mestre, O., Domonkos, P., Picard, F., Auer, I., Robin, S., Lebarbier, E., Böhm, R., Aguilar, E., Guijarro, J., Vertachnik, G., Klancar, M., Dubuisson, B. and Stepanek, P. (2013) HOMER: a homogenization software – methods and applications. *IDOJARAS - Quarterly Journal of the Hungarian Meteorological Service*, 117(1), 47–67.

Moberg, A. and Alexandersson, H. (1997) Homogenization of Swedish temperature data. Part II: homogenized gridded air temperature compared with a subset of global gridded air temperature since 1861. *International Journal of Climatology*, 17, 35–54. https://doi.org/10.1002/(SICI)1097-0088(199701)17:1<35::AID-JOC104>3.0.CO;2-F.

Morid, S., Smakhtin, V. and Moghaddasi, M. (2006) Comparison of seven meteorological indices for drought monitoring in Iran. *International Journal of Climatology*, 26(7), 971–985. https://doi.org/10.1002/joc.1264.

Nematchoua, M.K. (2019) A study of climate change and energy consumption in Madagascar Island. *Health and Environment*, 1 (1), 9–27. https://doi.org/10.25082/he.2019.01.002.

Nematchoua, M.K., Ricciardi, P., Orosa, J.A. and Buratti, C. (2018) A detailed study of climate change and some vulnerabilities in Indian Ocean: a case of Madagascar Island. *Sustainable Cities and Society*, 41, 886–898. https://doi.org/10.1016/j.scs.2018.05.040.

New, M., Hewitson, B., Stephenson, D.B., Tsiga, A., Kruger, A., Manhique, A., Gomez, B., Coelho, C.A.S., Masisi, D.N., Kululanga, E., Mbambalala, E., Adesina, F., Saleh, H., Kanyanga, J., Adosi, J., Bulane, L., Fortunata, L., Mdoka, M.L. and Lajoie, R. (2006) Evidence of trends in daily climate extremes over southern and West Africa. *Journal of Geophysical Research-Atmospheres*, 111(14), 1–11. https://doi.org/10.1029/2005JD006289.

Niang, I., Ruppel, O.C., Abdrabo, M.A., Essel, A., Lennard, C., Padgham, J. and Urquhart, P. (2015) Africa. In: Barros, V.R., Field, C.B., Dokken, D.J., Mastrandrea, M.D., Mach, K.J., Bilir, T.E., Chatterjee, M., Ebi, K.L., Estrada, Y.O., Genova, R. C., Girma, B., Kissel, E.S., Levy, A.N., MacCracken, S., Mastrandrea, P.R. and White, L.L. (Eds.) *Climate Change 2014: Impacts, Adaptation and Vulnerability: Part B: Regional Aspects: Working Group II Contribution to the Fifth Assessment Report of the Intergovernmental Panel on Climate Change*. Cam: Cambridge University Press, pp. 1199–1266. https://doi.org/10.1017/CBO9781107415386.002.

Nogueira, L.P., Longa, F.D. and van der Zwaan, B. (2020) A cross-sectoral integrated assessment of alternatives for climate mitigation in Madagascar. *Climate Policy*, 20, 1257–1273. https://doi.org/10.1080/14693062.2020.1791030.

Pérez-Zanón, N., Sigró, J., Aguilar, E., Guijarro, J.A., van der Schrier, G., Stepanek, P., Zahradnicek, P., Coscarelli, R., Engström, E., Curley, M., Caloiero, T., Lledó, L., Ramon, J., Valente, M.A. and Carvalho, S. (2018): First steps towards a benchmarking experiment in quality control and homogenization of observed data. EMS Annual Meeting (Budapest, 3-7 September)

Peterson, T.C., Easterling, D.R., Karl, T.R., Groisman, P., Nicholls, N., Plummer, N., Torok, S., Auer, I., Boehm, R., Gullett, D., Vincent, L., Heino, R., Tuomenvirta, H., Mestre, O., Szentimrey, T., Salinger, J., Førland, E.J., Hanssen-Bauer, I., Alexandersson, H., Jones, P. and Parker, D. (1998) Homogeneity adjustments of *in situ* atmospheric climate data: a review. *International Journal of Climatology*, 18(13), 1493–1517. https://doi.org/10.1002/(SICI)1097-0088(19981115)18:13<1493::AID-JOC329>3.0.CO;2-T.

Randriamahefasoa, T.S.M. and Reason, C.J.C. (2017) Interannual variability of rainfall characteristics over southwestern Madagascar. *Theoretical and Applied Climatology*, 128(1–2), 421–437. https://doi.org/10.1007/s00704-015-1719-0.

Ratna, S.B., Behera, S., Ratnam, J.V., Takahashi, K. and Yamagata, T. (2013) An index for tropical temperate troughs over southern Africa. *Climate Dynamics*, 41(2), 421–441. https://doi.org/10.1007/s00382-012-1540-8.

Raven, P.H., Gereau, R.E., Phillipson, P.B., Chatelain, C., Jenkins, C.N. and Ulloa, C.U. (2020) The distribution of biodiversity richness in the tropics. *Science Advances*, 6(37), eabc6228. https://doi.org/10.1126/sciadv.abc6228.

Raxworthy, C.J., Pearson, R.G., Rabibisoa, N., Rakotondrazafy, A. M., Ramanamanjato, J.B., Raselimanana, A.P., Wu, S., Nussbaum, R.A. and Stone, D.A. (2008) Extinction vulnerability of tropical montane endemism from warming and upslope displacement: a preliminary appraisal for the highest massif in Madagascar. *Global Change Biology*, 14(8), 1703–1720. https://doi.org/10.1111/j.1365-2486.2008.01596.x.

Sato, H., Ichino, S. and Hanya, G. (2014) Dietary modification by common brown lemurs (*Eulemur fulvus*) during seasonal drought conditions in western Madagascar. *Primates*, 55(2), 219–230. https://doi.org/10.1007/s10329-013-0392-0.

Sen, P.K. (1968) Estimates of the regression coefficient based on Kendall's tau. *Journal of the American Statistical Association*, 63 (324), 1379–1389. https://doi.org/10.1080/01621459.1968.10480934.

Skrynyk, O., Aguilar, E., Guijarro, J., Randriamarolaza, L.Y.A. and Bubin, S. (2021) Uncertainty evaluation of Climatol's adjustment algorithm applied to daily air temperature time series. *International Journal of Climatology*, 41(Suppl. 1), E2395–E2419. https://doi.org/10.1002/joc.6854.

Squintu, A.A., van der Schrier, G., Štěpánek, P., Zahradníček, P. and Tank, A.K. (2020) Comparison of homogenization methods for daily temperature series against an observation-based benchmark dataset. *Theoretical and Applied Climatology*, 140 (1–2), 285–301. https://doi.org/10.1007/s00704-019-03018-0.

Tadross, M., Randriamarolaza, L., Rabefitia, Z. and Yip, Z.K. (2008) *Climate Change in Madagascar: Recent, Past and Future*. Washington, DC: World Bank.

Tara James, C. and Stacia, Y. (2014) Climate change adaptation in the Southwest Indian Ocean: case study of the perception of risk, common coping strategies and the potential for micro-insurance. *Journal of Geography & Natural Disasters*, 04 (02), 2–9. https://doi.org/10.4172/2167-0587.1000129.

Trewin, B. (2010) Exposure, instrumentation, and observing practice effects on land temperature measurements. *WIREs Climate Change*, 1(4), 490–506. https://doi.org/10.1002/wcc.46.

Ummenhofer, C.C., England, M.H., Mclntosh, P.C., Meyers, G.A., Pook, M.J., Risbey, J.S., Gupta, A.S. and Taschetto, A.S. (2009) What causes Southeast Australia's worst droughts? *Geophysical Research Letters*, 36(4), L04706. https://doi.org/10.1029/2008GL036801.

Venema, V., Mestre, O., Aguilar, E., Auer, I., Guijarro, J.A., Domonkos, P., Vertacnik, G., Szentimrey, T., Stepanek, P., Zahradnicek, P., Viarre, J., Muller-Westermeier, G., Lakatos, M., Williams, C.N., Menne, M., Lindau, R., Rasol, D., Rustemeier, E., Kolokythas, K., Marinova, T., Andresen, L., Acquaotta, F., Fratianni, S., Cheval, S., Klancar, M., Brunetti, M., Gruber, C., Duran, M.P., Likso, T., Esteban, P. and Brandsma, T. (2012) Benchmarking monthly homogenization algorithms. *Climate of the Past*, 8, 89–115. https://doi.org/10.5194/cp-8-89-2012.

Vicente-Serrano, S.M., Beguería, S. and López-Moreno, J.I. (2010) A multiscalar drought index sensitive to global warming: the standardized precipitation evapotranspiration index. *Journal of Climate*, 23(7), 1696–1718. https://doi.org/10.1175/2009JCLI2909.1.

Vicente-Serrano, S.M., Quiring, S.M., Peña-Gallardo, M., Yuan, S. and Domínguez-Castro, F. (2020) A review of environmental droughts: increased risk under global warming? *Earth-Science Reviews*, 201, 102953. https://doi.org/10.1016/j.earscirev.2019.102953.

Vincent, L.A., Aguilar, E., Saindou, M., Hassane, A.F., Jumaux, G., Roy, D., Booneeady, P., Virasmi, R.,

Randriamarolaza, L.Y.A., Faniriantsoa, F.R., Amelie, V., Seeward, H. and Montfraix, B. (2011) Observed trends in indices of daily and extreme temperature and precipitation for the countries of the western Indian Ocean, 1961-2008. *Journal of Geophysical Research-Atmospheres*, 116(10), 1–12. https://doi.org/10.1029/2010JD015303.

Vincent, L.A., Zhang, X., Bonsal, B.R. and Hogg, W.D. (2002) Homogenization of daily temperatures over Canada. *Journal of Climate*, 15(11), 1322–1334. https://doi.org/10.1175/1520-0442(2002)015<1322:HODTOC>2.0.CO;2.

Whan, K., Alexander, L.V., Imielska, A., Mcgree, S., Jones, D., Ene, E., Finaulahi, S., Inape, K., Jacklick, L., Kumar, R., Laurent, V., Malala, H., Malsale, P., Pulehetoa-Mitiepo, R., Ngemaes, M., Peltier, A., Porteous, A., Seuseu, S., Skilling, E., Tahani, L., Toorua, U. and Vaiimene, M. (2014) Trends and variability of temperature extremes in the tropical Western Pacific. *International Journal of Climatology*, 34(8), 2585–2603. https://doi.org/10.1002/joc.3861.

World Meteorological Organization (WMO), 2020: Guidelines on Homogenization (WMO-No. 1245). Geneva.

Xu, W., Li, Q., Wang, X.L., Yang, S., Cao, L. and Feng, Y. (2013) Homogenization of Chinese daily surface air temperatures and analysis of trends in the extreme temperature indices. *Journal of Geophysical Research-Atmospheres*, 118(17), 9708–9720. https://doi.org/10.1002/jgrd.50791.

Yosef, Y., Aguilar, E. and Alpert, P. (2019) Changes in extreme temperature and precipitation indices: using an innovative daily homogenized database in Israel. *International Journal of Climatology*, 39(13), 5022–5045. https://doi.org/10.1002/joc.6125.

Yosef, Y., Aguilar, E. and Alpert, P. (2021) Is it possible to fit extreme climate change indices together seamlessly in the era of accelerated warming? *The International Journal of Climatology*, 41(S1), E952–E963. https://doi.org/10.1002/joc.6740.

Zhang, X., Alexander, L., Hegerl, G.C., Jones, P., Tank, A.K., Peterson, T.C., Trewin, B. and Zwiers, F.W. (2011) Indices for monitoring changes in extremes based on daily temperature and precipitation data. *WIREs Climate Change*, 2, 851–870. https://doi.org/10.1002/wcc.147.

Zhang, X., Vincent, L.A., Hogg, W.D. and Niitsoo, A. (2000) Temperature and precipitation trends in Canada during the 20th century. *Atmosphere-Ocean*, 38(3), 395–429. https://doi.org/10.1080/07055900.2000.9649654.

How to cite this article: Randriamarolaza, L. Y. A., Aguilar, E., Skrynyk, O., Vicente-Serrano, S. M., & Domínguez-Castro, F. (2021). Indices for daily temperature and precipitation in Madagascar, based on quality-controlled and homogenized data, 1950–2018. *International Journal of Climatology*, 1–24. https://doi.org/10.1002/joc.7243

CHAPTER 4 Extreme temperatures detection and attribution related to external forcing in Madagascar

Received: 6 May 2022 | Revised: 3 March 2023 | Accepted: 4 March 2023

DOI: 10.1002/joc.8065

RESEARCH ARTICLE

International Journal of Climatology RMetS

Extreme temperatures detection and attribution related to external forcing in Madagascar

Luc Yannick Andréas Randriamarolaza[1,2] | **Enric Aguilar**[1] | **Oleg Skrynyk**[3]

[1]Center for Climate Change (C3), Institut Universitari de Recerca en Sostenibilitat, Canvi Climàtic i Transició Energètica (IU-RESCAT), Universitat Rovira i Virgili, Tarragona, Spain

[2]Direction Générale de la Météorologie, Antananarivo, Madagascar

[3]Ukrainian Hydrometeorological Institute, Kyiv, Ukraine

Correspondence
Luc Yannick Andréas Randriamarolaza, Center for Climate Change (C3), Institut Universitari de Recerca en Sostenibilitat, Canvi Climàtic i Transició Energètica (IU-RESCAT), Universitat Rovira i Virgili, Tarragona 43480, Spain.
Email: lucyannickandreas.randriamarolaza@estudiants.urv.cat and luc.randriamarolaza@gmail.com

Funding information
FORMAS (SE), DLR (DE), BMWFW (AT), IFD (DK), MINECO (ES), ANR (FR), European Union, Grant/Award Number: 690462

Abstract

In this article, we use standard extreme temperature indices to detect and attribute external forcing in Madagascar. These indices are calculated from observations and multi-model ensemble mean responses on anthropogenic-plus-natural (ALL), greenhouse gases (GHG), natural (NAT) and anthropogenic (ANT) which are subtracted from ALL and NAT forcings over 1950–2018. Correlation analysis emphasizes that the observed changes are more influenced by ENSO events, especially in minimum temperature. The observed changes are regressed or combined with model simulations from the sixth phase of the Coupled Model Intercomparison Project (CMIP6) to assess human impacts in indices. CMIP6 models with ALL, GHG and ANT forcings correspond well with the observations for the frequency indices than the intensity indices. Moreover, decadal trends indicate the existence of anthropogenic warming according to observations and multi-model ensembles with ALL, GHG and ANT forcings. Detection and attribution parties identify and justify the causes of the observed changes. We do this by performing the single-signal and two-signal analysis using the Regularized Optimal Fingerprinting (ROF) method with Total Least Square (TLS) regression. We estimate internal climate variability by means of control model simulations. As a result, we note an inconsistency in the warming trend with the NAT forcing. The influence of ALL, GHG and ANT forcings is detectable for standard extreme temperature indices between 1950 and 2018. Nearly, observed changes are attributed to GHG and ANT forcings except for coldest night and warm nights in Madagascar.

KEYWORDS

attribution, detection, extreme temperature indices, fingerprint, Madagascar, model simulations

1 | INTRODUCTION

During the last decades, the scientific community has identified global and regional warming trends. In this regard, IPCC AR6 indicates that global temperatures now are 1.07°C warmer than those from the preindustrial times. In Madagascar, the yearly mean of the minimum and maximum temperatures increased by 0.24°C/decade

and 0.21°C/decade, respectively (Randriamarolaza et al., 2021). Many authors have attempted to attribute the detected trends to human activities, for example, Santer et al. (1996) or Bindoff et al. (2013). However, most of the studies in D&A analysis focus on mid-latitudes. Otto et al. (2015), Peterson et al. (2012) or Peterson et al. (2013), stressed the lack of studies to attribute extreme climate events in Africa. Furthermore, the African continent suffers from poor quality and scarcity of observational data (Otto et al., 2013, 2015) which can interfere with the development adequate D&A studies. Nonetheless, Otto et al. (2020) provided some suggestions to address these problems. Following their advice, the purpose of this article is to apply the D&A analysis on extreme temperature changes in Madagascar by using a rare quality controlled and homogenized observational dataset (Randriamarolaza et al., 2021). Namely, we seek to understand the influence of external forcing (anthropogenic and natural) and to identify their robustness separately on extreme temperature changes. We apply a standard regression-based optimal fingerprinting approach, similar to Sonali and Kumar (2020). It is noteworthy that variant approaches exist depending on the transformation of the variables. For instance, a standard approach is applied directly with the indices by Morak et al. (2011, 2013), Christidis and Stott (2016) and Dong et al. (2018). Variables are converted to probability-based indices in Zhang et al. (2013), Min et al. (2013) and Kim et al. (2016) or fit an extreme value distribution in Wang et al. (2020) before implementing a standard approach. Since the majority of studies use the standard approach directly with the indices, we adopt it to simplify and facilitate the comparison of results. The remainder of this article is organized as follows: Section 2 describes the data and methodology. Section 3 presents key findings. Finally, Section 4 sets out both the discussion and the conclusion.

2 | DATA AND METHODOLOGY

2.1 | Observational data

For this study, we used the observational dataset of Malagasy daily minimum and maximum air temperatures developed by Randriamarolaza et al. (2021). The dataset contains 26 synoptic weather stations in Madagascar (see Table 1), quality-controlled with the INQC package (available at https://CRAN.R-project.org/package=INQC) and homogenized with the Climatol (available at https://CRAN.R-project.org/package=climatol) software. Inhomogeneities were detected at the monthly scale before adjusting daily data by interpolating monthly factors. Skrynyk et al. (2021) analysed the effects of Climatol homogenization on daily data and found substantial improvements in the accuracy and reliability of the temperature indices trends. Indices calculation was performed with ClimInd (Domínguez-Castro et al., 2020). The indices are categorized as intensity and frequency (see Table 2). Their anomalies were derived by subtracting a corresponding average value calculated based on the WMO reference period 1961–1990, as in Vincent et al. (2011) and Randriamarolaza et al. (2021). Subsequently, the regional anomaly time series were computed as the average of the anomalies across all stations. Lastly, regional anomaly series were smoothed using a 5-year moving average.

2.2 | Sea surface temperature data

The monthly Extended Reconstructed Sea Surface Temperature, version 5 (ERSST V5), with a resolution of $2° \times 2°$ (Huang et al., 2017), was employed in our analysis in order to construct a time series of the El Niño Southern Oscillation Index (ENSO). Therefore, we delimited the ENSO region from 160° E to 80° W in longitude and from 5° S to 5° N in latitude. Sea surface temperature (SST) is averaged at all grid points of the ENSO region to obtain a single time series of monthly values. This time series is further used to compute the annual SST. The annual anomalies are then calculated according to the reference period 1961–1990. El Niño and La Niña events occur when SST anomalies are higher than 0.5°C and lower than −0.5°C, respectively (refer to Figure 1a). ENSO influence on the regional anomalies of the extreme temperature indices was analysed by using the Morlet wavelet function as in Torrence and Compo (1998) and Jevrejeva et al. (2003). Specifically, we used the wavelet coherence to measure the strength of the relationship between two time series as a function of frequency or period (see Section 2.4, for details). The performance of this method was highlighted by Torrence and Compo (1998), Yi and Shu (2012) and Liang et al. (2013). Figure 1b shows the wavelet power spectrum of the constructed ENSO index time series. ENSO events' cycle which is around 2–7 years can be clearly seen in the figure. The extreme ENSO events such as El Niño at 1982–1983 and 1997–1998 (also pointed out by Santoso et al., 2017) were captured by the wavelet transform.

2.3 | Model simulations data

Model simulation data sets on daily minimum and maximum temperatures, used to estimate the expected responses of the climate system to external forcings, were

TABLE 1 List of synoptic stations in Madagascar.

Stations	Longitude (°)	Latitude (°)	Elevation (m)	WMO numbers
Ambohitsilaozana	48.5	−17.7	786	67067
Analalava	47.8	−14.6	57	67019
Antalaha	50.3	−15.0	6	67025
Antananarivo	47.5	−18.9	1310	67085
Antsirabe	47.1	−19.9	1540	67107
Antsiranana	49.3	−12.4	105	67009
Antsohihy	48.0	−14.9	28	67020
Besalampy	44.5	−16.8	36	67037
Farafangana	47.8	−22.8	6	67157
Fianarantsoa	47.1	−21.5	1106	67137
Ivato	47.5	−18.8	1264	67083
Maevatanana	46.8	−17.0	77	67045
Mahajanga	46.4	−15.7	22	67027
Mahanoro	48.8	−19.8	5	67113
Maintirano	44.0	−18.1	25	67073
Mananjary	48.4	−21.2	6	67143
Morombe	43.4	−21.8	4	67131
Morondava	44.3	−20.3	8	67117
NosyBe	48.3	−13.3	11	67012
Ranohira	45.4	−22.6	823	67152
SainteMarie	49.8	−17.1	9	67072
Sambava	50.2	−14.3	5	67023
Taolagnaro	47.0	−25.0	8	67197
Toamasina	49.4	−18.1	6	67095
Toliary	43.7	−23.4	9	67161
Vohemar	50.0	−13.4	5	67017

TABLE 2 List of climate indices used in the study.

Category	Index	Indicator name	Definition	Unit
Intensity	TNn	Coldest night	annual minima of daily minimum temperature	°C
	TXn	Coldest day	annual minima of daily maximum temperature	°C
	TNx	Warmest night	annual maxima of daily minimum temperature	°C
	TXx	Warmest day	annual maxima of daily maximum temperature	°C
Frequency	TN10P	Cold nights	Percentage of days with Tmin <10th percentile	%
	TX10P	Warm nights	Percentage of days with Tmax <10th percentile	%
	TN90P	Cold days	Percentage of days with Tmin >90th percentile	%
	TX90P	Warm days	Percentage of days with Tmax >90th percentile	%
	TN1P	Very cold night	Count of days with Tmin <1st percentile	days
	TX99P	Very warm day	Count of days with Tmax >99th percentile	days

obtained from the Sixth Phase of the Coupled Model Inter-comparison Project (CMIP6) archive (available at https://esgf-node.llnl.gov/search/cmip6/, visited on December 9, 2020). CMIP6 historical model simulations differ depending on four elements: realization, initialization methods, perturbed physics and forcing. All

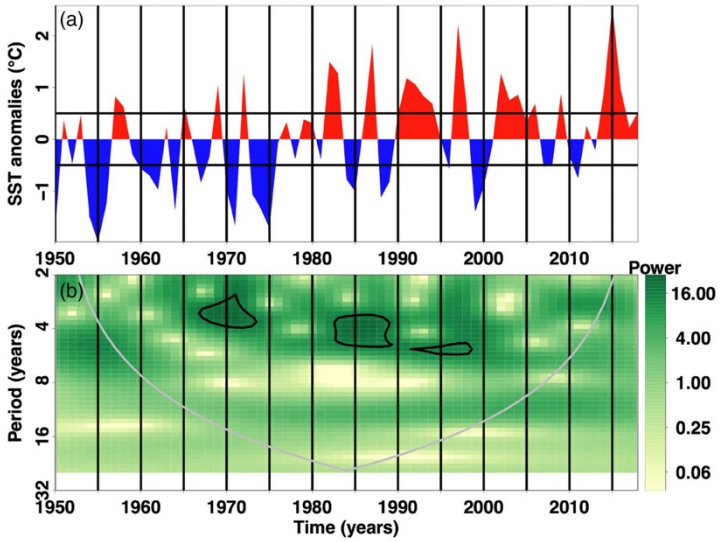

FIGURE 1 (a) Time series of ENSO index. (b) Wavelet power spectrum of ENSO index. The bold contours represent a significant area at level 0.05 against red noise. The cone of influence indicates where the effect of edge is important.

Minimum temperature					Maximum temperature			
Members	**ALL**	**GHG**	**NAT**	**CTL**	**ALL**	**GHG**	**NAT**	**CTL**
r1i1p1f1	4	8	8	12	5	4	4	11
r2i1p1f1	0	8	8	0	0	3	3	0
r3i1p1f1	3	8	8	0	3	4	4	0
r4i1p1f1	1	2	2	0	1	1	1	0
r5i1p1f1	1	2	2	0	1	1	1	0
r6i1p1f1	1	1	1	0	1	1	1	0
r7i1p1f1	1	1	1	0	1	1	1	0
r8i1p1f1	1	1	1	0	1	1	1	0
r9i1p1f1	1	1	1	0	1	1	1	0
r10i1p1f1	1	1	1	0	1	1	1	0
Total	14	33	33	12	15	18	18	11

TABLE 3 The number of model simulations per ensemble member.

historical model simulations with similar elements are grouped in an ensemble member. In our study, we choose 10 ensemble members with different realizations but similar initialization methods, perturbed physics and forcing.

Each ensemble member contained historical model simulations with anthropogenic-plus-natural (ALL), greenhouse gases (GHG) and natural (NAT) forcings. The GHG simulations represent climates with well-mixed greenhouse gases composed primarily of carbon dioxide, methane and nitrous oxide (Meinshausen et al., 2017). Table 3 shows that more than 50% of the runs were performed under the first three ensemble members. In addition, Table 4 illustrates that values of minimum and maximum temperatures were taken from 95 and 62 runs, respectively. These runs were produced using 19 models. However, only the ensemble member r1i1p1f1 had control or pre-industrial simulations (CTL runs). The most repeated model, which has more than 10% in all runs, is CanESM5 (Swart et al., 2019).

O'Neill et al. (2016) described the pathways of societal development, the Shared Socioeconomic Pathways (SSPs), as the future evolution of society with respective emissions scenarios used to drive climate models. Ssp245 is a central scenario in which trends continue their historical patterns without substantial deviations. The

TABLE 4 Numbers of model simulations for all ensemble members.

	Minimum temperature				Maximum temperature			
Models	**ALL**	**GHG**	**NAT**	**CTL**	**ALL**	**GHG**	**NAT**	**CTL**
ACCESS-CM2	0	0	0	1	0	0	0	1
ACCESS-ESM1-5	0	3	3	1	0	3	3	1
AWI-CM-1-1-MR	0	0	0	1	0	0	0	0
AWI-ESM-1-1-LR	0	0	0	1	0	0	0	1
BCC-CSM2-MR	0	3	3	0	1	2	2	0
CanESM5	8	10	10	0	8	10	10	0
CESM2	0	3	3	0	0	3	3	0
FIO-ESM-2-0	0	0	0	1	0	0	0	1
FGOALS-g3	2	3	3	0	3	0	0	0
HadGEM3-GC31-LL	0	0	0	1	0	0	0	1
MIROC6	1	3	3	0	1	0	0	0
MRI-ESM2-0	2	5	5	0	1	0	0	0
MPI-ESM-1-2-HAM	0	0	0	1	0	0	0	1
MPI-ESM1-2-HR	0	0	0	1	0	0	0	1
MPI-ESM1-2-LR	0	0	0	1	0	0	0	1
NESM3	1	0	0	0	1	0	0	0
NorES2-LM	0	3	3	1	0	0	0	1
NorESM2-MM	0	0	0	1	0	0	0	1
TaiESM1	0	0	0	1	0	0	0	1
Total	14	33	33	12	15	18	18	11

corresponding CMIP6 experiment ssp245 is considered as reference one in CMIP6-endorsed Model Intercomparison Projects (MIPs) and is employed to extend the historical simulation period beyond 2015 in detection and attribution MIP (O'Neill et al., 2016). For example, Gillett et al. (2016) used ssp245 to continue the historical simulation period to 2020. In our study, we selected model simulations that existed simultaneously in ssp245 and with ALL forcing for all members. As the historical simulation with ALL forcing period was only from 1850 to 2014 (Eyring et al., 2016), we extracted the time period over 1950–2014 then extended it from 2015 to 2018 by using ssp245. Thereafter, we uniformed their grid resolution to 1° by 1°.

A multi-model ensemble mean was built by averaging daily minimum and maximum temperature at each grid point of all model simulations and all members for each forcing, respectively. Therefore, regional time series were computed by averaging temperature over all grid points for multi-model ensemble mean with ALL, GHG and NAT. Thereafter, we computed annual indices by using ClimInd software for each grid point and regional time series. Annual index anomalies were calculated by taking WMO reference 1961–1990 as in the observational data. These steps were applied to all the considered runs (ALL, GHG, NAT and CTL). From these results, the anthropogenic (ANT) forcing was formed by subtracting ALL and NAT forcings. Therefore, ANT includes GHG and short-lived gases and aerosols. The CTL runs were split into two parts to create two independent estimations of internal variability, following Ribes et al. (2013). Finally, 5-year moving averages were calculated with regional average index anomaly time series for model simulations, CTL runs and multi-model ensemble means with ALL, GHG, ANT and NAT forcings.

2.4 | Methods

2.4.1 | Wavelet coherence

The wavelet analysis is often used to extract isolated and time-localized events (Lilly, 2017) or to analyse localized intermittent oscillation in time series. It also can be used to study the linkage between two time series (Grinsted et al., 2004). We use wavelet analysis, following the approach described in Torrence and Compo (1998), to assess the strength of relationship between observational intensity and frequency indices and ENSO index based on period or frequency. Torrence and Compo (1998)

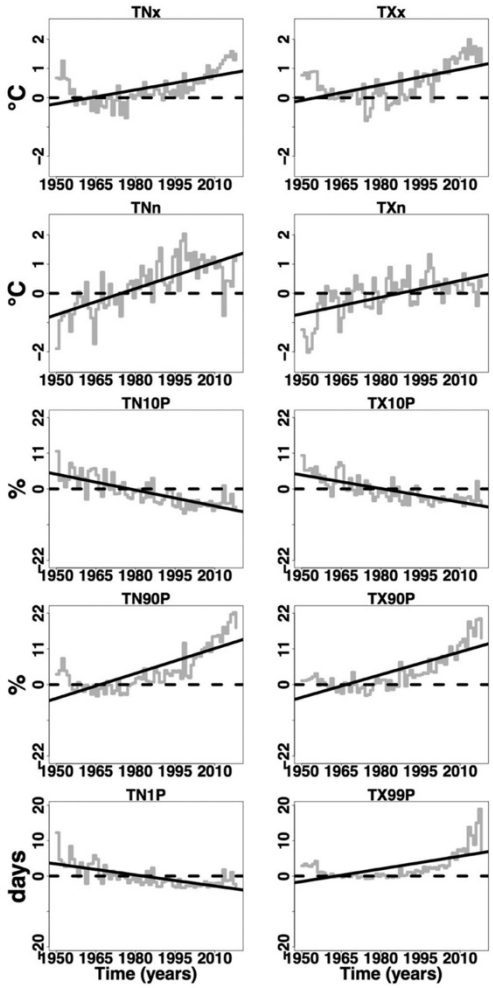

FIGURE 2 Regional average anomalies time series and the fitted trend lines for intensity and frequency indices over 1950–2018.

pointed out that the choice of a wavelet basis function was crucial, but it depended on the type of analysed data. The Morlet wavelet function is a complex sine-shaped Gaussian function, mostly employed with climate data, for example, by Yi and Shu (2012) and Ruwangika et al. (2020). We adopt it to derive the continuous wavelet transform of intensity and frequency indices' time series. Their significance correlation is assessed by using the wavelet coherence method. We use the R package 'biwavelet' (Tarik et al., 2018) to conduct this method.

2.4.2 | Trend calculation

We use trend analysis to quantify long-term changes over 1950–2018. As in Randriamarolaza et al. (2021), we use the Sen's slope method (Sen, 1968), implemented by Zhang et al. (2000) to calculate station-by-station and regional index trends and their confidence intervals. This approach is applied to observational time series, individual model simulations, CTL runs and multi-model ensemble mean with ALL, GHG, ANT and NAT forcings. The method is applied for each grid point to have spatial distribution of indices trends. The R package 'zyp', (Bronaugh & Werner, 2019), method, is used for calculation. This package has been employed in many articles such as Barry et al. (2018), Yosef et al. (2019, 2020) and Randriamarolaza et al. (2021). Besides, trends' sign comparison was done between multi-model ensemble mean and each model simulation. Then we filtered the grid points where 75% of model simulations under ALL, GHG, ANT and NAT forcings had the similar trends' sign and significant at 0.05 level than in multi-model ensemble mean under ALL forcing (see Figures 2 and 3).

2.4.3 | Standard optimal fingerprinting

The standard optimal fingerprinting method proposed by Allen and Tett (1999) and Allen and Stott (2003) with generalized linear regression Equation (1) is expressed as

$$Y=(X-\nu)\beta+\varepsilon, \quad (1)$$

where Y is observations, X is multi-model ensemble mean, ν is internal variability which is due to the interaction between atmosphere and ocean (Dima et al., 2005), β is scaling factor and ε is regression residual. It is used to quantify influences from external forcing. The amplitude of scaling factor measures presence or absence of signals in the observations. However, uncertainty arises mainly from quantification of internal climate variability of the climate system. Mostly, control simulations of climate models are used to assess the internal climate variability (Curry & Webster, 2011). Therefore, two independent noises from CTL runs are used to obtain the best estimate of scaling factors and their 5%–95% uncertainty levels (i.e., confidence intervals at 0.05 level) and to run the residual consistency check (RCC). RCC is performed to test the hypothesis if model simulation internal variability is consistent with observations. According to Stott et al. (2011), Dong et al. (2018) and Dileepkumar et al. (2018), if the best estimate of scaling factor and their uncertainty are greater than zero, we detect the influence of forcing. Besides, if the best estimate of scaling factor is

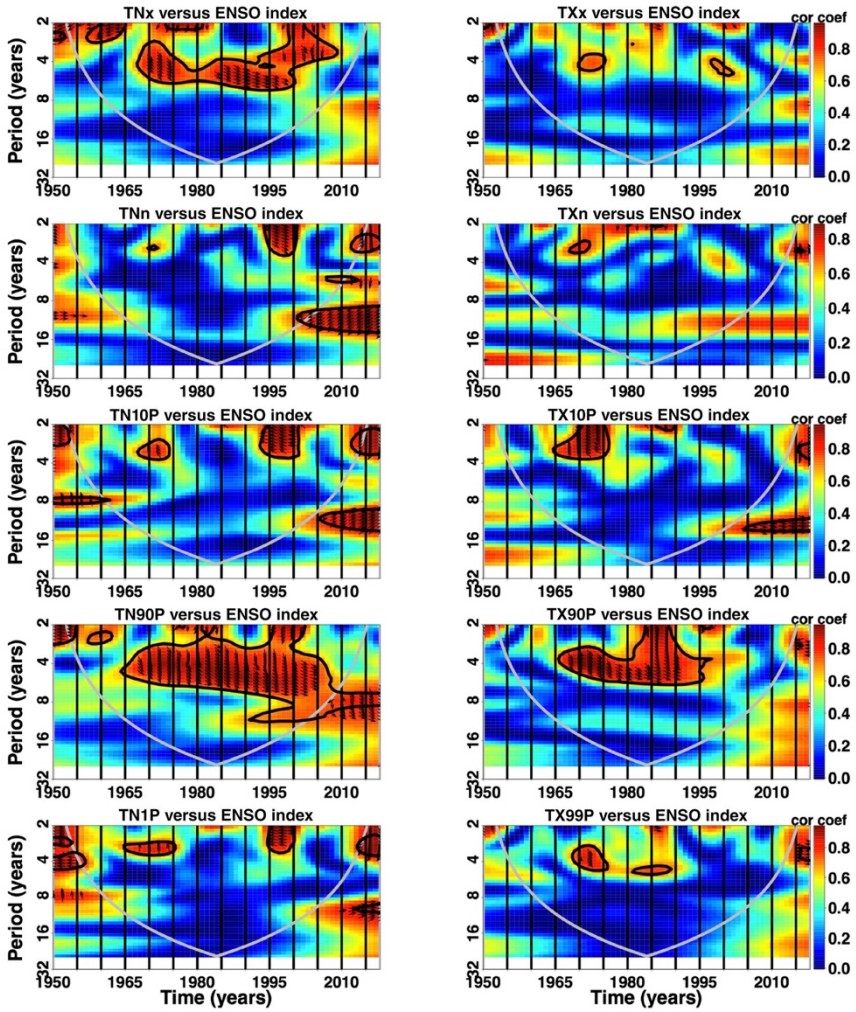

FIGURE 3 Wavelet coherence between intensity and frequency indices and ENSO events over 1950–2018. The bold contours represent a significant area at level 0.05 against red noises and right (left) arrows indicate if their direction is in phase (anti-phase). The cone of influence indicates where the effect of edge is important. Cor. coef. means correlation coefficient.

consistent with the unit (i.e., scaling factor uncertainty interval contains the unit), we attribute an observed change to this forcing.

Ribes et al. (2013) developed an alternative to the standard optimal fingerprinting method called ' Regularized Optimal Fingerprinting (ROF)'. ROF method avoids the use of a truncated Empirical Orthogonal Function (EOF) projection to estimate the scaling factor β in the Equation (1). This method was used by Ribes et al. (2013), Wan et al. (2014), Lo et al. (2016) and Dileepkumar et al. (2018). It is implemented in the R Package ECOF-V1, which stands for Environment Canada's Optimal Fingerprint coded by Feng Yang (https://www.wcrp-climate.org/ictp-2014-tutorials. Accessed August 2, 2020), adapting the original code used in Ribes et al. (2013). We carry out single-signal and two-signal analyses by using

TABLE 5 Regional trends with its confidence intervals (in brackets) in the observations (OBS) and multi-model ensemble mean responses on anthropogenic-plus-natural (ALL), greenhouse gases (GHG) forcings over 1950–2018

		Decadal trends (confidence interval)		
Index	**Units**	**OBS**	**ALL**	**GHG**
TNn	°C/10 years	**0.29** (0.19,0.39)	**0.15** (0.12;0.19)	**0.17** (0.16;0.20)
TXn	°C/10 years	**0.11** (0.00;0.22)	**0.16** (0.13;0.19)	**0.17** (0.15;0.19)
TNx	°C/10 years	**0.24** (0.11;0.36)	**0.20** (0.16;0.25)	**0.20** (0.18;0.21)
TXx	°C/10 years	**0.23** (0.07;0.36)	**0.21** (0.17;0.26)	**0.22** (0.20;0.24)
TN10P	%/10 years	**−1.52** (−1.90;−1.18)	**−2.17** (−2.54;−1.80)	**−2.36** (−2.58;−2.17)
TX10P	%/10 years	**−1.31** (−1.72;−0.86)	**−2.24** (−2.62;−1.84)	**−2.28** (−2.51;−2.08)
TN90P	%/10 years	**3.01** (1.84;4.28)	**5.54** (1.20;2.65)	**4.42** (3.49;5.29)
TX90P	%/10 years	**2.38** (1.27;3.49)	**4.02** (2.78;5.25)	**3.72** (3.01;4.64)
TN1P	days/10 years	**−0.79** (−1.12;−0.49)	**−0.89** (−1.09;−0.72)	**−1.05** (−1.25;−0.85)
TX99P	days/10 years	**0.82** (0.17;1.54)	**1.09** (0.50;1.67)	**1.25** (0.73;1.97)

Note: Bold face indicates significant trends at 0.05 level.

the ROF method with Total Least Squares (TLS) regression as implemented in this package. On the one hand, the single-signal analysis performs the regression of the observations against the multi-model ensemble mean responses to ALL, GHG, ANT and NAT forcings, respectively. The objective is to check if the influence of each forcing can be detected in the observed changes. On the other hand, the two-signal analysis objective is to detect if the influence of ANT and NAT can be separated in presence of other signals. We use the 5-year moving averages of the regional anomaly time series of the observations and multi-model ensemble mean with ALL, GHG, ANT, NAT and CTL runs to carry out the D&A analysis over 1950–2018. This approach was used by Lu et al. (2018) to reduce data dimensionality.

3 | RESULTS

3.1 | Observed changes in extremes

Figure 2 shows regional indices anomalies and their trends. The changes in regional temperature extremes are significant at 0.05 level and in agreement with warming. Changes in intensity indices are similar except for TXn from 1950 to 2018. However, TNx and TXx increase at a faster rate than TNn and TXn. Warm-frequency events (i.e., indices related to maximum temperature) increase and cold-frequency events (i.e., indices related to minimum temperature) decrease. Similar as pointed out by Randriamarolaza et al. (2021), warm frequency events are changing with a faster rate than cold frequency events (see Figure 2). Observations' trend values ascertain these results (see Table 5). On the one hand, Figure 3 shows that intensity indices associated with minimum temperature are mostly correlated to ENSO events and they are in phase. This correlation may explain the peak of TNn around 1997/1998. On the other hand, frequency indices are mostly in phase with ENSO events except the TN90P, TN10P and TN1P (see Figure 3). On the other hand, intensity and frequency are well correlated to minimum and maximum temperatures at a 0.05 significance level, except for TXn (see Table 6). The cold nights (TN10P) and warm days (TX90P) have the highest correlation coefficients with minimum and maximum temperatures, respectively. Moreover, TN10P (TX90P) and minimum temperature (maximum temperature) evolve in the opposite direction (similar direction). However, the minimum and maximum temperatures only explain 76% and 82% of the variance of TN10P and TX90P, respectively.

3.2 | Spatial and temporal patterns in observations and simulations

Tables 5 and 7, presented in the previous section, shows also the regionally averaged trends for ALL, GHG, ANT and NAT forcings. On the one hand, trends of the multi-model ensemble mean under ALL, GHG and ANT forcings agree in sign and significance at 0.05 level with OBS, although OBS trends are mainly larger and smaller for intensity and frequency indices, respectively. We may explain this situation using Figure 4, which shows the Taylor diagrams (Taylor, 2001) and combines three parameters (standard deviation, root-mean-square [RMS]

TABLE 6 Correlation between temperature extremes and yearly mean of the minimum and maximum temperatures with 95% confidence interval.

	Yearly mean of minimum temperature		Yearly mean of maximum temperature	
Index	**Coefficient of correlation**	**Coefficient of determination**	**Coefficient of correlation**	**Coefficient of determination**
TNn	0.74 [0.61;0.83]	55%	0.64 [0.48;0.76]	41%
TXn	0.42 [0.20;0.60]	18%	0.48 [0.28;0.65]	23%
TNx	0.74 [0.61;0.83]	55%	0.74 [0.60;0.86]	54%
TXx	0.73 [0.60;0.82]	53%	0.78 [0.66;0.86]	60%
TN10P	−0.87 [−0.92;−0.80]	76%	−0.78 [−0.86;−0.66]	60%
TX10P	−0.77 [−0.85;−0.66]	60%	−0.81 [−0.88;−0.71]	66%
TN90P	0.86 [0.79;0.91]	75%	0.85 [0.77;0.90]	72%
TX90P	0.84 [0.75;0.90]	70%	0.90 [0.85;0.94]	82%
TN1P	−0.74 [−0.83;−0.61]	55%	−0.66 [−0.78;−0.50]	44%
TX99P	0.66 [0.51;0.78]	44%	0.72 [0.58;0.82]	52%

TABLE 7 Regional trends with its confidence intervals (in brackets) in the multi-model ensemble mean responses on anthropogenic (ANT) and natural (NAT) forcings over 1950–2018.

		Decadal trends (confidence interval)	
Index	**Units**	**ANT**	**NAT**
TNn	°C/10 years	**0.17** (0.14;0.19)	0.01 (−0.02;0.04)
TXn	°C/10 years	**0.17** (0.15;0.20)	0.01 (−0.03;0.05)
TNx	°C/10 years	**0.19** (0.16;0.21)	0.01 (−0;02;0.04)
TXx	°C/10 years	**0.21** (0.18;0.25)	0.00 (−0.03;0.04)
TN10P	%/10 years	**−2.22** (−2.58;−2.17)	0.01 (−0.21;0.88)
TX10P	%/10 years	**−2.27** (−2.50;−2.03)	0.02 (−0.25;0.30)
TN90P	%/10 years	**4.85** (3.85;5.84)	−0.11 (−0.53;0.63)
TX90P	%/10 years	**4.07** (3.25;4.91)	**−0.37** (−0.71;−0.05)
TN1P	days/10 years	**−0.99** (−1.16;−0.80)	0.06 (−0.08;0.20)
TX99P	days/10 years	**1.45** (0.94;2.05)	−0.15 (−0.31;0.00)

Note: Bold face indicates significant trends at 0.05 level.

difference and correlation coefficient) to match patterns between OBS and multi-model ensemble mean responses on ALL, GHG, ANT and NAT forcing. The amplitudes of variation (standard deviations) of OBS are greater and lower than multi-model ensemble means under ALL, GHG and ANT forcings for intensity and frequency indices, respectively. For instance, the coldest (warmest) day and night of the multi-model ensemble mean with ALL, GHG and ANT are less (well) correlated with OBS and have high (low) RMS. Their spatial interpolation of trends (Figures 5 and 6) indicates that more individual model simulations are in concordance with the multi-model ensemble mean for the warmest day and night compared to the coldest day and night. Besides, frequency indices of the multi-model ensemble mean with ALL, GHG and ANT forcings are well correlated with OBS. Nevertheless, warm events (TN90P, TX90P and TX99P) are more scattered than cold events (TN10P, TX10P and TN1P) of the multi-model ensemble mean with ALL, GHG and ANT forcings. In general, OBS changes are consistent with the multi-model ensemble mean responses on ALL, GHG and ANT forcings (see Figures 5 and 6). However, individual model and multi-model ensemble mean responses on ALL, GHG and ANT show discrepancies for some very extreme indices such as TN1P and TX99P. The North Western (NW) region is the hottest area in Madagascar and, in this region, the frequency of TXn and TX10P decrease and increase, respectively (see Figure 5). This situation is the opposite of the global warming effect. Therefore, it may be due to microclimate effects or to the homogeneity aspect and missing data filling in climate data records. On the other hand, the multi-model ensemble mean under NAT forcing trends are non-significant except for TX90P, with the

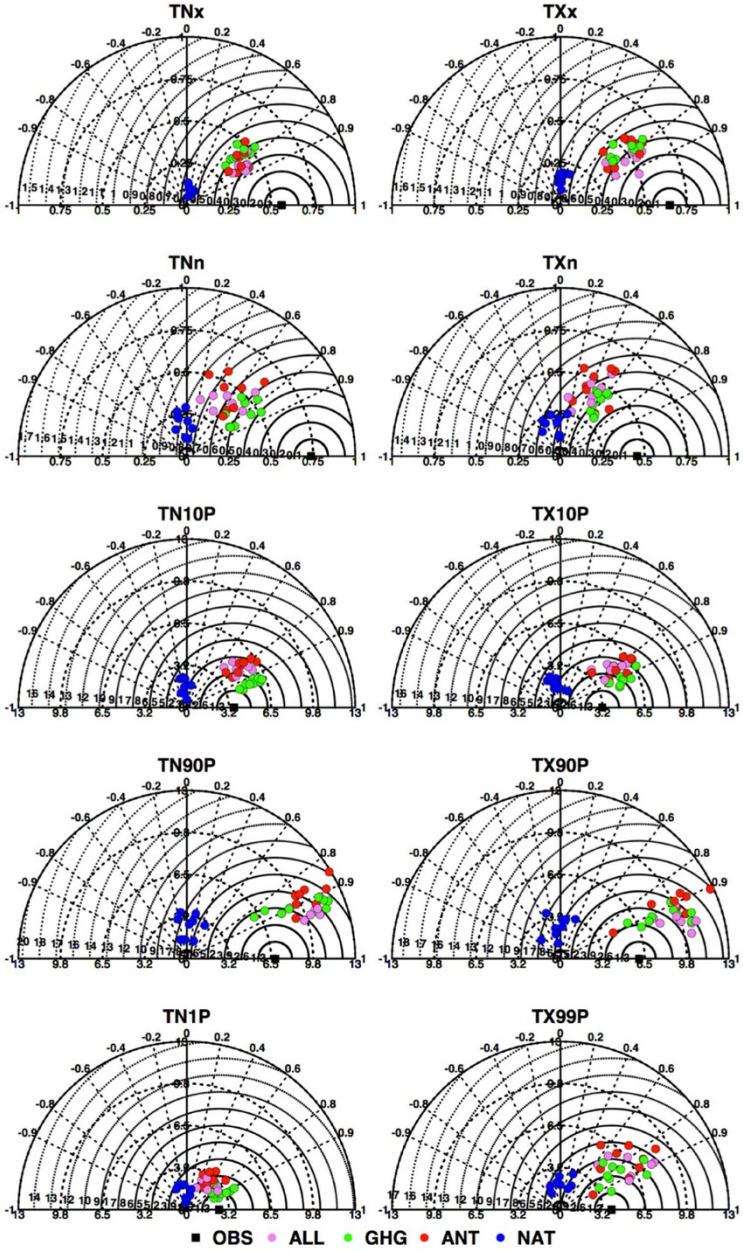

FIGURE 4 Taylor diagrams of intensity and frequency indices. The square on the x-axis indicates OBS considered as a reference. Dots indicate the 5-year mean regional of multi-model ensemble members under ALL, GHG, ANT and NAT forcings. Concentric circles from OBS and origin represent centred root-mean-square (RMS) difference and standard deviation, respectively. Radial axis indicates the correlation coefficients between OBS and ensemble member.

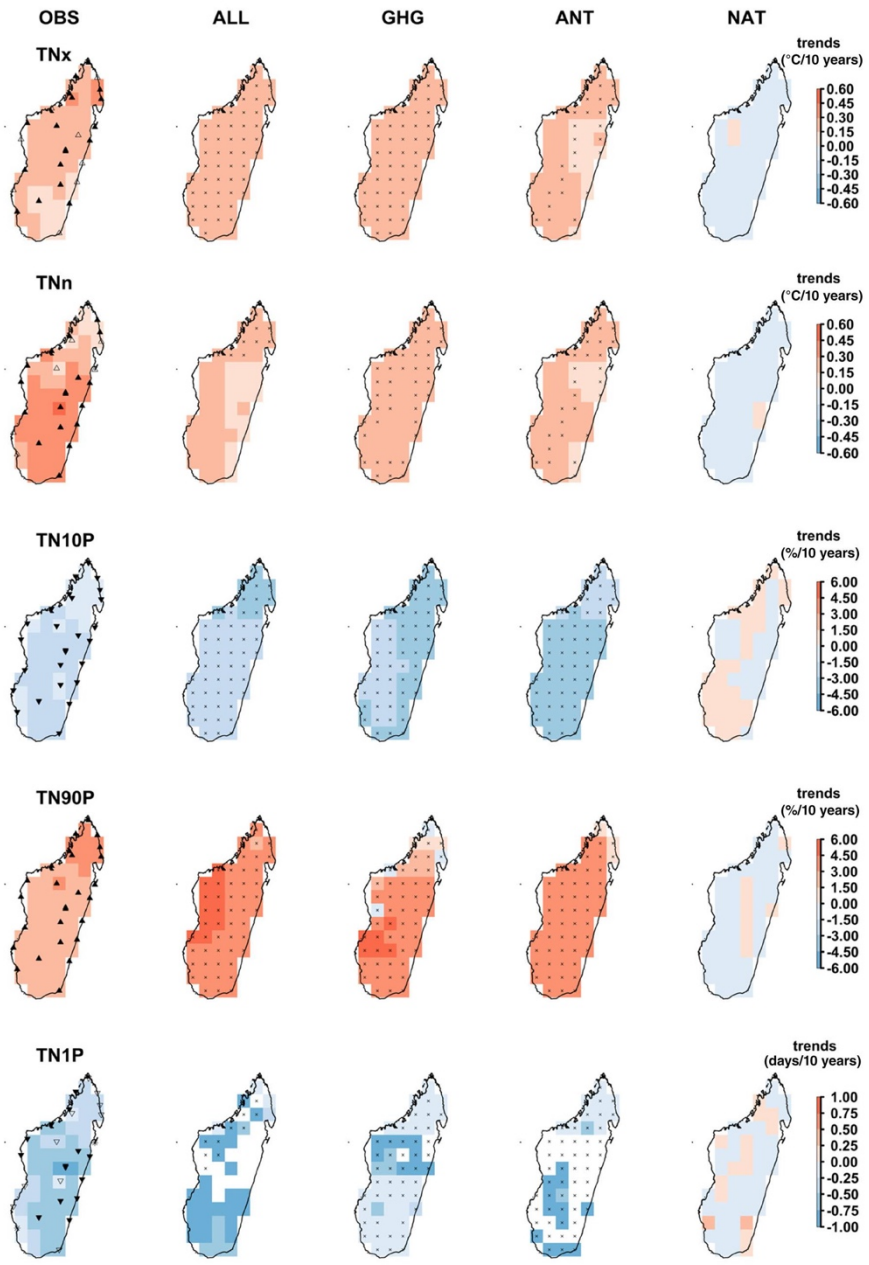

FIGURE 5 Spatial distribution trends over 1950–2018 of intensity and frequency indices related to minimum temperature in the observation and multi-model ensemble mean responses to ALL, GHG, ANT and NAT forcings. Crosses mark the agreement of at least 75% of the model simulations on the trends' significance at 0.05 level and sign with multi-model ensemble mean.

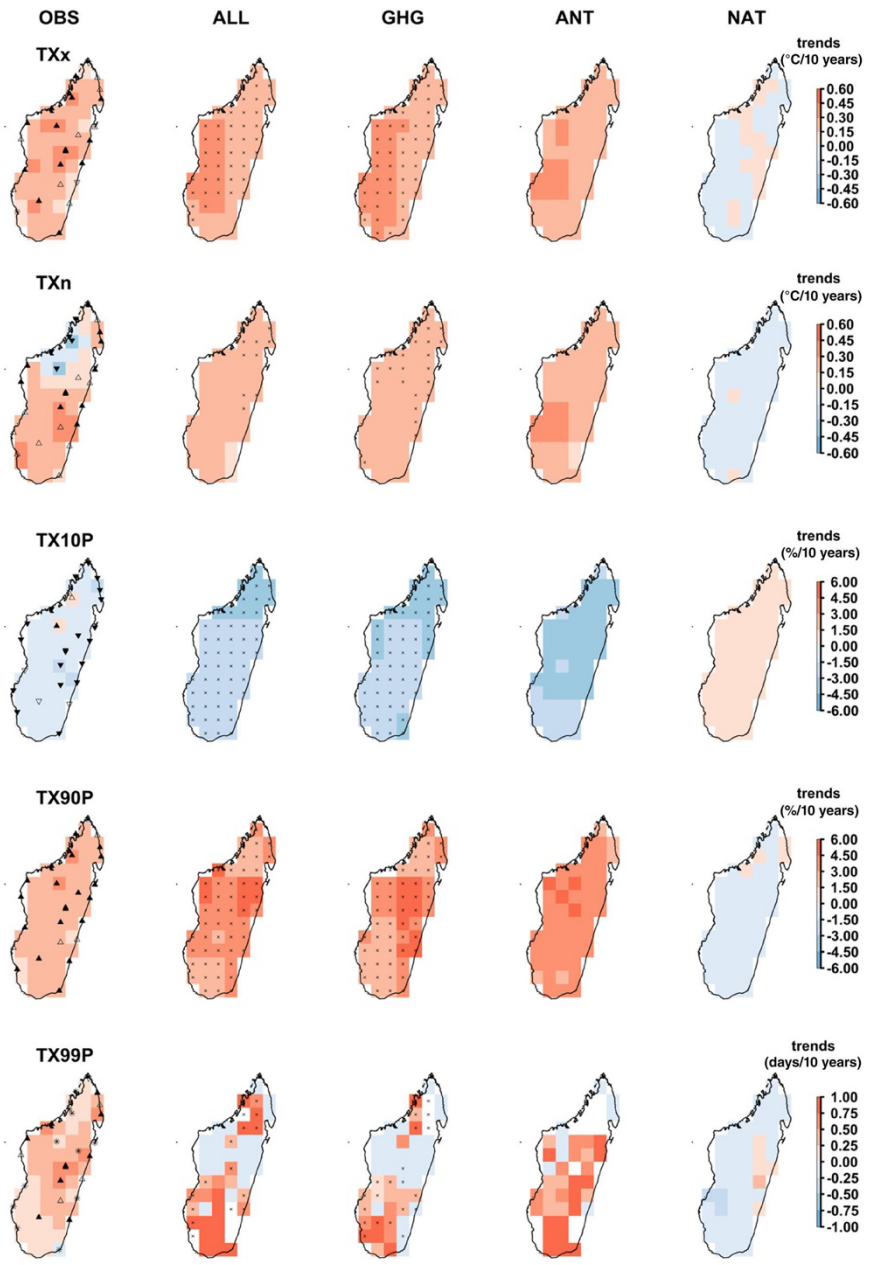

FIGURE 6 Spatial distribution trends over 1950–2018 of intensity and frequency indices related to maximum temperature in the observation and multi-model ensemble mean responses to ALL, GHG, ANT and NAT forcings. Crosses mark the agreement of at least 75% of the model simulations on the trends' significance at 0.05 level and sign with multi-model ensemble mean under ALL forcing.

opposite sign to the other time series. Figure 4 shows any variation compared to OBS. Beyond this, any individual model under NAT forcing agrees with the multi-model ensemble mean under ALL forcing on indices trend sign and significance. Figure 6 shows a similar situation with ANT forcing related to intensity and frequency indices associated with maximum temperature. This is due to small numbers of individual models. Figure 7 represents the 5-year moving averages of the regional anomaly time series of the observational and multi-model ensemble means with ALL, GHG, ANT and NAT forcings over 1950–2018. Regional average anomaly time series of OBS are mainly included in the model simulation ranges (i.e., 5%–95%), especially for ALL, GHG and ANT forcings. On the contrary, the regional multi-model ensemble mean response on NAT forcing anomaly time series oscillate around the mean (see Figure 7).

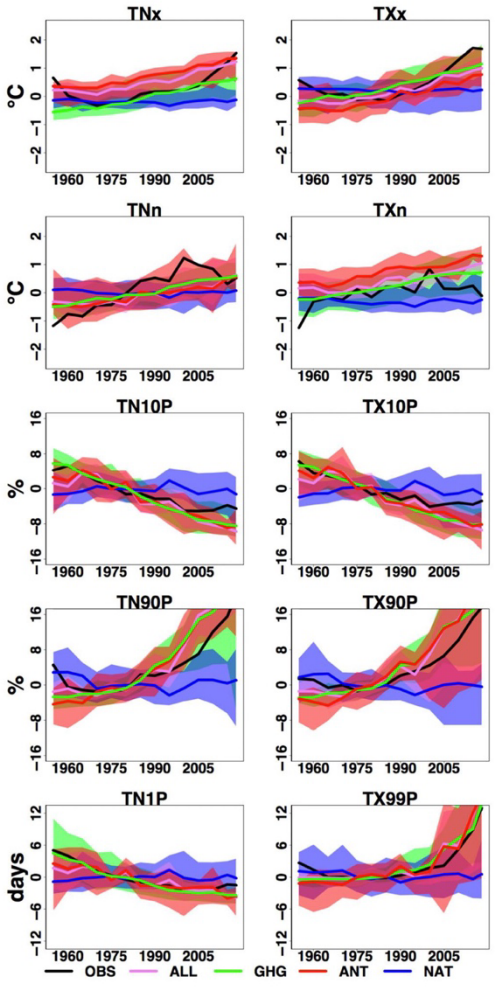

FIGURE 7 5-year moving averages of the regional anomaly time series of the observational and multi-model ensemble simulations. Shaded area show 5%–95% confidence interval of the selected model simulations.

3.3 | Detection and attribution results

The single-signal analysis result is shown in Figure 8. It indicates that the intensity and frequency indices' scaling factors and lower limits of confidence intervals are greater than zero under ALL, GHG and ANT forcings. Therefore ALL, GHG and ANT influences are detected. Notice that observed changes are attributed to an external forcing if its influence is detected and the confidence interval of a corresponding scaling factor includes the unit. As ALL and ANT are composed by different forcing, single-signal analysis highlights this combined effect. On the one hand, observed changes of TXx, TNn, TN10P, TX10P, TN90P and TX90P are not attributed to ALL forcing. On the other hand, similar results are observed with ANT forcing except for TXx and TN10P. However, most observed changes are attributed to GHG forcing except for TNn and TX10P. Besides, observed changes of TNx, TXn, TN1P and TX99P are attributed to all external forcing except NAT. However, any external forcing is attributed to TNn and TX10P. Most RCC tests fail for NAT forcing except for TXx. It means that NAT forcing is inconsistent with observed changes.

We perform a two-signal analysis with ANT and NAT forcings to determine whether their influence can be detected separately. Figure 9 ascertains that NAT and ANT influences are detected for TXx and its observed changes are attributed only to ANT forcing. It also displays that observed changes of TNx, TN10P and TX99P are attributed to ANT forcing. On the contrary to single-signal analysis, observed changes of TX90P are attributed to ANT forcing. Moreover, observed changes of TNn, TXn and TN1P are inconsistent with ANT and NAT forcings. The other indices are consistent with NAT forcing even if NAT influence is not detected. In a nutshell, most observed changes are attributed to GHG and ANT forcings.

4 | DISCUSSION AND CONCLUSIONS

This article presents for a very first time a D&A analysis for Madagascar. Our results demonstrate that on the one

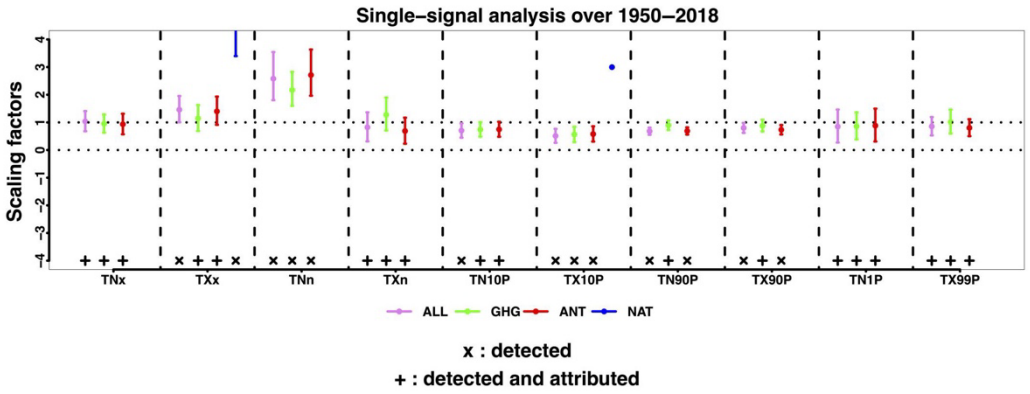

FIGURE 8 Single-signal analysis of best estimates of scaling factors (dots) and their 5%–95% uncertainty levels (bars) from multi-model ensembles under ALL, GHG, ANT and NAT forcings. If the residual consistency check (RCC) is failed or no detection found (scaling factor is less than zero), bars are missing.

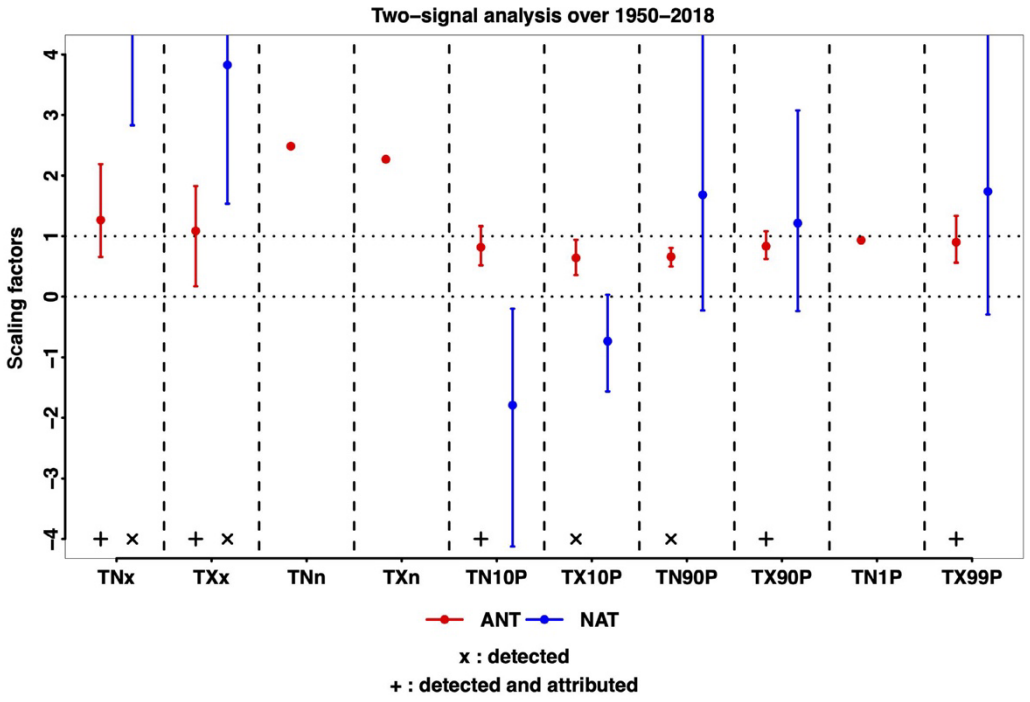

FIGURE 9 Two-signal analysis of best estimates of scaling factors (dots) and their 5%–95% uncertainty levels (bars) from multi-model ensembles under ANT and NAT forcing. If the residual consistency check (RCC) is failed or no detection found (scaling factor is less than zero), bars are missing.

hand, regional and station-by-station trends in intensity and frequency indices point to the effects of global warming in Madagascar. Moreover, regional intensity and frequency indices are influenced by ENSO events, particularly indices associated with minimum temperature. On the other hand, observational and multi-model ensemble simulations with ALL, GHG and ANT forcings are well-matched in terms of regional intensity and frequency indices. Almost similar patterns are observed between OBS and multi-model ensemble members with ALL, GHG and ANT forcings, particularly for frequency indices, based on the Taylor diagram. However, any relationship found between OBS and multi-model ensemble members with NAT forcing. Spatial distribution of trends in intensity and frequency indices ascertain these findings. The ROF method demonstrates that the observed changes of intensity and frequency indices are mostly influenced by ALL, GHG and ANT forcings. Moreover, observed changes are mainly attributed to ANT and GHG forcings. Any observed changes in intensity and frequency indices are influenced by NAT forcing.

The state-of-the-art on D&A analysis recommends using a high-quality observational dataset (Coumou & Rahmstorf, 2012), so we used quality-controlled and homogenized observations of daily minimum and maximum temperatures (Randriamarolaza et al., 2021). According to Zhai et al. (2018), uncertainties might come from methods' selection in D&A analysis. In this article, we applied the standard optimal fingerprinting method by using ROF with TLS regression to drive single-signal and two-signal analyses against ALL, GHG, ANT and NAT forcings. ROF method used an inverse of the covariance matrix avoiding projection steps, providing improved accuracy (see Ribes et al., 2013). As underlined by Hannart et al. (2014), errors might arise from internal variability, model error or observational error in D&A analysis. They suggested that if all errors shared the same covariance, TLS was the best statistical method to perform D&A analysis. Nevertheless, the robustness of results was based on model simulations and statistical methods used as pointed out by Hegerl and Zwiers (2011) and Zhai et al. (2018). In this article, we selected model simulations, which contributed to the IPCC AR6 from the CMIP6 archive. Model simulations had similar initialization methods, perturbed physics and forcing, but they had different realizations. We built multi-model ensemble mean responses on forcing to overcome uncertainties. Before assessing D&A analysis, we analysed the relationship between indices and ENSO events. Moreover, we compared CMIP6 ensemble members under ALL, GHG, ANT and NAT forcings with observations using the Taylor diagram method. Finally, we made spatial and temporal comparisons between observed and model simulation trends over 1950–2018.

Our findings are consistent with those for the global and regional scales. The observed indices trends were consistent with our previous analysis (Randriamarolaza et al., 2021). However, this article was completed with a brief assessment of ENSO's influence on indices by using wavelet coherence method. As underlined by Dong et al. (2018) for Asia, warm event changes were also more pronounced after the 1980s. On the other hand, the influence of external forcing was detectable in observations for intensity and frequency indices in temperature extremes over 1950–2018 in Madagascar. Mostly, observed changes of intensity and frequency indices were attributed to GHG and ANT forcings. These results were mostly consistent with Global and Europe results over 1961–2010 and Asia results over 1958–2012 found by Christidis and Stott (2016) and Dong et al. (2018), respectively. However, the influence of GHG forcing on TNn and TXn were not detected in Europe. The influence of ALL forcing on TNx, TXx, TNn and TXn were not credible in Asia for lower and higher latitudes, respectively. Moreover, regional average index trend behaviours were comparable to Globally and European average index trends in Christidis and Stott (2016). For percentile-based indices, Morak et al. (2013) found similar warming trends by telling that TX10P, TX90P, TN10P and TN90P decreased and increased over 1951–2013, respectively. These observed changes were influenced by external forcing at 5% level. Noticed that Morak et al. (2013) and Christidis and Stott (2016) did not adopt a multi-model approach but they employed indices directly with optimal fingerprinting method. Nevertheless, Min et al. (2013) and Kim et al. (2016) employed a multi-model approach, but they transformed variables to probability-based index before applying standard optimal fingerprinting methods. They found that observed changes of TXn, TXx, TNn and TXx were influenced by external forcing. Then Kim et al. (2016) observed that CMIP5 models agreed better with observed changes in TNx and TXx than the previous study with CMIP3. We also found similar agreement between CMIP6 models and observed changes, especially for frequency indices in Madagascar.

We recognize, as a setback of this article, that we did not evaluate model performance at regional levels. Moreover, individual model numbers might be insufficient. However, we selected ensemble members with similar initialization methods, perturbed physics and forcing. Besides, index regional time series of OBS, ALL, GHG, ANT and NAT forcings were compared to capture their evolution (see Figures 6 and 7). But we might add the validation of models against observation as adopted by Otto et al. (2013) to improve our results. Therefore, this research might be improved by tackling these gaps issues and implementing standard optimal fingerprinting methods with a

probability-based index or extreme value theory. We might also extend the study with other indices (e.g., indices related to precipitation). However, it was important to think about how to apply these findings on real time to assess actual risks by connecting them to sector impacts such as agriculture, health and so on.

AUTHOR CONTRIBUTIONS

Luc Yannick Andréas RANDRIAMAROLAZA: Conceptualization; data curation; formal analysis; investigation; methodology; software; validation; visualization; writing – original draft; writing – review and editing. **Enric Aguilar:** Conceptualization; formal analysis; funding acquisition; methodology; project administration; supervision; validation; writing – review and editing. **Oleg Skrynyk:** Conceptualization; formal analysis; methodology; validation; writing – review and editing.

ACKNOWLEDGEMENTS

This study was not completed without the climate data from Directorate General of Meteorology of Madagascar and the financial support from the INDECIS project. It is a part of ERA4CS, an ERA-NET initiated by JPI Climate, and funded by FORMAS (SE), DLR (DE), BMWFW (AT), IFD (DK), MINECO (ES), ANR (FR) with co-funding by the European Union (Grant 690462). The authors thank all those who helped to improve this study, particularly Xuebin Zhang and the anonymous reviewers for their in-depth reading of the manuscript and their valuable comments and suggestions.

ORCID

Luc Yannick Andréas Randriamarolaza https://orcid.org/0000-0002-2939-2250
Enric Aguilar https://orcid.org/0000-0002-8384-377X
Oleg Skrynyk https://orcid.org/0000-0001-8827-0280

REFERENCES

Allen, M.R. & Stott, P.A. (2003) Estimating signal amplitudes in optimal fingerprinting, Part I: theory. *Climate Dynamics*, 21, 477–491. Available from: https://doi.org/10.1007/s00382-003-0313-9

Allen, M.R. & Tett, S.F.B. (1999) Checking for model consistency in optimal fingerprinting. *Climate Dynamics*, 15, 419–434. Available from: https://doi.org/10.1007/s003820050291

Barry, A.A., Caesar, J., Klein, T.A.M.G., Aguilar, E., McSweeney, C., Cyrille, A.M. et al. (2018) West Africa climate extremes and climate change indices. *International Journal of Climatology*, 38, e921–e938. Available from: https://doi.org/10.1002/joc.5420

Bindoff, N.L., Stott, P.A., Achuta Rao, K.M., Allen, M.R., Gillett, N., Gutzler, D. et al. (2013) Detection and attribution of climate change: from global to regional. In: Stocker, T.F., Qin, D., Plattner, G.K., Tignor, M., Allen, S.K., Boschung, J. et al. (Eds.) *Climate Change 2013: The Physical Science Basis. Contribution of Working Group I to the Fifth Assessment Report of the Intergovernmental Panel on Climate Change*. Cambridge, UK; New York, NY: *Cambridge University Press*. Available from: https://doi.org/10.1017/CBO9781107415324.022

Bronaugh, D. & Werner, A. (2019) Package 'zyp'. https://CRAN.R-project.org/package=zyp

Christidis, N. & Stott, P.A. (2016) Attribution analyses of temperature extremes using a set of 16 indices. *Weather and Climate Extremes*, 14, 24–35. Available from: https://doi.org/10.1016/j.wace.2016.10.003

Coumou, D. & Rahmstorf, S. (2012) A decade of weather extremes. *Nature Climate Change*, 2, 491–496. Available from: https://doi.org/10.1038/nclimate1452

Curry, J.A. & Webster, P.J. (2011) Climate science and the uncertainty monster. *Bulletin of the American Meteorological Society*, 92, 1667–1682. Available from: https://doi.org/10.1175/2011BAMS3139.1

Dileepkumar, R., AchutaRao, K. & Arulalan, T. (2018) Human influence on sub-regional surface air temperature change over India. *Scientific Reports*, 8, 8967. Available from: https://doi.org/10.1038/s41598-018-27185-8

Dima, M., Lohmann, G. & Dima, I. (2005) Solar-induced and internal climate variability at decadal time scales. *International Journal of Climatology*, 25(6), 713–733. Available from: https://doi.org/10.1002/joc.1156

Domínguez-Castro, F., Reig, F., Vicente-Serrano, S.M., Aguilar, E., Peña-Angulo, D., Noguera, I. et al. (2020) A multidecadal assessment of climate indices over Europe. *Scientific Data*, 7, 125. Available from: https://doi.org/10.1038/s41597-020-0464-0

Dong, S., Sun, Y., Aguilar, E., Zhang, X., Peterson, T.C., Song, L. et al. (2018) Observed changes in temperature extremes over Asia and their attribution. *Climate Dynamics*, 51, 339–353. Available from: https://doi.org/10.1007/s00382-017-3927-z

Eyring, V., Bony, S., Meehl, G.A., Senior, C.A., Stevens, B., Stouffer, R.J. et al. (2016) Overview of the Coupled Model Intercomparison Project Phase 6 (CMIP6) experimental design and organization. *Geoscientific Model Development*, 9, 1937–1958. Available from: https://doi.org/10.5194/gmd-9-1937-2016

Gillett, N.P., Shiogama, H., Funke, B., Hegerl, G., Knutti, R., Matthes, K. et al. (2016) The Detection and Attribution Model Intercomparison Project (DAMIP v1.0) contribution to CMIP6. *Geoscientific Model Development*, 9, 3685–3697. Available from: https://doi.org/10.5194/gmd-9-3685-2016

Grinsted, A., Moore, J.C. & Jevrejeva, S. (2004) Application of the cross wavelet transform and wavelet coherence to geophysical time series. *Nonlinear Processes in Geophysics*, 11, 561–566. Available from: https://doi.org/10.5194/npg-11-561-2004

Hannart, A., Ribes, A. & Naveau, P. (2014) Optimal fingerprinting under multiple sources of uncertainty. *Geophysical Research Letters*, 41, 1261–1268. Available from: https://doi.org/10.1002/2013GL058653

Hegerl, G. & Zwiers, F. (2011) Use of models in detection and attribution of climate change. *WIREs Climate Change*, 2, 570–591. Available from: https://doi.org/10.1002/wcc.121

Huang, B., Thorne, P.W., Banzon, V.F., Boyer, T., Chepurin, G., Lawrimore, J.H. et al. (2017) Extended Reconstructed Sea Surface Temperature, Version 5 (ERSSTv5): upgrades, validations,

and intercomparisons. *Journal of Climate*, 30, 8179–8205. Available from: https://doi.org/10.1175/JCLI-D-16-0836.1

Jevrejeva, S., Moore, J.C. & Grinsted, A. (2003) Influence of the Arctic Oscillation and El Niño-Southern Oscillation (ENSO) on ice conditions in the Baltic Sea: the wavelet approach. *Journal of Geophysical Research: Atmospheres*, 108(21), 1–11. Available from: https://doi.org/10.1029/2003jd003417

Kim, Y.H., Min, S.K., Zhang, X., Zwiers, F., Alexander, L.V., Donat, M.G. et al. (2016) Attribution of extreme temperature changes during 1951–2010. *Climate Dynamics*, 46, 1769–1782. Available from: https://doi.org/10.1007/s00382-015-2674-2

Liang, L., Li, L., Liu, C. & Cuo, L. (2013) Climate change in the Tibetan Plateau Three Rivers Source Region: 1960–2009. *International Journal of Climatology*, 33, 2900–2916. Available from: https://doi.org/10.1002/joc.3642

Lilly, J.M. (2017) Element analysis: a wavelet-based method for analysing time-localized events in noisy time series. *Proceedings of the Royal Society A: Mathematical, Physical and Engineering Sciences*, 473, 20160776. Available from: https://doi.org/10.1098/rspa.2016.0776

Lo, Y., Charlton-Perez, A., Lott, F. & Highwood, E. (2016) Detecting sulphate aerosol geoengineering with different methods. *Scientific Reports*, 6, 39169. Available from: https://doi.org/10.1038/srep39169

Lu, C., Sun, Y. & Zhang, X. (2018) Multimodel detection and attribution of changes in warm and cold spell durations. *Environmental Research Letters*, 13(7), 074013. Available from: https://doi.org/10.1088/1748-9326/aacb3e

Meinshausen, M., Vogel, E., Nauels, A., Lorbacher, K., Meinshausen, N., Etheridge, D.M. et al. (2017) Historical greenhouse gas concentrations for climate modelling (CMIP6). *Geoscientific Model Development*, 10(5), 2057–2116. Available from: https://doi.org/10.5194/gmd-10-2057-2017

Min, S.K., Zhang, X., Zwiers, F., Shiogama, H., Tung, Y.S. & Wehner, M. (2013) Multimodel detection and attribution of extreme temperature changes. *Journal of Climate*, 26, 7430–7451. Available from: https://doi.org/10.1175/jcli-d-12-00551.1

Morak, S., Hegerl, G.C. & Christidis, N. (2013) Detectable changes in the frequency of temperature extremes. *Journal of Climate*, 26, 1561–1574. Available from: https://doi.org/10.1175/JCLI-D-11-00678.1

Morak, S., Hegerl, G.C. & Kenyon, J. (2011) Detectable regional changes in the number of warm nights. *Geophysical Research Letters*, 38, L17703. Available from: https://doi.org/10.1029/2011GL048531

O'Neill, B.C., Tebaldi, C., van Vuuren, D.P., Eyring, V., Friedlingstein, P., Hurtt, G. et al. (2016) The Scenario Model Intercomparison Project (ScenarioMIP) for CMIP6. *Geoscientific Model Development*, 9, 3461–3482. Available from: https://doi.org/10.5194/gmd-9-3461-2016

Otto, F.E.L., Boyd, E., Jones, R.G., Cornforth, R.J., James, R., Parker, H.R. et al. (2015) Attribution of extreme weather events in Africa: a preliminary exploration of the science and policy implications. *Climatic Change*, 132, 531–543. Available from: https://doi.org/10.1007/s10584-015-1432-0

Otto, F.E.L., Harrington, L., Schmitt, K., Philip, S., Kew, S., van Oldenborgh, G.J. et al. (2020) Challenges to understanding extreme weather changes in lower income countries. *Bulletin of the American Meteorological Society*, 101, E1851–E1860. Available from: https://doi.org/10.1175/BAMS-D-19-0317.1

Otto, F.E.L., Jones, R.G., Halladay, K. & Allen, M.R. (2013) Attribution of changes in precipitation patterns in African Rainforests. *Philosophical Transactions of the Royal Society B: Biological Sciences*, 368, 20120299. Available from: https://doi.org/10.1098/rstb.2012.0299

Peterson, T.C., Hoerling, M.P., Stott, P.A. & Herring, S.C. (2013) Explaining extreme events of 2012 from a climate perspective. *Bulletin of the American Meteorological Society*, 94, S1–S74. Available from: https://doi.org/10.1175/BAMS-D-13-00085.1

Peterson, T.C., Stott, P.A. & Herring, S.C. (2012) Explaining extreme events of 2011 from a climate perspective. *Bulletin of the American Meteorological Society*, 93, 1041–1067. Available from: https://doi.org/10.1175/BAMS-D-12-00021.1

Randriamarolaza, L.Y.A., Aguilar, E., Skrynyk, O., Vicente-Serrano, S.M. & Domínguez-Castro, F. (2021) Indices for daily temperature and precipitation in Madagascar, based on quality-controlled and homogenized data, 1950–2018. *International Journal of Climatology.*, 42, 265–288. Available from: https://doi.org/10.1002/joc.7243

Ribes, A., Planton, S. & Terray, L. (2013) Application of regularised optimal fingerprinting to attribution. Part I: method, properties and idealised analysis. *Climate Dynamics*, 41, 2817–2836. Available from: https://doi.org/10.1007/s00382-013-1735-7

Ruwangika, A.M., Perera, A. & Rathnayake, U. (2020) Comparison of statistical, graphical, and wavelet transform analyses for rainfall trends and patterns in Badulu Oya Catchment, Sri Lanka. *Complexity*, 2020, 7146593. Available from: https://doi.org/10.1155/2020/7146593

Santer, B.D., Wigley, T.M.L., Barnett, T.P. & Anyamba, E. (1996) Detection of climate change and attribution of causes. In: *Climate Change 1995: The Science of Climate Change. Contribution of Working Group I to the Second Assessment Report of the Intergovernmental Panel on Climate Change*, Vol. 30. Cambridge, UK: Cambridge Unversity Press, pp. 91–109. Available from: https://doi.org/10.4324/9780203876213.ch1

Santoso, A., Mcphaden, M.J. & Cai, W. (2017) The defining characteristics of ENSO extremes and the strong 2015/2016 El Niño. *Reviews of Geophysics*, 55, 1079–1129. Available from: https://doi.org/10.1002/2017RG000560

Sen, P.K. (1968) Estimates of the regression coefficient based on Kendall's tau. *Journal of the American Statistical Association*, 63, 1379–1389. Available from: https://doi.org/10.1080/01621459.1968.10480934

Skrynyk, O., Aguilar, E., Guijarro, J., Randriamarolaza, L.Y.A. & Bubin, S. (2021) Uncertainty evaluation of Climatol's adjustment algorithm applied to daily air temperature time series. *International Journal of Climatology*, 41, E2395–E2419. Available from: https://doi.org/10.1002/joc.6854

Sonali, P. & Kumar, D.N. (2020) Review of recent advances in climate change detection and attribution studies: a large-scale hydroclimatological perspective. *Journal of Water and Climate Change*, 11, 1–29. Available from: https://doi.org/10.2166/wcc.2020.091

Stott, P.A., Jones, G.S., Christidis, N., Zwiers, F.W., Hegerl, G. & Shiogama, H. (2011) Single-step attribution of increasing frequencies of very warm regional temperatures to human influence. *Atmospheric Science Letters*, 12, 220–227. Available from: https://doi.org/10.1002/asl.315

Swart, N.C., Cole, J.N.S., Kharin, V.V., Lazare, M., Scinocca, J.F., Gillett, N.P. et al. (2019) The Canadian Earth System Model

version 5 (CanESM5.0.3). *Geoscientific Model Development*, 12, 4823–4873. Available from: https://doi.org/10.5194/gmd-12-4823-2019

Tarik, C.G., Grinsted, A. & Simko, V. (2018) *R package biwavelet: Conduct Univariate and Bivariate Wavelet Analyses (Version 0.20.17)*. Available at: https://github.com/tgouhier/biwavelet

Taylor, K.E. (2001) Summarizing multiple aspects of model performance in a single diagram. *Journal of Geophysical Research Atmospheres*, 106(D7), 7183–7192. Available from: https://doi.org/10.1029/2000JD900719

Torrence, C. & Compo, G. (1998) A practical guide to wavelet analysis. *Bulletin of the American Meteorological Society*, 79, 61–78. Available from: https://doi.org/10.1175/1520-0477(1998)079<0061:APGTWA>2.0.CO;2

Vincent, L.A., Aguilar, E., Saindou, M., Hassane, A.F., Jumaux, G., Roy, D. et al. (2011) Observed trends in indices of daily and extreme temperature and precipitation for the countries of the western Indian Ocean, 1961–2008. *Journal of Geophysical Research-Atmospheres*, 116(10), 1–12. Available from: https://doi.org/10.1029/2010JD015303

Wan, H., Zhang, X., Zwiers, F. & Min, S.K. (2014) Attributing northern high-latitude precipitation change over the period 1966–2005 to human influence. *Climate Dynamics*, 45, 1713–1726. Available from: https://doi.org/10.1007/s00382-014-2423-y

Wang, Z., Jiang, Y., Wan, H., Yan, J. & Zhang, X. (2020) Toward optimal fingerprinting in detection and attribution of changes in climate extremes. *Journal of the American Statistical Association*, 116, 1–13. Available from: https://doi.org/10.1080/01621459.2020.1730852

Yi, H. & Shu, H. (2012) The improvement of the Morlet wavelet for multi-period analysis of climate data. *Comptes Rendus Geoscience*, 344, 483–497. Available from: https://doi.org/10.1016/j.crte.2012.09.007

Yosef, Y., Aguilar, E. & Alpert, P. (2019) Changes in extreme temperature and precipitation indices: using an innovative daily homogenized database in Israel. *International Journal of Climatology*, 39, 5022–5045. Available from: https://doi.org/10.1002/joc.6125

Yosef, Y., Aguilar, E. & Alpert, P. (2020) Is it possible to fit extreme climate change indices together seamlessly in the era of accelerated warming? *International Journal of Climatology*, 41, E952–E963. Available from: https://doi.org/10.1002/joc.6740

Zhai, P., Zhou, B. & Chen, Y. (2018) A review of climate change attribution studies. *Journal of Meteorological Research*, 32, 671–692. Available from: https://doi.org/10.1007/s13351-018-8041-6

Zhang, X., Vincent, L.A., Hogg, W.D. & Niitsoo, A. (2000) Temperature and precipitation trends in Canada during the 20th century. *Atmosphere-Ocean*, 38, 395–429. Available from: https://doi.org/10.1080/07055900.2000.9649654

Zhang, X., Wan, H., Zwiers, F.W., Hegerl, G.C. & Min, S.K. (2013) Attributing intensification of precipitation extremes to human influence. *Geophysical Research Letters*, 40, 5252–5257. Available from: https://doi.org/10.1002/grl.51010

How to cite this article: Randriamarolaza, L. Y. A., Aguilar, E., & Skrynyk, O. (2023). Extreme temperatures detection and attribution related to external forcing in Madagascar. *International Journal of Climatology*, 1–18. https://doi.org/10.1002/joc.8065

CHAPTER 5 Rainy season and crop calendars comparison between past (1950-2018) and future (2030-2100) in Madagascar

Received: 3 May 2023 | Revised: 5 July 2023 | Accepted: 25 July 2023

DOI: 10.1002/met.2146

RESEARCH ARTICLE

Meteorological Applications
Science and Technology for Weather and Climate
RMetS

Rainy season and crop calendars comparison between past (1950–2018) and future (2030–2100) in Madagascar

Luc Yannick Andréas Randriamarolaza[1,2] | **Enric Aguilar**[1]

[1]University Institute on Sustainability, Climate Change and Energy Transition (IU-RESCAT), Center for Climate Change (C3), Universitat Rovira i Virgili, Vila-Seca, Tarragona, Spain

[2]Direction Générale de la Météorologie, Antananarivo, Madagascar

Correspondence
Enric Aguilar, University Institute on Sustainability, Climate Change and Energy Transition (IU-RESCAT), Center for Climate Change (C3), Universitat Rovira i Virgili, Joanot Martorell 15, Vila-Seca, Tarragona, 43480, Spain.
Email: enric.aguilar@urv.cat

Funding information
FORMAS (SE), DLR (DE), BMWFW (AT), IFD (DK), MINECO (ES), ANR (FR), European Union, Grant/Award Number: 690462

Abstract

This paper analyzes rainfall data to characterize the rainy season and define rice and maize crop calendars for current and future conditions in Madagascar. The daily rainfall data are taken from observational climate records and climate model simulations from the CMIP6 under the SSP245 and SSP585 scenarios. Rainy season characteristics are calibrated to fit rice and maize crop growth stages. The comparison between the past (1950–2018) and the future (2030–2100) highlights changes in the onset and cessation dates, which happen later and earlier, respectively. This causes the reduction of the rainy season duration, which affects the rice and maize crop calendars, especially its sowing or seeding periods. The worst (best) case is mainly observed in the southeast (southwest). On the one hand, the southwestern region may need to adapt to grow rice and maize crops with short or medium crop cycles in the future. In the Highland or Central land, the length of the sowing or seeding period increases. On the other hand, the North and East face a significant reduction in the length of the sowing or seeding period. Rice endures more than maize. Growing rice crops twice a year may not be possible in the future. But rather, we observe minor changes in the West. Our analysis suggests the imperative necessity to advise smallholder farmers to rely on short crop cycle varieties of rice and maize crops. Predominantly, the harvesting period is postponed. It is recommended to carefully consider our results for the definition of food policies.

KEYWORDS

climate projection, Madagascar, maize and rice crop calendars, rainy season

1 | INTRODUCTION

The rapid population growth pressures global food security (Gerardeaux et al., 2012), especially in Africa (Sasson, 2012). Rice and maize are among the world's most important crops to support food security. For instance, they are a staple food and main crops in Madagascar.

Rice crops can grow under three environments such as irrigated, rainfed upland, and lowland. Madagascar has the largest rice fields, which represent around 15% of

all of Africa (Diagne et al., 2013). However, the rice fields, which have been divided for generations, diminish in size in the Highland of Madagascar (Andrianantoandro & Bélières, 2015). Moreover, smallholder farmers had constraints due to pests and weeds for rainfed rice and water management and infrastructure problems for irrigated rice in the eastern part of Madagascar (Dröge et al., 2020). On the other hand, global climate change effects would affect rice crop growth and production (Lanka, 2004; van Oort & Zwart, 2018). Randriamarolaza et al. (2022) found that the amount of precipitation decreased, and drought events appeared frequently during September–October–November. Therefore, some studies have been set up to tackle such issues. For instance, Saito et al. (2018) focused their research on the improvement of crop varieties in the tropics, especially for rainfed upland rice crops. Fujisaka (1990) established for the western part of Madagascar, three and four research priorities on rainfed lowland and upland rice, respectively. In Madagascar, promoting upland rice cultivation is one key major to increasing rice production.

In Africa, Baskin (2022) noticed that climate change might decrease maize production as it affected the growth stages of maize crops. Therefore, Epule et al. (2022) highlighted that increasing maize yields did not depend only on increasing harvest area. They recommended thinking about high-yielding and drought-tolerant varieties as well as climate-smart information to brief farmers about changes in the growing season. For instance, Kostandini et al. (2013) indicated the benefits earned from drought-tolerant maize.

The objective of this work is to understand the effects of the changing climate on rainfed maize and rice crops in Madagascar by studying the characteristics of the rainy season, its onset, duration, and cessation, and formulating crop calendars for the present and future based on observed and projected climate data.

The remainder of the paper is organized as follows: Section 2 describes the data and methodology. Section 3 presents key findings. Finally, Section 4 sets out both the discussion and the conclusion.

2 | DATA AND METHODOLOGY

2.1 | Data

This study uses observational data (OBS) provided by the Directorate General of Meteorology of Madagascar (DGM) and Global climate projection data from the Sixth Phase of the Coupled Model Inter-comparison Project (CMIP6).

OBS consists of 26 quality controlled and homogenized time series of daily atmospheric precipitation sums. The time series were developed by Randriamarolaza et al. (2022). The spatial location of the corresponding weather stations on the territory of Madagascar is shown in Figure 1. Their data period covers 1950–2018.

Global Climate Models (GCMs) projection data are obtained from the CMIP6 under the Shared Socioeconomic Pathways SSP245 and SSP585 scenarios. Their data range from 2030 to 2100. They are publicly available through the Earth System Grid Federation (https://esgf-node.llnl.gov/, last visited on May 2022). Three criteria were set out to select the GCMs, which are:

- Native resolution of GCMs is 100 km
- GCMs products contain daily precipitation
- GCMs are chosen from the five ensemble members, which have different realizations but similar initialization methods, perturbed physics, and forcing as in Randriamarolaza et al. (2023). However, ensemble members should contain at least two GCMs.

The selected GCMs are listed in Table 1. The number of GCMs and ensemble members is the same for both SSP245 and SSP585 scenarios. A Madagascar land mask was used to extract daily precipitation from GCMs. Then, the data of spatial resolution were converted to 1 degree by 1 degree using "remapbil" function in the Climate Data Operators (CDO) package (Schulzweida et al., 2017). Afterward, we created a multimodel ensemble mean for each five ensemble members by employing "ensmean" function in CDO. Then, all multimodel ensemble means were ensembled to build a super-ensemble model. From the super-ensemble model, the data were interpolated to the weather station locations by means of the nearest-neighbor method.

2.2 | Methodology

Our analysis consists of two steps: the determination of the rainfall season characteristics (onset, cessation, length) defined according to the local climate and the needs of each crop and the definition of the crop calendar. The analysis, detailed in the remainder of this section, is performed with self-developed software INCLICS, available at https://github.com/Lucmto/INCLICS.

2.2.1 | Rainy season characteristics

Madagascar is an island in the Indian Ocean. It is boarded by the Indian Ocean at the East and Mozambique channel at the West. The rainy season straddles 2 years. Climatologically, the rainy season lasts from November to April. As the rainy season may start and end either earlier or later,

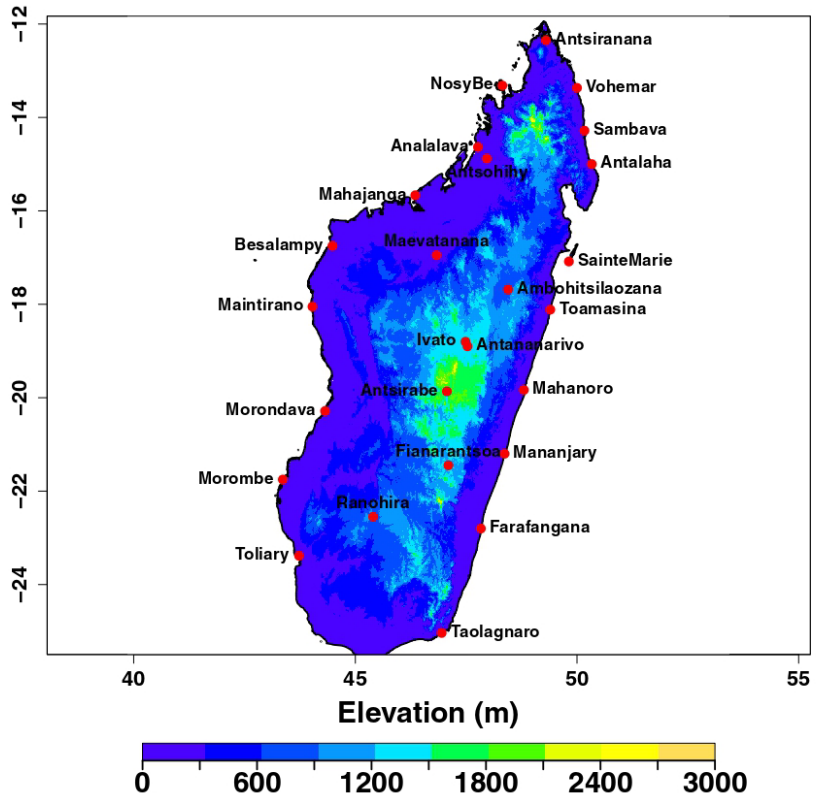

FIGURE 1 Spatial location of the synoptic weather stations on the territory of Madagascar and its topography.

TABLE 1 GCMs list.

	MRI-ESM2-0	CESM2-WACCM	CESM2	BCC-CSM2-MR
r1i1p1f1	x	x		x
r2i1p1f1	x	x		
r3i1p1f1	x	x		
r4i1p1f1	x	x	x	
r5i1p1f1	x	x		

we set the rainy season from August to July. Rice and maize are the main crops in Madagascar. Oldeman (1990) established the agroclimatology zones favorable for growing rice in Madagascar. He calculated the monthly precipitation and potential evapotranspiration ratio to define water availability. He found nine zones to be potentially adequate for rice cultivation. However, a poor irrigated rice system exists in Africa and Madagascar.

Therefore, most farmers especially smallholder farmers grow rice and maize crops following the rainy season. Rainfed lowland and upland rice are the types of rice cultivation in Madagascar.

In this paper, we improve the criteria by using daily precipitation instead of monthly precipitation to define the onset and cessation dates of the rainy season. Liebmann et al. (2012) determined that the onset and cessation dates occurred when daily precipitation are greater and lower than the annual daily average respectively. However, this definition gives only potential dates of the start and end of the rainy season. This may cause a high

TABLE 2 Literature review of onset and cessation dates definition.

ZAE	Onset definitions	Cessation definitions	Countries	Crops	References
Sahel	First occasion after May 1 that the 10- day total exceeds half the evaporation assuming a daily evaporation of 5 mm. Date after 1 May when rainfall accumulated over three consecutive days was at least 20 mm and when no dry spell within the next 30 days exceeded 7 days.		Mali Southern Sahelian and Sudanian of West Africa	Cereal crops (maize, millet, sorghum)	Akinseye et al., (2016), Sivakumar, (1988)
Savanna	20 mm in 2 days or at least 2 days of rainy days within 7 days and no dry spell within the next 21 days exceeded 7 days. 30 mm within 10 days, after which there is no dry spell longer than seven (7) days within the next 30 days.	10 mm in 10 days after which no rain falls for the next 10 days.	Mali Ghana	Cereal crops (maize, millet, sorghum) Maïze	Akinseye et al., (2016), Kasei & Afuakwa, (1991)
Guinea	20 mm in 2 days or at least 2 days of rainy days within 7 days and no dry spell within the next 21 days exceeded 7 days.			Cereal crops (maize, millet, sorghum)	Akinseye et al., (2016)
	Def1: 25 mm in 5 days and at least 2 days of rainy days (which are 0.1 mm) and no dry spell more than 7 days within 30 days. Def2: 25 mm in 6 days and no dry spell more than 10 days within 40 days.		Mali and Burkina Faso		Dodd & Jolliffe, (2001)
	First occasion after May 1st with more than 20 mm of rain in 2 days and with no dry spell of 10 days or more in the next 30 days.	First day after September 1st when soil with a 60 mm water-holding capacity gets completely depleted, assuming daily evapotranspiration rate of 5 mm and remains depleted for at least 5 consecutive days without recovering to maximum capacity in the next 15 days respectively.	Southwest Burkina Faso and Upper East Ghana.		Boansi et al., (2019)

rate of false alarms, especially for onset dates. Therefore, we learn from the knowledge of different research studies listed in Table 2. Rice crops are more sensitive to drought than maize crops. Moreover, water stress is more important in rice than in maize crops. We establish two definitions of the onset of the rainy season according to the rice and maize crops respectively. For rice crops, we define the onset dates as the first day after August 1 with more than 20 mm of rain in 2 days and at least 2 days of rainy days within 5 days and no dry spell within the next 21 days exceeding 7 days. This definition ascertains the availability of water for juvenile rice plants, especially for upland rice. For maize crops, we define the onset dates as the first day after August 1 with more than 25 mm of rain in 7 days and no dry spell within the next 21 days exceeding 10 days. Maize crops can grow without excessive rainy days. Notice that a dry day is a day with less than 0.85 mm of rainfall. These definitions avoid false alarms.

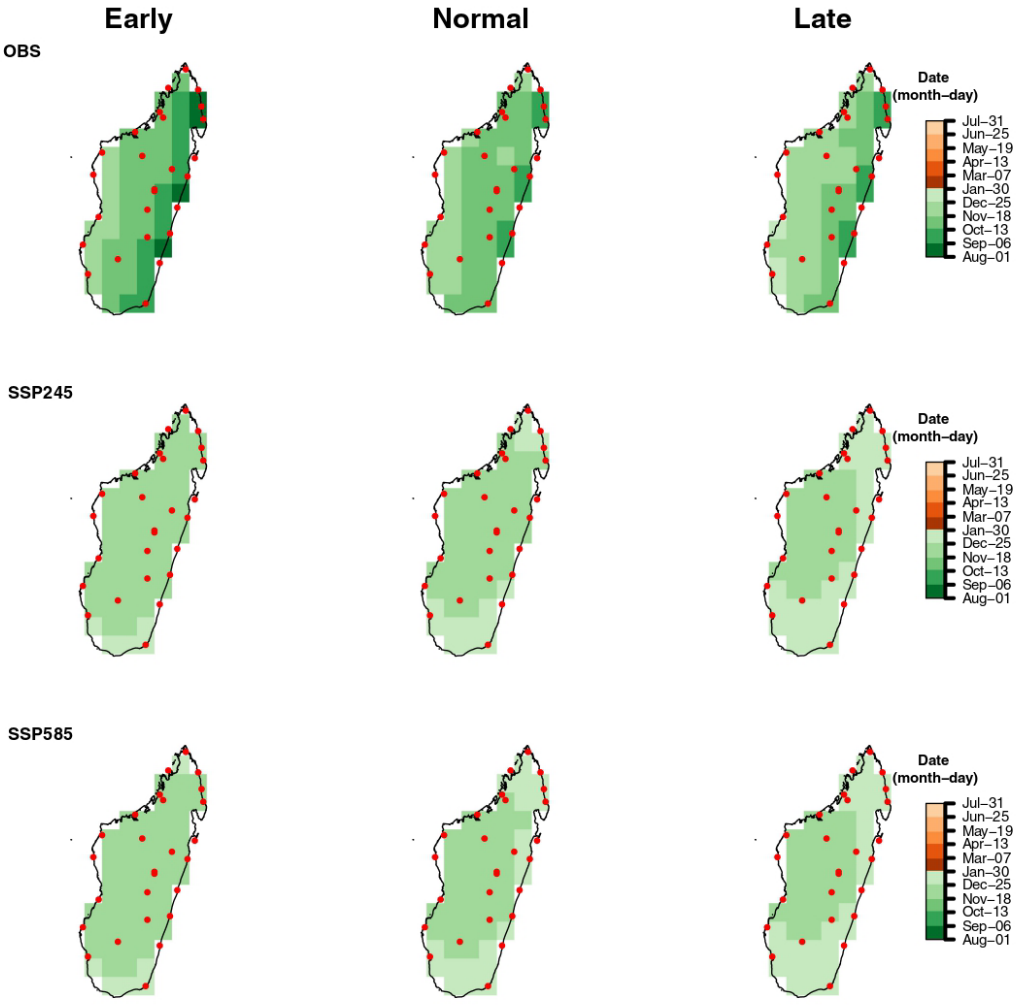

FIGURE 2 (a) Rainy season onset dates for rice crops. Dots represent synoptic weather stations. (b) Rainy season onset dates for maize crops. Dots represent synoptic weather stations.

The similar cessation dates definition adopted by Boansi et al. (2019) depending on the soil's water-holding capacity and daily evapotranspiration (PET) is applied. Soil's water-holding capacity depends on soil texture and other factors such as soil preparation on fertilizers and nutrients. Mostly, soil texture is defined by sand, silt, and clay percentage. Oldeman (1990) described that Ferrallisol is the major soil type in Madagascar. In the middle West of Madagascar, the percentage of sand, silt, and clay are 47%, 21%, and 32%, respectively (Fujisaka, 1990). According to a workshop note prepared by Armstrong et al. (2001), this texture is classified as clay loam. Therefore, its water-holding capacity is 150 mm. Oldeman (1990) found that PET reaches more than 6 mm/day during the summertime, especially in the western part. It decreases to 2 mm/day over the wintertime, especially in the highland or central land of Madagascar. Therefore, we set the PET value to 5 mm/day. By gathering those elements, we define the cessation dates as the first day after March 1 when soil with a 150 mm water-holding capacity gets completely depleted, assuming a daily evapotranspiration rate of 5 mm/day and remains depleted for at least five consecutive days without recovering to maximum

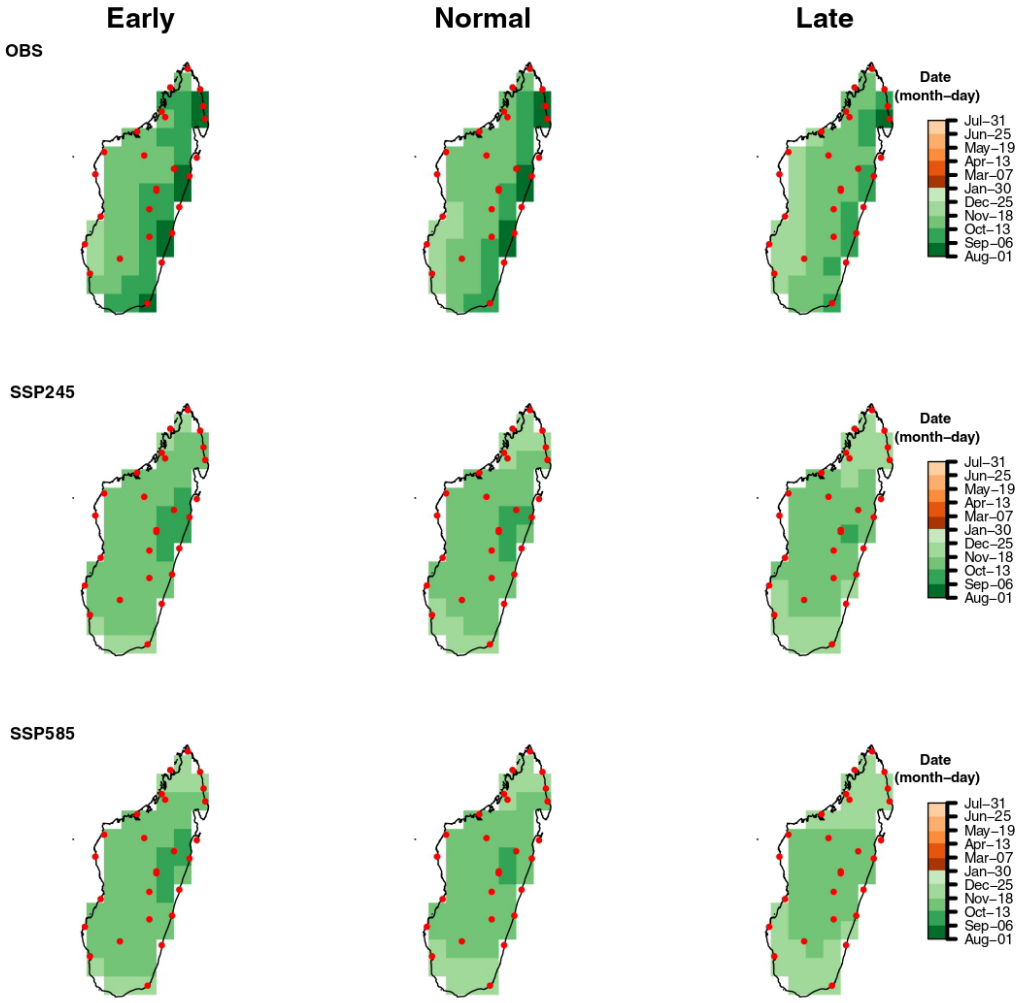

FIGURE 2 (Continued)

capacity in the next 15 days respectively. This definition is applied to rice and maize crops.

As explained by de Shannon (2021), onset and cessation dates are supposed to be normally distributed. Then they are classified as early, normal, and late when their probabilities are less than 0.33, between 0.33 and 0.67, and greater than 0.67, respectively. The length of the rainy season is the number of days between the onset and cessation dates.

These definitions have been applied to OBS and CMIP6 under SSP245 and SSP585 scenarios.

The onset dates, cessation dates, and the length of rainy season deduced from OBS are spatialized using inverse distance weighted (IDW) interpolation to 1 degree by 1 degree resolution. IDW was predominantly used to interpolate rainfall as Chen and Liu (2012), Muzakky et al. (2022), and de Oliveira Aparecido et al. (2022) used it to estimate spatial rainfall in Tawain, Indonesia, and Brazil, respectively. This step converts the onset dates, cessation dates, and length of rainy season deduced from OBS to have the same resolution as CMIP6 under SSP245 and SSP585 scenarios. This permits to calculate the spatial differences between OBS and CMIP6 under SSP245 and SSP585 scenarios. The results highlight the evolution of onset dates, cessation dates, and length of rainy season in the future.

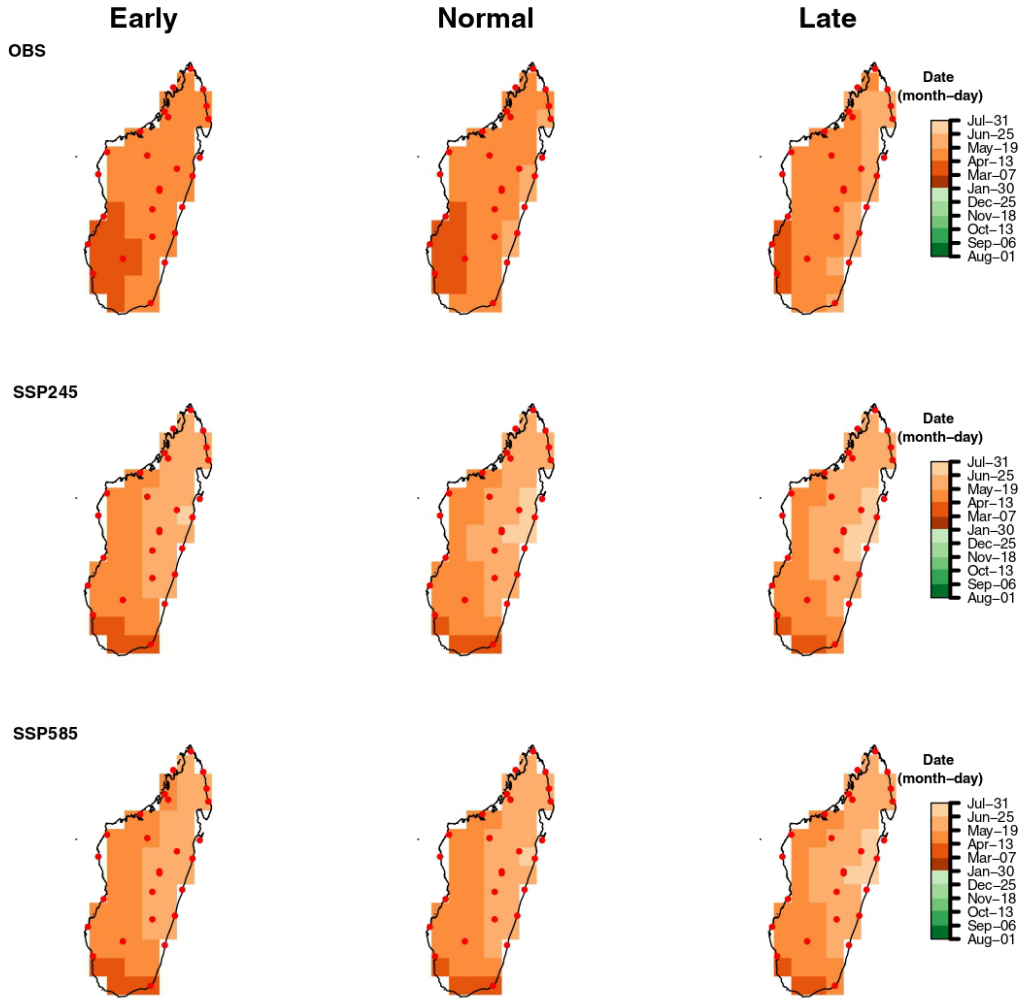

FIGURE 3 Rainy season cessation dates for rice and maize crops. Dots represent synoptic weather stations.

2.2.2 | Crop calendars

In general, farmers needed decadal information on climate or weather to manage crop growth. The rice and maize crop calendars are established by referring to the latest date for sowing or seeding. The seeding period is the dates range between the earliest and latest of seeding dates. Thus, the harvesting period is defined by the earliest and latest dates to start the harvest. In this paper, we transform the rainy season to fit the rice and maize crops' growing seasons. Crop varieties are different following their length of crop cycle (LCC). In Madagascar, LCC is classified into three categories: short (S), medium (M), and long (L). It is 105, 130, and 145 days (90, 120, and 150 days) for rice (maize) crop varieties respectively. We suppose that the growing season does not end later than late cessation dates. Then, we combine crop cycle lengths and late cessation dates to determine the latest dates for sowing or seeding. Thereafter, crop

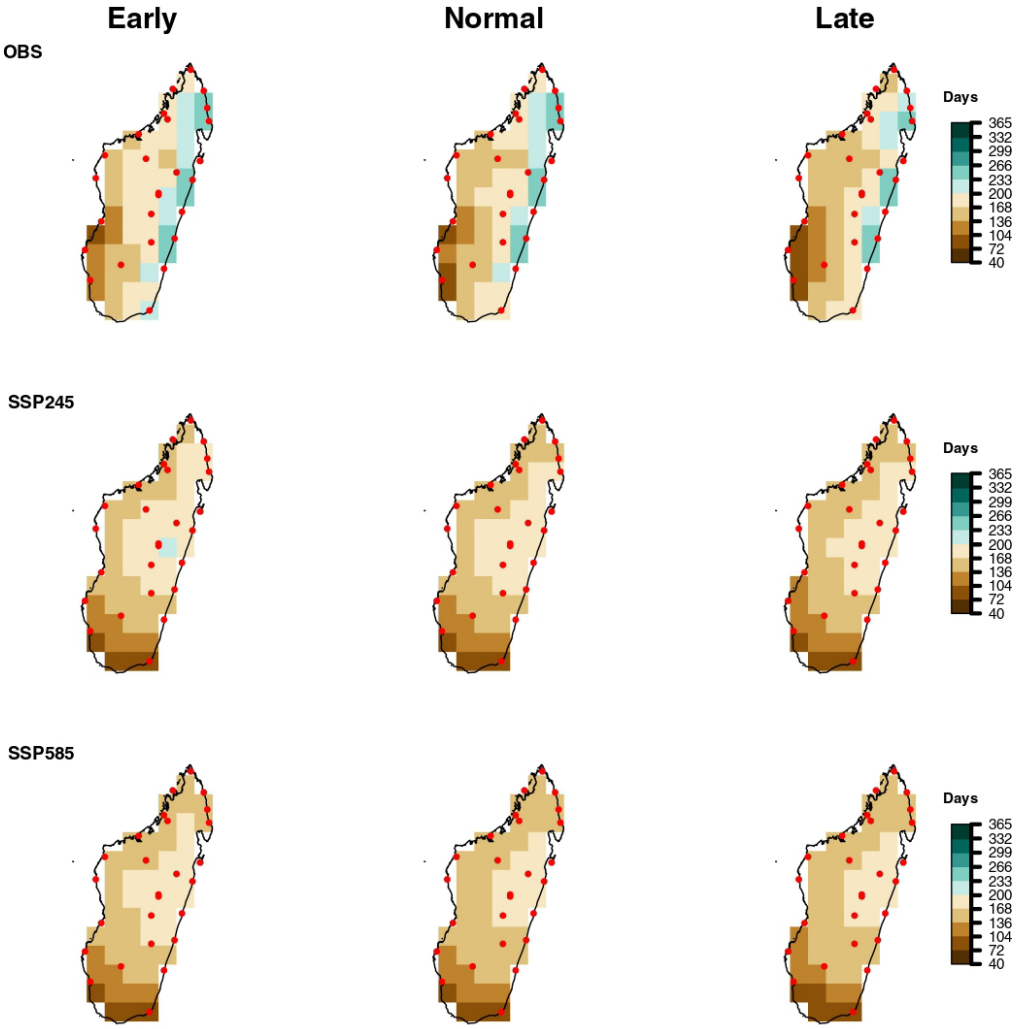

FIGURE 4 (a) Rainy season duration for rice crops. Dots represent synoptic weather stations. (b) Rainy season duration for maize crops. Dots represent synoptic weather stations.

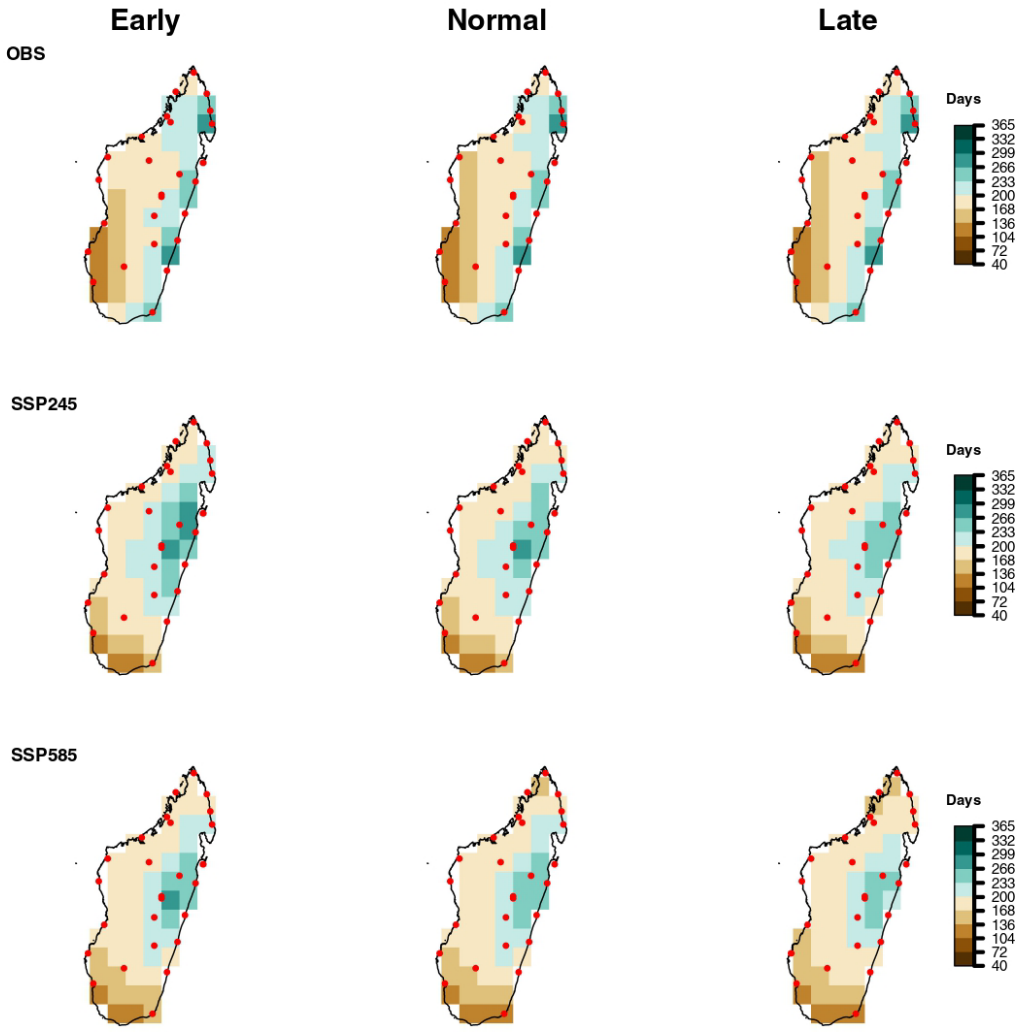

FIGURE 4 (Continued)

calendars are established and contained the sowing or seeding and harvesting periods. The crop calendars are established for each weather station location. They are grouped in five regions such as North (NosyBe, Antsiranana, Vohemar, Antalaha, Sambava), West (Mahajanga, Maintirano, Besalampy, Maevatanana, Analalava, Antsohihy), Highland (Ambohitsilaozana, Antananarivo, Ivato, Antsirabe, Fianarantsoa, Ranohira), East (Sainte Marie, Toamasina, Mahanoro, Mananjary, Farafangana, Taolagnaro), South-west (Toliary, Morombe, Morondava). Then the results obtained from OBS and CMIP6 under SSP245 and SSP585 scenarios are compared, especially the mean length of sowing or seeding period for each region.

3 | RESULTS

3.1 | Rainy season characteristics

Figure 2a, b shows onset dates for rice and maize. In the past, the earliest, and latest onset dates happen in the East (August–September) and the South-west

(December–January) respectively. Rice onset dates lagged maize 1 month, that is, November–December (October–November) see the majority of normal onset dates for rice (maize). In the future, the onset dates are delayed. They shift from November (October) to January (December) for rice (maize). Moreover, we observe the latest onset dates in the North and the South. Instead of September–October, the onset dates become December–January for rice during the late rainy season in the East.

Figure 3 displays cessation dates for rice and maize. The earliest and latest cessation dates are March–April and June–July, respectively. The earliest cessation dates remain in the South. However, this situation is more tangible in the South-east than South-west in the future. Furthermore, the cessation dates extend to May–June in Highland in the future. Generally, the early (late) onset dates are associated with the late (early) cessation dates.

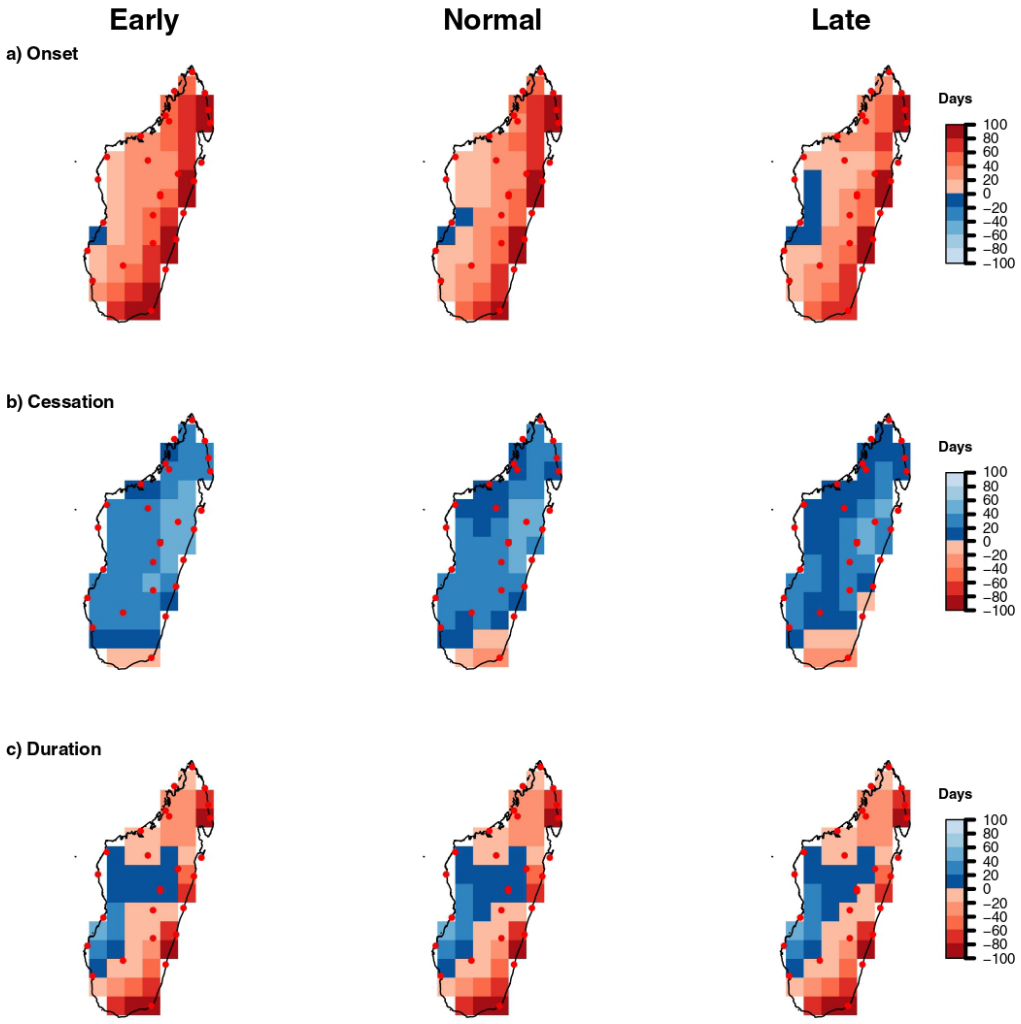

FIGURE 5 (a) Spatial differences between OBS and CMIP6 under SSP245 scenario according to rice growing conditions. Dots represent synoptic weather stations. (b) Spatial differences between OBS and CMIP6 under SSP585 scenario according to rice growing conditions. Dots represent synoptic weather stations.

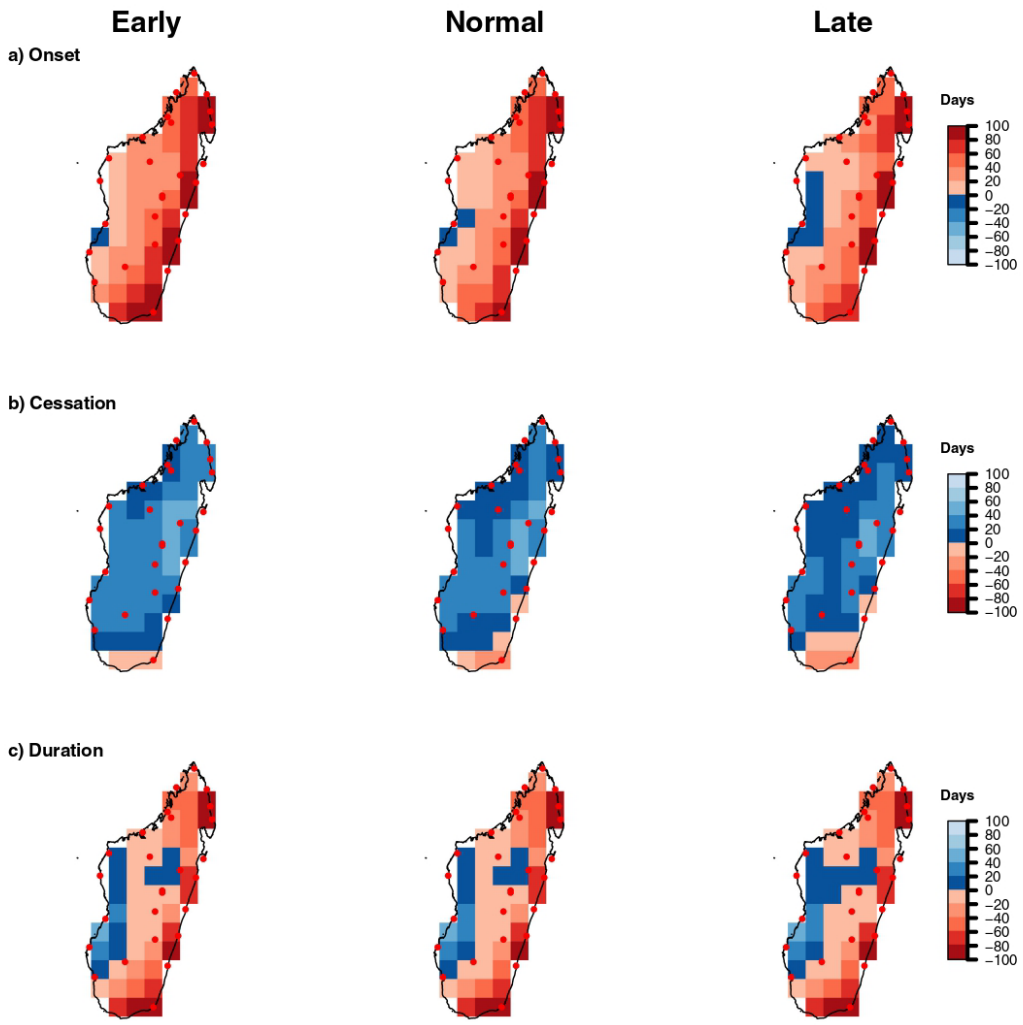

FIGURE 5 (Continued)

These results reflect the variability of the rainy season duration. Figure 4a, b exhibits that the rainy season duration is more than 200 days in the East and the North. Nevertheless, It becomes less than 200 days for rice in the future. Alongside, a significant improvement in rainy season duration, more than 200 days, is seen for maize on Highland. Mostly, the reduction of rainy season duration affects the North, East, and South-east in the future. The reduction is between 20 and 80 days.

This is because the onset and cessation dates are late and early, respectively. For instance, the worst situation is in the South-east. However, some parts of West and Highland or Central land benefit from the lengthening of the rainy season duration. For instance, the best illustration is the case of the South-west (see Figures 5a, b, and 6a, b).

3.2 | Rice and maize crop calendars

The sowing or seeding period starts principally from August to December for rice and maize crops in the observation period. It is shifted from November to January,

especially for rice crops in the future. This situation postpones the harvesting period. On the one hand, the negative impacts are more important for rice than maize crops, especially in the North and East. For instance, all districts grew predominately rice and maize crops twice a year in the North and East. Nevertheless, any and short rice crops can be grown twice a year respectively for North and East in the future (Figures 7a and 8a). Regarding maize crops, all (i.e., short, medium, and long) and only short varieties may be grown for East and North respectively, but the harvesting period is postponed in January instead of November (Figures 7b and 8b). Moreover, Tables 3 and 4 ascertain the decreases in the length of sowing or seeding period of more than 75 (70) and 100 (35) days for rice (maize) crops in the North and East, respectively. Insignificant changes are seen for the West as the length of sowing

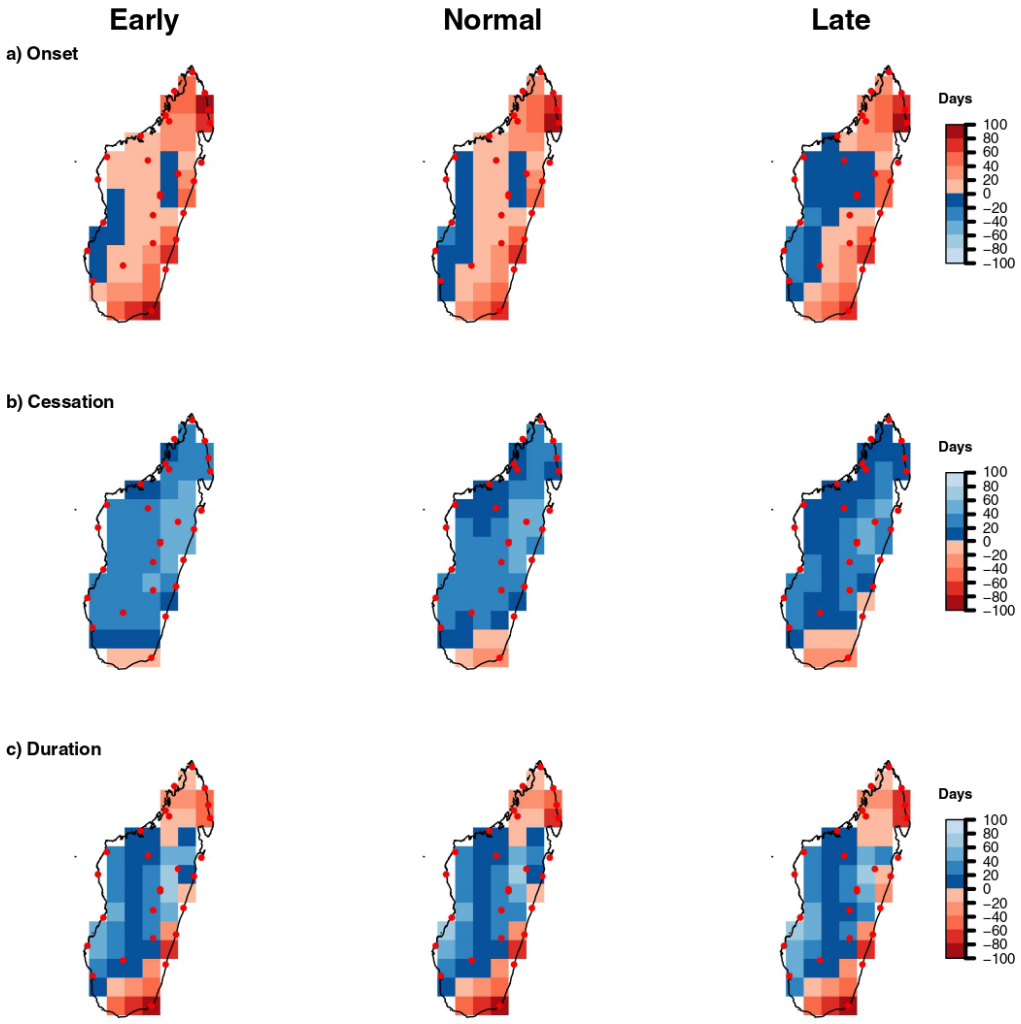

FIGURE 6 (a) Spatial differences between OBS and CMIP6 under SSP245 scenario according to maize growing conditions. Dots represent synoptic weather stations. (b) Spatial differences between OBS and CMIP6 under SSP585 scenario according to maize growing conditions. Dots represent synoptic weather stations.

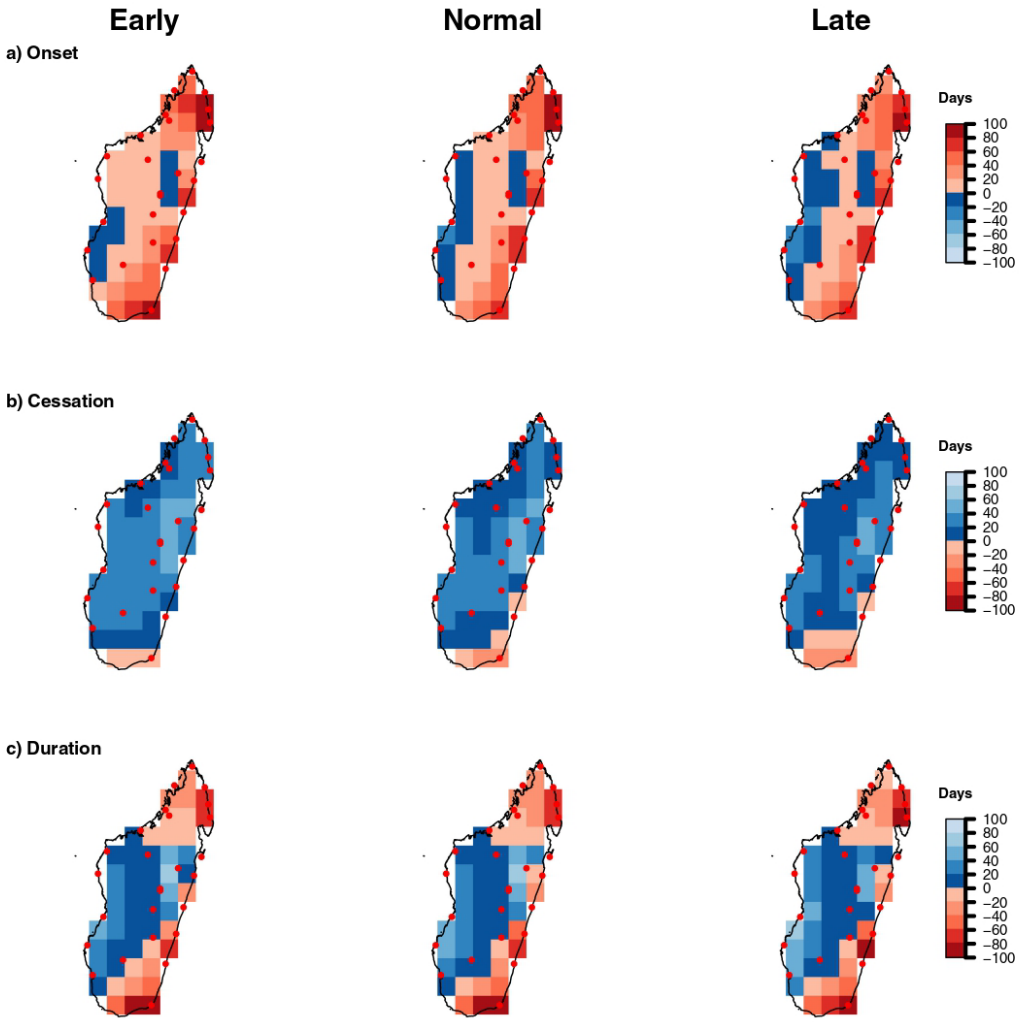

FIGURE 6 (Continued)

or seeding period diminishes around 10 and 2 days for rice and maize crops respectively in the future (Figures 9a, b, Tables 3 and 4). On the other hand, the positive impacts are observed in the Highland and South-west. The length of the sowing or seeding period increases to around 10 and 30 days for rice and maize crops respectively in the future (Tables 3 and 4). The granary rice of Madagascar (i.e., Ambohitsilaozana) may have a chance to improve rice growth conditions (Figure 10a). As the South has a dry climate, rice crops are mostly not suitable. However, a new opportunity may be observed in the future as far as growing rice and maize crops are concerned (Figure 11a, b).

4 | DISCUSSION AND CONCLUSIONS

This paper uses the state-of-the-art science to produce climate and weather information critically important for agriculture sectors. The quality of climate and weather datasets

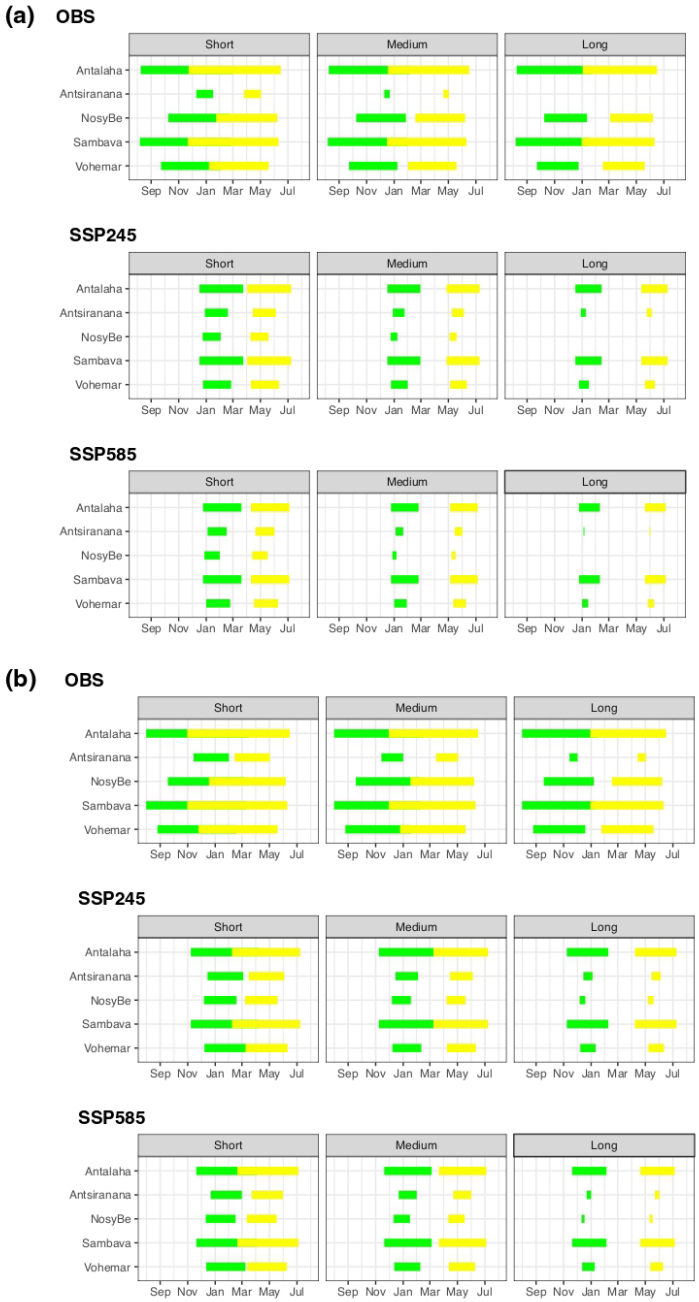

FIGURE 7 (a) Rice crop calendars for North. Green and Yellow colors represent the sowing or seeding and harvesting periods respectively. (b) Maize crop calendars for North. Green and Yellow colors represent the sowing or seeding and harvesting periods respectively.

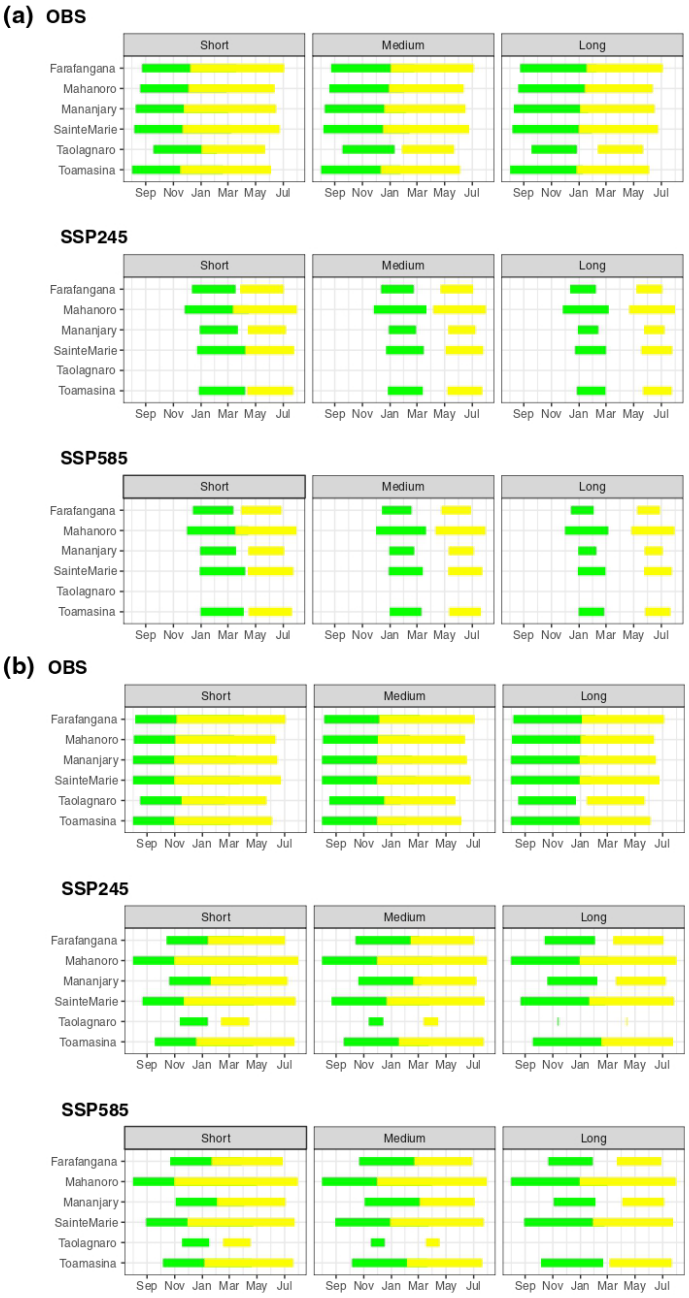

FIGURE 8 (a) Rice crop calendars for East. Green and Yellow colors represent the sowing or seeding and harvesting periods respectively. (b) Maize crop calendars for East. Green and Yellow colors represent the sowing or seeding and harvesting periods respectively.

is assessed. For instance, OBS datasets are quality controlled and homogenized (Randriamarolaza et al., 2022). Climate model simulation datasets are taken from the Sixth Phase of the Coupled Model Inter-comparison Project

TABLE 3 Mean length of sowing or seeding period for rice crops in days.

Regions	North			West			Highland			East			South-west		
LCC	S	M	L	S	M	L	S	M	L	S	M	L	S	M	L
OBS	142	117	103	59	34	20	70	45	30	192	168	153	0	0	0
SSP245	69	45	30	49	24	9	83	58	43	88	68	56	19	5	0
SSP585	60	35	21	47	22	7	80	54	40	83	62	50	21	6	1

TABLE 4 Mean length of sowing or seeding period for maize crops in days.

Regions	North			West			Highland			East			South-west		
LCC	S	M	L	S	M	L	S	M	L	S	M	L	S	M	L
OBS	174	145	115	91	61	31	100	70	40	221	192	162	9	0	0
SSP245	109	80	50	90	60	30	134	104	75	190	160	130	58	29	9
SSP585	98	69	39	88	58	28	128	99	69	179	149	119	57	29	9

(Eyring et al., 2016) under the Shared Socioeconomic Pathway SSP245 and SSP585 scenarios (O'Neill et al., 2017). Babaousmail et al. (2021) showed that the multi-model ensemble had a performance in simulating the spatial pattern of rainfall over North Africa. Monteverde et al. (2022) ascertained the performance of GCMs, especially with the ensemble model, to produce precipitation in the Amazon River Basin in Brazil. This paper studies daily rainfall to draw rainy season characteristics and crop calendars. Based on these previous studies, we built a super-ensemble model. The CDO software, written by Schulzweida et al. (2017), is used to realize the spatial comparisons between observation and projection datasets. Besides, in-depth research on literature review was helpful to define and set up criteria for rainy season characteristics, which fit rainfed rice and maize crops on water needs. Then crop calendars were deduced by mixing rainy season characteristics and the length of crop cycles. The main results on rainy season characteristics indicate that the past results agree with Oldeman (1990). The early and late onset dates are always started in the East and the South respectively. The opposite is observed for the cessation dates. The length of rainy season is between 70 (in the South) and 300 (in the East) days. Major zones have a length of rainy season between 100 and 200 days. They are mostly found in Central land or Highland. Oldeman (1990) identified that these zones represented 36% and rainy season was from November to April. Precisely, early and late onset dates may occur in October and December, respectively. Moreover, early and late cessation dates may be April and May, respectively.

The consideration of climate projections under SSP245 and SSP585 scenarios allows us to value the opportunities and constraints for growing rice and maize crops in the future. Mostly, the onset and cessation dates became late (December–January) and early (March–April), respectively. This involves the shortening of the rainy season duration as well as the displacement of the sowing or seeding period. Therefore, rice crops were principally more sensitive to the changes than maize crops. Egbebiyi et al. (2019) also noticed that the suitability of maize crop growth conditions was improved than cassava and pineapple crops in West Africa. On the one hand, positive impacts were observed in Highland and South. Crop calendars stated that the South might have a chance to grow short or medium rice and maize crops. These opportunities might be due to the increase in rainfall associated with tropical cyclones under climate change effects (Otto et al., 2022). Moreover, Fitchett and Grab (2014) pointed out that no statistically significant trends were found for the frequency of tropical cyclone landfalls in Madagascar and Mozambique, despite their trajectories seeming to move to the South of Madagascar. Besides, Gerardeaux et al. (2012) showed the positive effects of climate change on rice production in the Highland. We find an extension of the sowing or seeding period, especially for rice granaries in Ambohitsilaozana. Barimalala et al. (2021) highlighted that the 2.0°C global warning level generated an increase in total rainfall during the summertime, especially for West and South-west regions. These findings lined up with our findings, as the rice and maize growing conditions are improving in the West and South-west. For instance, the length of rainy season increases in the future. On the other hand, negative impacts were seen in the North and East of Madagascar. For instance, the South-east was mainly affected. The length of the rainy

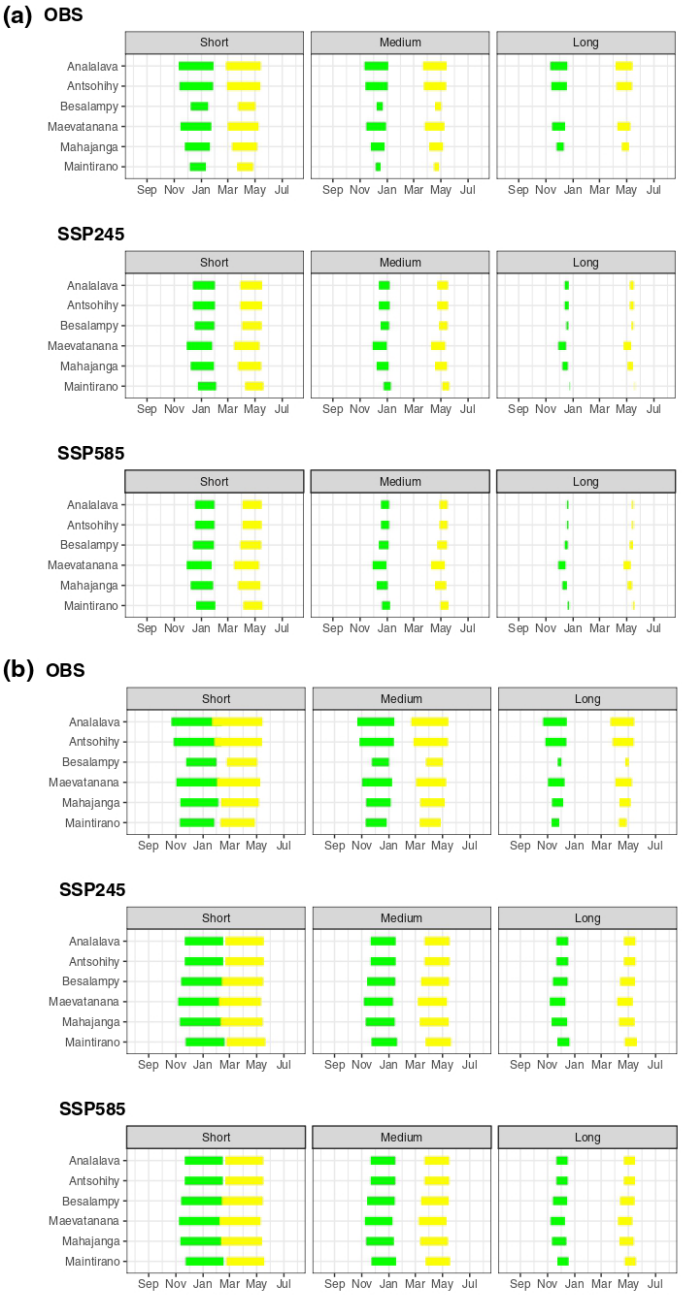

FIGURE 9 (a) Rice crop calendars for West. Green and Yellow colors represent the sowing or seeding and harvesting periods respectively. (b) Maize crop calendars for West. Green and Yellow colors represent the sowing or seeding and harvesting periods respectively.

season was from 70 (100) to 100 (140) days concerning rice (maize) crop needs. A previous paper by Dröge et al. (2020) confirmed that pests and water were the factors limiting rice yields in eastern Madagascar. Furthermore, Barimalala

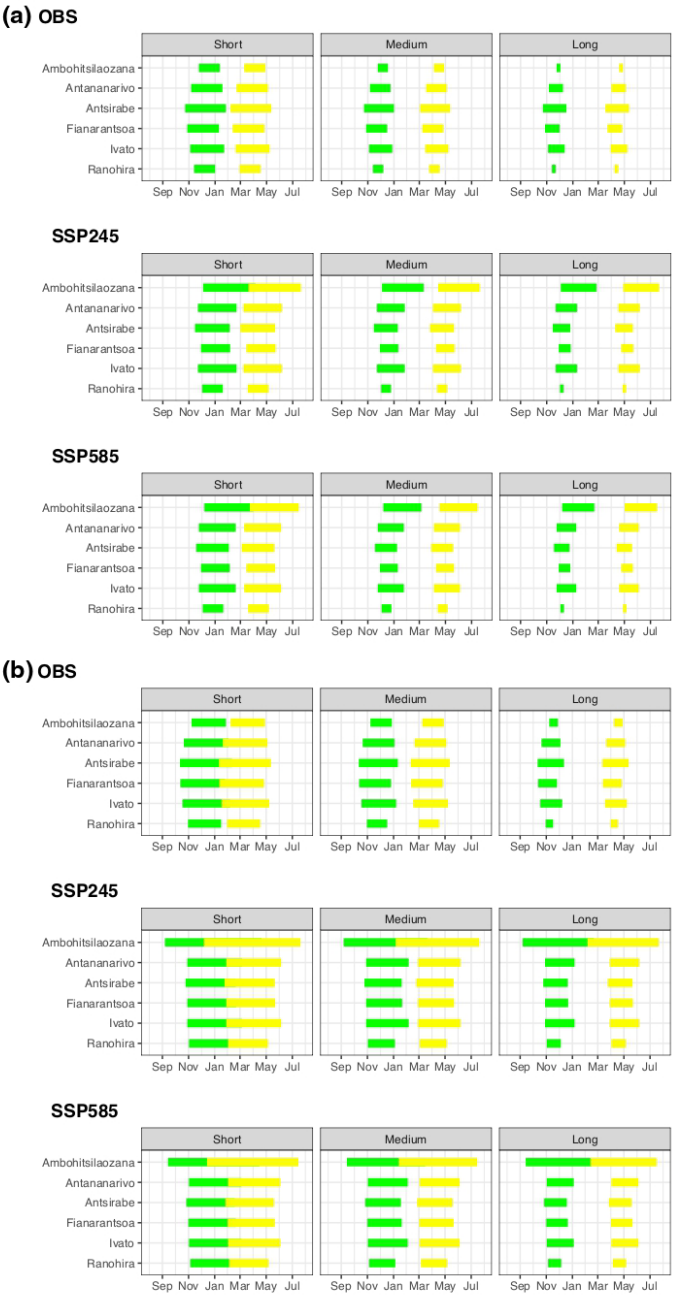

FIGURE 10 (a) Rice crop calendars for Highland or Central land. Green and Yellow colors represent the sowing or seeding and harvesting periods respectively. (b) Maize crop calendars for Highland or Central land. Green and Yellow colors represent the sowing or seeding and harvesting periods respectively.

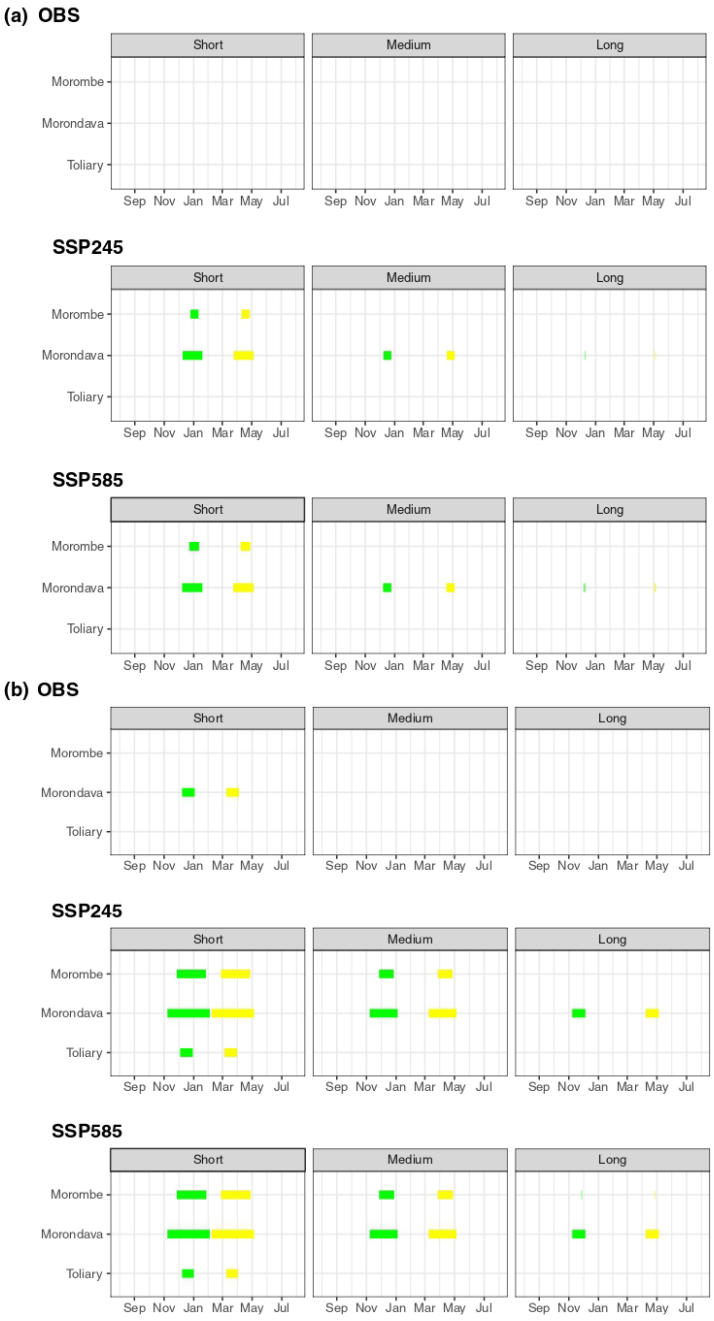

FIGURE 11 (a) Rice crop calendars for South-west. Green and Yellow colors represent the sowing or seeding and harvesting periods respectively. (b) Maize crop calendars for South-west. Green and Yellow colors represent the sowing or seeding and harvesting periods respectively.

et al. (2021) pointed out that the North and East were subject to a deficit in total rainfall. In the North and East, a significant diminution in the length of the sowing or seeding period was observed. Nevertheless, the interpretation of the results should be taken with caution for food policies.

As climate change adaptation and coping strategies, Madagascar has implemented a system of rice intensification (Thakur & Uphoff, 2017) and conservation agriculture (Bruelle et al., 2015). New seeds, with shortened crop cycles, drought tolerance, and resistance to storm damage, were developed and introduced. For instance, new rice crop varieties were tested such as NERICA stands for New Rice for Africa (Somado et al., 2008). This variety supports the temperate climate in Highland or Central land where the minimum temperature may reach lower than 5°C. Our findings might reinforce and contribute to improving these techniques for increasing rice or maize yield production. Nevertheless, this paper could be upgraded by adding other variables than precipitation, by focusing on crops' phenology for further details on crops calendars. Further research might concern the seasonal forecast of onset and cessation dates as done in East and West Africa (MacLeod, 2018; Rauch et al., 2019).

AUTHOR CONTRIBUTIONS

Luc Yannick Andréas Randriamarolaza: Conceptualization (equal); data curation (equal); formal analysis (equal); investigation (equal); methodology (equal); resources (equal); software (equal); visualization (equal); writing – original draft (equal); writing – review and editing (equal). **Enric Aguilar:** Conceptualization (equal); funding acquisition (equal); methodology (equal); project administration (equal); resources (equal); software (equal); supervision (equal); validation (equal); writing – review and editing (equal).

ACKNOWLEDGEMENTS

We acknowledge the Directorate General of Meteorology in Madagascar for sharing the climate data. We are also thankful to WMO's CREWS (see https://www.crews-initiative.org/en/projects visited on 22 December 2022), APA, and ENANDES projects (see https://www.adaptation-fund.org/project/chile-colombia-peru-enhancing-adaptive-capacity-andean-communities-climate-services-enandes/visited on 22 December 2022).

FUNDING INFORMATION

This work is done with the financial support of the INDECIS project, which is a part of ERA4CS, an ERA-NET initiated by JPI Climate, and funded by FORMAS (SE), DLR (DE), BMWFW (AT), IFD (DK), MINECO (ES), ANR (FR) with co-funding by the European Union (Grant 690462).

DATA AVAILABILITY STATEMENT

The observational records that support the findings of this study are available on request from the corresponding author. The data are not publicly available due to privacy or ethical restrictions. However, the climate data simulations from CMIP6 are publicly available at the following URL/DOI: https://esgf-node.llnl.gov/search/cmip6/.

ORCID

Luc Yannick Andréas Randriamarolaza https://orcid.org/0000-0002-2939-2250
Enric Aguilar https://orcid.org/0000-0002-8384-377X

REFERENCES

Akinseye, F.M., Agele, S.O., Traore, P.C.S., Adam, M. & Whitbread, A.M. (2016) Evaluation of the onset and length of growing season to define planting date—"a case study for Mali (West Africa)". *Theoretical and Applied Climatology*, 124(3–4), 973–983. Available from: https://doi.org/10.1007/s00704-015-1460-8

Andrianantoandro, V.T. & Bélières, J.F. (2015) L'agriculture Familiale Malgache Entre Survie et Développement: Organisation Des Activités, Diversification et Différenciation Des Ménages Agricoles de La Région Des Hautes Terres. *Revue Tiers Monde*, 1(1), 69. Available from: https://doi.org/10.3917/rtm.221.0069

Armstrong, D., Cotching, B. & Bastick, C. (2001) Assessing your soil resources for irrigation. *Tasmanian Departement of Primary Industries, Water and Environment* no. September, pp. 1–42.

Babaousmail, H., Hou, R., Ayugi, B., Ojara, M., Ngoma, H., Karim, R. et al. (2021) Evaluation of the performance of Cmip6 models in reproducing rainfall patterns over North Africa. *Atmosphere*, 12(4), 475. Available from: https://doi.org/10.3390/atmos12040475

Barimalala, R., Raholijao, N., Pokam, W. & Reason, C.J.C. (2021) Potential impacts of 1.5°C, 2°C global warming levels on temperature and rainfall over Madagascar. *Environmental Research Letters*, 16(4), 044019. Available from: https://doi.org/10.1088/1748-9326/abeb34

Baskin, C.C. (2022) Effects of climate change on annual crops: the case of maize production in Africa. In: *Plant regeneration from seeds: a global warming perspective*. Cambridge, MA: Academic Press, pp. 213–228. Available from: https://doi.org/10.1016/B978-0-12-823731-1.00020-2

Boansi, D., Tambo, J.A. & Müller, M. (2019) Intra-seasonal risk of agriculturally-relevant weather extremes in west African Sudan savanna. *Theoretical and Applied Climatology*, 135(1–2), 355–373. Available from: https://doi.org/10.1007/s00704-018-2384-x

Bruelle, G., Naudin, K., Scopel, E., Domas, R., Rabeharisoa, L. & Tittonell, P. (2015) Short-to mid-term impact of conservation agriculture on yield variability of upland Rice: evidence from Farmer's fields in Madagascar. *Experimental Agriculture*, 51(1), 66–84. Available from: https://doi.org/10.1017/S0014479714000155

Chen, F.W. & Liu, C.W. (2012) Estimation of the spatial rainfall distribution using inverse distance weighting (IDW) in the middle of Taiwan. *Paddy and Water Environment*, 10(3), 209–222. Available from: https://doi.org/10.1007/s10333-012-0319-1

de Oliveira Aparecido, L.E., da Silva Cabral de Moraes, J.R., de Lima, R.F. & Torsoni, B.G. (2022) Spatial interpolation techniques to map rainfall in Southeast Brazil. *Revista Brasileira de Meteorologia*, 37(1), 141–155. Available from: https://doi.org/10.1590/0102-77863710015

de Shannon, R. (2021) Manual for creating a weather-based crop calendar. WMO agricultural meteorology report series.

Diagne, A., Amovin-Assagba, E., Futakuchi, K. & Wopereis, M.C.S. (2013) Estimation of cultivated area, number of farming households and yield for major rice-growing environments in Africa. *Realizing Africa's Rice Promise*, no. September 2015, 35–45. Available from: https://doi.org/10.1079/9781845938123.0035

Dodd, D.E.S. & Jolliffe, I.T. (2001) Early detection of the start of the wet season in semiarid tropical climates of Western Africa. *International Journal of Climatology*, 21(10), 1251–1262. Available from: https://doi.org/10.1002/joc.640

Dröge, S., Poudyal, M., Hockley, N., Mandimbiniaina, R., Rasoamanana, A., Andrianantenaina, N.S. et al. (2020) Constraints on rice cultivation in eastern Madagascar: which factors matter to smallholders and which influence food security? *Human Ecology*, 50, no. 0123456789, 493–513. Available from: https://doi.org/10.1007/s10745-022-00336-2

Egbebiyi, T.S., Crespo, O. & Lennard, C. (2019) Defining crop-climate departure in West Africa: improved understanding of the timing of future changes in crop suitability. *Climate*, 7(9), 10–12. Available from: https://doi.org/10.3390/cli7090101

Epule, T.E., Chehbouni, A. & Dhiba, D. (2022) Recent patterns in maize yield and harvest area across Africa. *Agronomy*, 12, 374. Available from: https://doi.org/10.3390/agronomy12020374

Eyring, V., Bony, S., Meehl, G.A., Senior, C.A., Stevens, B., Stouffer, R.J. et al. (2016) Overview of the coupled model intercomparison project phase 6 (CMIP6) experimental design and organization. *Geoscientific Model Development*, 9(5), 1937–1958. Available from: https://doi.org/10.5194/gmd-9-1937-2016

Fitchett, J.M. & Grab, S.W. (2014) A 66-year tropical cyclone record for South-East Africa: temporal trends in a global context. *International Journal of Climatology*, 34(13), 3604–3615. Available from: https://doi.org/10.1002/joc.3932

Fujisaka, S. (1990) Rice research priorities for Madagascar's middle west. IRRI research paper series 144.

Gerardeaux, E., Giner, M., Ramanantsoanirina, A. & Dusserre, J. (2012) Positive effects of climate change on rice in Madagascar. *Agronomy for Sustainable Development*, 32(3), 619–627. Available from: https://doi.org/10.1007/s13593-011-0049-6

Kasei, C.N. & Afuakwa, J.J. (1991) Determination of optimum planting date and growing season of maize in the northern savanna zone of Ghana. *IAHS-AISH Publication*, 199, 593–600.

Kostandini, G., La Rovere, R. & Abdoulaye, T. (2013) Potential impacts of increasing average yields and reducing maize yield variability in Africa. *Food Policy*, 43(December), 213–226. Available from: https://doi.org/10.1016/j.foodpol.2013.09.007

Lanka, S. (2004) Global climate changes and Rice food security. Delta, no. Table 1: 24–30. http://www.hechoenperu.org.pe/fao/docs/Agriculture/3-Nguyen.pdf

Liebmann, B., Bladé, I., Kiladis, G.N., Carvalho, L.M.V., Senay, G.B., Allured, D. et al. (2012) Seasonality of African precipitation from 1996 to 2009. *Journal of Climate*, 25(12), 4304–4322. Available from: https://doi.org/10.1175/JCLI-D-11-00157.1

MacLeod, D. (2018) Seasonal predictability of onset and cessation of the east African rains. *Weather and Climate Extremes*, 21(June), 27–35. Available from: https://doi.org/10.1016/j.wace.2018.05.003

Monteverde, C., de Sales, F. & Jones, C. (2022) Evaluation of the CMIP6 performance in simulating precipitation in the Amazon River basin. *Climate*, 10(8), 122. Available from: https://doi.org/10.3390/cli10080122

Muzakky, I., Noor, M., Prasetyowati, S. & Sibaroni, Y. (2022) Prediction map of rainfall classification using random forest and inverse distance weighted (IDW). *Building of Informatics, Technology and Science (BITS)*, 4(2), 723–731. Available from: https://doi.org/10.47065/BITS.V4I2.1978

Oldeman, L.R. (1990) An Agroclimatic characterization of Madagascar. International Soil Reference and Information Centre. ISRIC Technical paper 21.

O'Neill, B.C., Kriegler, E., Ebi, K.L., Kemp-Benedict, E., Riahi, K., Rothman, D.S. et al. (2017) The roads ahead: narratives for shared socioeconomic pathways describing world futures in the 21st century. *Global Environmental Change*, 42, 169–180. Available from: https://doi.org/10.1016/j.gloenvcha.2015.01.004

Otto, F.E.L., Zachariah, M., Wolski, P., Pinto, I., Barimalala, R., Nhamtumbo, B. et al. (2022) Climate change increased rainfall associated with tropical cyclones hitting highly vulnerable communities in Madagascar, Mozambique & Malawi. WWA-MMM-TS-Scientific Report, no. February.

Randriamarolaza, L.Y.A., Aguilar, E. & Skrynyk, O. (2023) Extreme temperatures detection and attribution related to external forcing in Madagascar. *International Journal of Climatology*, 43(8), 3907–3924. Available from: https://doi.org/10.1002/joc.8065

Randriamarolaza, L.Y.A., Aguilar, E., Skrynyk, O., Vicente-Serrano, S.M. & Domínguez-Castro, F. (2022) Indices for daily temperature and precipitation in Madagascar, based on quality-controlled and homogenized data, 1950–2018. *International Journal of Climatology*, 42(1), 265–288. Available from: https://doi.org/10.1002/joc.7243

Rauch, M., Bliefernicht, J., Laux, P., Salack, S., Waongo, M. & Kunstmann, H. (2019) Seasonal forecasting of the onset of the rainy season in West Africa. *Atmosphere*, 10(9), 528. Available from: https://doi.org/10.3390/atmos10090528

Saito, K., Asai, H., Zhao, D., Laborte, A.G. & Grenier, C. (2018) Progress in varietal improvement for increasing upland Rice productivity in the tropics. *Plant Production Science*, 21(3), 145–158. Available from: https://doi.org/10.1080/1343943X.2018.1459751

Sasson, A. (2012) Food security for Africa: an urgent global challenge. *Agriculture and Food Security*, 1(1), 1–16. Available from: https://doi.org/10.1186/2048-7010-1-2

Schulzweida, U., Kornblueh, L. & Quast, R. (2017) CDO user's guide. Guide, no. June: 1–206. https://code.zmaw.de/projects/cdo/embedded/cdo.pdf

Sivakumar, M.V.K. (1988) Predicting rainy season potential from the onset of rains in southern Sahelian and Sudanian climatic zones of West Africa. *Agricultural and Forest Meteorology*, 42(4), 295–305. Available from: https://doi.org/10.1016/0168-1923(88)90039-1

Somado, E.A., Guei, R.G. & Keya, S.O. (2008) *NERICA: the new rice for Africa – a compendium*. Cotonou, Benin: WARDA, p. 210.

Thakur, A.K. & Uphoff, N.T. (2017) How the system of rice intensification can contribute to climate-smart agriculture. *Agronomy Journal*, 109(4), 1163–1182. Available from: https://doi.org/10.2134/agronj2016.03.0162

van Oort, P.A.J. & Zwart, S.J. (2018) Impacts of climate change on rice production in Africa and causes of simulated yield changes. *Global Change Biology*, 24(3), 1029–1045. Available from: https://doi.org/10.1111/gcb.13967

How to cite this article: Randriamarolaza, L. Y. A., & Aguilar, E. (2023). Rainy season and crop calendars comparison between past (1950–2018) and future (2030–2100) in Madagascar. *Meteorological Applications*, *30*(5), e2146. https://doi.org/10.1002/met.2146

PART III: GENERAL DISCUSSION, CONCLUSION, AND FUTURE PERSPECTIVES

CHAPTER 6 General discussion and conclusion

This thesis uses the state-of-the-art science on climate change developed during the INDECIS project. This project focused on the development of users-oriented climate indicators for GFCS high-priority sectors. Agriculture is one of the priority sectors. This project followed the GFCS concept to produce science-based climate information. The findings of the INDECIS project contributed to alleviating challenges, realizing goals, and implementing principles of GFCS as stated by Hewitt et al. (2012). For instance, the improvement of climate data quality, the integration of climate information in decision-making, and the exchange of scientific methods and tools were some of the challenges, goals, and principles respectively. Therefore, this thesis capitalizes on and applies these concepts, tools, and software to assess climate change effects in Madagascar, especially in the agriculture sector. The key findings of this thesis are found in the chapters 3 to 5.

Chapter 3 groups the results on quality control, homogenization of climate data, and climate indices. The results indicate that:

- Around 0.06% (1,182/2,116,968) of daily raw data are checked. Then 4%, 34%, and 62% of checked data are validated as correct, corrected using online materials, and replaced with missing values respectively (see Table 3).
- Two different homogenization methods, automatic and semi-automatic modes, produce similar results according to annual and seasonal trends. Moreover, homogenized data is out of missing data (see Figure 5).
- The changes corroborate with global warming in Madagascar. On the one hand, air temperature increases. For instance, the change rate of minimum temperature is greater than the maximum temperature then the number of cold and hot events diminish and increase respectively (see Table 6). On the other hand, atmospheric precipitation decreases, and an intensified drying period is observed from the last fifteen years i.e., 2000-2018 (see Figures 8 and 9). This fact is justified by the frequency of drought events (see Figures 11 and 12).

C**hapter 4** concerns the detection and attribution of extreme temperatures in Madagascar. The findings show that:

- The ENSO events influence the extreme temperature indices, especially those related to minimum temperature (see Figure 3).

- Agreement between climate models under anthropogenic-plus-natural (ALL), greenhouse gases (GHG) and anthropogenic (NAT) forcings and observations are obvious with frequency than intensity indices (see Figure 4).
- The changes in extreme temperature indices are mainly detected and attributed to anthropogenic forcing (see Figures 8 and 9).

C**hapter 5** focuses on the rainy season characteristics and rice and maize growing conditions. The observed and projected outputs are compared. The results indicate that:

- Late onset and early cessation are increasingly observed (see Figures 5 and 6).
- Short cycle lengths of rice and maize crops are advised to be planted by farmers in Madagascar (see Figures 7 to 11).

These main results are obtained by challenging the constraints on the reliability of climate datasets and the efficiency of science-based methods adopted to develop climatic and agroclimatic indicators in Madagascar. This section will concentrate on the discussion of these constraints.

6.1 Reliability of climate datasets

Much research uses climate datasets to develop information on climate change and variability for policymakers and private sectors (Lacagnina et al. 2022). In this fact, reliable climate datasets are important as shown by Sorrentino et al. (2012) and Ait Issad et al. (2019) for solar radiation energy and smart agriculture respectively. To trust climate datasets, it is recommended to check certain quality aspects. This step ascertains their reliability and usability (Lacagnina et al. 2022). Climate datasets quality aspects are mainly based on inhomogeneities which are due to collecting, digitizing, processing, transferring, storing, and transmitting of climate data. However, it is a big challenge to ensure climate datasets quality as nowadays, research treats daily Essential Climate Variables (ECV) which are massive amounts of weather and climate data (Ribeiro et al. 2016). Moreover, Nightingale et al. (2019) identified the ten science knowledge gaps to ensure quality aspects of in-situ observations and satellite data. They remarked on the lack of consistent and standard quality flags to compare different data from different providers. In addition, Dinku (2019) identified quality data gaps in Africa such as poor quality due to missing data and low density of weather stations' network. These situations reflect the Madagascar case. This thesis overcomes these challenges by implementing science-based methods of quality control and homogenization developed and applied by the INDECIS project.

In this thesis, climate datasets include in-situ observations and climate model data. In-situ observations are the long-time series of daily precipitation and maximum and minimum temperatures collected from 26 synoptic weather stations in Madagascar. These daily raw data cover the period 1950-2018. The climate model data are the daily projection data taken from the Sixth Phase of the Coupled Model Inter-comparison Project (CMIP6). The daily projection data range from 2030 to 2100.

6.2 Quality control and homogenization of in-situ observations

As the World Meteorological Organization (WMO) recommends having high-quality climate data to satisfy user needs through climate services, they confirm that quality control and homogenization of climate data are mandatory and recommended.

6.2.1 Quality control

Quality control consists of checking data highly suspicious to be erroneous. Many tools were developed to achieve these goals. For instance, Dinku et al. (2022) built the Climate Data Tool (CDT). The quality control of our in-situ observations was done with an R package called INQC (Aguilar 2019). INQC stands for Indecis Quality Control of Climatological Daily Time Series. It is available at https://CRAN.R-project.org/package=INQC. Its main functions were detailed in Skrynyk et al. (2023). He remarked that INQC included 16 test functions then each tested value was flagged following six categories such as passed QC, true error, almost certain error, outlier, collectively suspect, and missing value. INQC software was used to assess the quality of European Climate Assessment & Dataset station data in the frame of the INDECIS project. The INQC tests showed that true errors were found in temperatures and precipitation such as minimum higher than maximum temperatures (e.g., seen in Fianarantsoa station) and precipitation amount higher than the fixed threshold (e.g., seen in Morondava station). However, almost certain errors are detected by labeling inter-diurnal differences in quantiles to be too large and isolating the extreme values that are not continuous in the distribution. Moreover, some outliers are detected by basing on the interquartile range. Lastly, the repeated consecutive equal values and decimals and too many consecutive wet or dry days are mostly the collectively suspect errors detected on temperatures and precipitation respectively. The missing values are the biggest issues as they reduce the reliability of the climate datasets and information. Reliable climate time series should not contain more than 10% missing values according to the recommendation by WMO. Massetti (2014) analyzed the effect of consecutive missing values on the calculation of monthly temperature indices and found that mean and standard deviation are mostly influenced by five consecutive rather than five random missing

values. Unfortunately, our time series on minimum temperature, maximum temperature, and precipitation contain 16.1%, 15.7%, and 10.2% missing values respectively. Therefore, our challenge is to have high-quality data by reducing missing value rates and correcting those suspect errors. Correcting those suspected errors is a big challenge as it is based on weather and climate archives. Without archives, corrections would be guessed or replaced by missing values. These two options are not a good way to proceed so we are investigating online materials to support our correction phase. After correction, the percentage of missing values reduces by 0.12% and 0.01% for minimum temperature and precipitation respectively. However, it increases by 0.65% for maximum temperature. This last parameter contains more errors than the two others. In the next section, we focus on imputation methods of data gaps, change points detection, and correction.

6.2.2 Homogenization

The goal of the homogenization task is to eliminate non-climatic factors in time series (Domonkos, Tóth, and Nyitrai 2023). Then the performance of the homogenization method depends on the detection and correction of the inhomogeneities. However, the efficiency of the detection method is based on its tolerance of missing data (Domonkos 2013). In addition, the high rate of missing data affects the reliability of climate data. Domonkos and Coll (2019) demonstrated that missing data impacted mainly on a monthly rather than an annual basis. Therefore, our task consists of filling these data gaps, detecting inhomogeneities, and producing homogenized in-situ observation data by using the homogenization method adopted by Climatol (Jose A Guijarro 2023).

As filling data gaps has been a challenge, many methods have been developed. Addi et al. (2022) identified 12 methods and found that the best imputation methods were regression, probabilities principal component analysis, and missForest for rainfall. Afrifa-Yamoah et al. (2020) focused on infilling gaps for temperature, humidity, and wind speed with three imputation methods and detected that the multiple linear regression was the best followed by autoregressive integrated moving average. Qin et al. (2021) are interested in time series with strong seasonality and spatial correlation. The imputation method was based on the decomposition of time series using spectral analysis. In the same idea, Climatol uses two simple methods of interpolation focused on the normal-ratio and 3-station-average (Paulhus and Kohler 1952).

The detection and adjustment of breakpoints or change points are crucial in the homogenization step. Several techniques or methods have been developed. Ducré-Robitaille et al. (2003) adopted and compared eight techniques and found that the standard normal homogeneity test

(SNHT) (Alexandersson 1986 ; Alexandersson and Moberg 1997) and multiple linear regression (MLR) (Lucie A Vincent 1998) were the best technique. Moreover, José A. Guijarro (2013) applied six methods on window running along the time series and ascertained that the classical t-test, Alexandersson's SNHT, and Squared Relative Mean Difference were the best tests. In this thesis, the SNHT method has been used as it is implemented in Climatol (see https://www.climatol.eu/climatol4-en.pdf). On the one hand, the breakpoints were detected on a monthly scale and in an automatic way as it was also set up by José A. Guijarro et al. (2023) to test the performance of freely available software packager on homogenization during the Spanish MULTITEST project. He highlighted that ACMANT and Climatol minimized the root mean squared errors and errors in the trends of the time series. On the other hand, the breakpoints were compared with breakpoints detected in a semi-automatic way done with the software HOMER. HOMER combined the best state-of-the-art homogenization methods such as PRODIGE, ACMANT, Climatol, and joint segmentation (Mestre et al. 2013). It is set up to run the pairwise detection, two rounds of joint detection/correction, and a month of change assessment. It detects more monthly breakpoints (around 1 to 3 per year) than Climatol on temperature and any breakpoint in precipitation. However, monthly breakpoint dates coincide with the metadata in Climatol than HOMER even if breakpoints shift 1 to 3 years, especially on minimum temperature. As the skill of homogenized methods did not depend on the instability of break detection as said by Coll et al. (2020), these findings ascertain the empowerment of Climatol to manage short time series, data gaps, and sparse networks. The correction of the daily time series was done by adjusting each homogenous fragment according to the monthly breakpoints. Therefore, one of the advantages of Climatol is that it produces many homogenous time series following the number of homogenous fragments. The default homogenous time series is the one built from the latest homogenous fragment, but the users can select or choose the homogenous time series fitted to their analysis. The default homogenized time series were used to calculate climate indices.

6.3 Climate change indices

The former steps were done to ascertain and improve previous analyses on climate indices and their trends in Madagascar, for instance, Tadross et al. (2008) and L. A. Vincent et al. (2011). They used the absolute homogenization method using RHtestV3 software (Wang and Feng 2010). In this thesis, the relative homogenization method was applied by using Climatol and HOMER softwares. Many projects on benchmarking of homogenization software showed that relative was more accurate than absolute mothed (José A. Guijarro et al. 2023). As missing

data and time series with short periods impose constraints on the calculation of climate indices, many observational datasets were discarded from the previous studies. Therefore, this thesis chose Climatol software to challenge these constraints as it includes a method to infill data gaps and manage short period time series, for instance, 26 synoptic weather stations were used instead of 21 and 19 in the Tadross et al. (2008) and L. A. Vincent et al. (2011) respectively. Moreover, 37 climate indices were calculated instead of 21 within the previous papers. Tadross et al. (2008) and L. A. Vincent et al. (2011) took climate indices from STARDEX (https://crudata.uea.ac.uk/projects/stardex/) and climdex (see https://www.climdex.org/learn/indices/) projects respectively. Most climate indices are common to those calculated by the ClimInd package (see https://cran.r-project.org/web/packages/ClimInd/index.html) developed during the INDECIS project (see http://www.indecis.eu/). Furthermore, this thesis introduces new 17 climate indices, for instance, drought characteristics (i.e., intensity, duration, and magnitude) and some extremes of precipitation and temperatures. Finally, the analysis period was increased to around 20 years. Results corroborate with global warming effects. Its comparison with previous papers ascertained the continuation of climate change impacts. The main results showed that nighttime indices had higher values than daytime as far as temperature extremes are concerned. In addition, an intensifying dry period was observed last 15 years (i.e., 2000-2018). This fact was highlighted by the frequent and intense drought events. For instance, drought events last longer from September-October-November. In Madagascar, drought has triggered a food crisis as stated by the conversation journal (see https://theconversation.com/how-climate-change-contributed-to-madagascars-food-crisis-167370). Militao et al. (2022) pointed out that climate change was one of the causes of food insecurity and for instance, Madagascar had a high prevalence according to the World Food Program's Hunger Map. Therefore, climate indices play important roles as indicators measuring changes and being considered in the decision-making process. This thesis also investigates to measure the influence of external forcing (i.e., anthropogenic, and natural) on extreme temperature indices.

6.4 Detection and attribution of temperature extremes

This step is crucial to justify the changes and understand the causes of climate change statistically. As stated by the first IPCC report, the main challenges were to have long and reliable observational time series and to reduce the climate model uncertainties, especially on past historical greenhouse gases (Wigley and Barnett 1990). Many efforts have been made since the second IPCC report to improve the resolution of the Atmosphere-Ocean General

Circulation Model (AOGCM) then the use of statistical or dynamic techniques permits to downscale of AOGCMs outputs to the regional scale. For instance, biases have been reduced (F. Giorgi 1996). However, the fifth IPCC report noticed that the robustness of detection and attribution depended on the correctness of internal variability simulation (Bindoff 2013). Therefore, Hegerl et al. (2010a) provided some recommendations for good practice in detection and attribution studies. They recommended to manage quality and data gaps in observational data. Easterling et al. (2016) ascertained that challenges in detection studies were data quality, coverage, and completeness. In this thesis, the reliability of the observational dataset and indices of temperature extremes are already discussed in the quality control and homogenization and climate indices sections respectively. As we are interested in the detection and attribution of temperature extremes by using the fingerprint-based method, Hegerl and Zwiers (2011) pointed out that the results' robustness depended on the climate simulation models or GCMs. They suggested building an ensemble (typically composed of 3 to 10) of climate simulation models to avoid uncertainty due to internal variability. For instance, Deser et al. (2012) confirmed the importance of considering the effect of internal variabilities of GCMs. Then the reliability of models was assessed by comparison with observational datasets. Climate simulation models under anthropogenic-plus-natural (ALL), greenhouse gases (GHG), natural (NAT), and anthropogenic (ANT) forcings were compared to observational datasets. We calculated from observational and climate simulation models datasets, indices based on threshold and absolute values of minimum and maximum temperatures. They are called frequency (TN10P, TX10P, TN90P, TX90P, TN1P, TX99P) and intensity (TNn, TXn, TNx, TXx) indices respectively. The relative contribution of different external forcing was analyzed. As recommended by Hegerl et al. (2010a), the greenhouse gas response from other anthropogenic forcing was separated. On the one hand, the analysis with wavelet coherence revealed the influence of ENSO events on temperature extremes in Madagascar. The findings showed that the frequency indices were more influenced than the intensity indices. Similar results were observed in Malaysia (Tan et al. 2021). On the other hand, considering the ALL, GHG, and ANT forcings, the results indicated that frequency and intensity indices were well correlated with a correlation value of more than 0.6 except for the coldest day and night. However, climate simulation models had low and high standard deviations for intensity and frequency indices respectively. The opposite was found for the centered root-mean-square. No consistency was seen with NAT forcing. The time series comparison ascertained that indices range values of GCMs under ALL, GHG, and ANT forcings aligned with observational behaviors at a regional scale. As we respect the guidance and recommendation on detection

and attribution studies, we trust the robustness of our conclusion saying that changes in temperature extremes are detected and attributed to anthropogenic forcing, especially GHG forcing. These results would help to issue decision-making on climate change impacts. Therefore, the next section deals with climate change impacts on the agriculture sector.

6.5 Effects of climate change on rainy season characteristics and growing season calendars for rice and maize crops

The agriculture sector is more vulnerable to climate change compared to other natural ecosystems (Tao et al. 2011). For instance, Müller et al. (2011) studies issued from climate change assessment literature, revealed that African agriculture was threatened by climate change and science should be involved to improve agricultural production in Africa. The sixth report of the Intergovernmental Panel on Climate Change (IPCC) ascertained with high confidence that climate change negatively affected the African food systems due to the shortening of growing season and water stress (Trisos et al. 2022). Andrianarimanana et al. (2023) assessed the importance of climate, land, and soil on the global supply of agricultural products and global food security. They discovered that climate lowered the soil quality and agricultural production in tropical regions. For instance, the negative impacts were obvious for low-income countries with low adaptive capacity such as Madagascar (Rakotonirina. et al. 2023). Moreover, Harvey et al. (2014) highlighted that smallholder farmers were extremely vulnerable in Madagascar. Then Mutengwa et al. (2023) and Rakotonirina et al. (2023) suggested that promoting the Climate-Smart-Agriculture (CSA) would be a solution to increase farmers' resilience in Southern Africa and Madagascar respectively. Rice and maize are widely grown as they are stapled foods in Madagascar. Therefore, this thesis part may contribute to the CSA approach by understanding the climate change effects on rainy season characteristics and growing season calendars for rice and maize crops. The onset and cessation of the rainy season were defined as the rainy season which could fit the growth and development of rice and maize crops. For instance, Van Nguyen and Ferrero (2006) and Prasad et al. (2017) assessed the challenges in rice production and found that rice was going to suffer because of the scarcity of water resources due mainly to dry spell events. For instance, only 22% of the cultivated area is irrigated in Madagascar according to an FAO report in 2013 (https://www.fao.org/3/ca0199fr/CA0199FR.pdf). Thus, the objective of this section is to establish a science-based technique on rainfed rice and maize crop calendars that ensures the availability of water for juvenile plants. The literature reviews permit to selection of the definitions of onset and cessation of the rainy season based on criteria of rainfall quantity and

dry spell length. With the approach done by Liebmann et al. (2012), we can define the potential onset and cessation dates of the rainy season. However, the potential dates may be followed by dry spell events which may affect juvenile development. Then the potential dates may be false alarms. For instance, chapter 2 showed that drought or dry spell events were mostly frequent at the beginning of the rainy season, especially during September-October-November in Madagascar. This period matches to germination phase which is one of the sensitive phases of crop development. A similar situation was found by Ibrahim et al. (2022) in Burkina Faso. To tackle this issue, the researcher tested different criteria to identify the real or effective onset dates from which crop conditions are satisfied according to Usman and AbdulKadir (2013). For instance, Stern et al. (1981) added the criteria on dry spell occurrence to define the earliest onset dates for West Africa. Then Sivakumar (1988) computed the early and normal in the Southern Sahaelian and Sudanian climatic zones. Akinseye et al. (2016) tested four definitions to detect the onset dates of the rainy season in the Malian agroecological zones. Through the findings of Akinseye et al. (2016), this thesis formulates the criteria for the total amount of rainfall, minimum numbers of rainy days, and maximum length of dry spells to determine the onset dates. As maize uses less water than rice (Ondrasek et al. 2014), fewer constraints are put on maize than rice crops as far as rainfall amount and length of dry spells are concerned. On the one hand, the potential (effective) onset date of the rainy season, which fits rice (maize) crop needs, is the first day after August 1st with more than 20 mm (25 mm) of rain in 2 days (7 days) and no dry spell within the next 21 days exceeded 7 days (10 days). However, the effective onset date of the rainy season for rice crops is when the potential onset date is followed by at least 2 days of rainy days within 5 days. This last condition is not necessary for maize crops as it can grow without excessive rainy days. For instance, Li et al. (2019) pointed out that excessive rainfall hurt maize yield in the United States. On the other hand, the effective cessation date, which fits rice and maize crop needs, is defined as the first day after March 1 when soil with a 150 mm water-holding capacity gets completely depleted, assuming a daily evapotranspiration rate of 5 mm/day and remains depleted for at least five consecutive days without recovering to maximum capacity in the next 15 days respectively. Then supposing that the rainy season starts and ends normally, the sowing or seeding period ranges from the lower bound of the normal onset period of the rainy season to the latest sowing or seeding date which is the date calculated from the upper bound of cessation normal period of the rainy season and the length of crop cycle. Moreover, the corresponding harvesting period is also computed. The period spans from sowing or seeding and harvesting periods are called growing seasons. As our goal is to compare past (1950-2018) and future (2030-2100) rice and maize growing

seasons, the findings show that the onset and cessation of rainy seasons are mainly late and early respectively. Then the duration of the rainy season decreases. This situation is mostly observed in the north and east parts of Madagascar. Similar situations were seen in East Africa (Dunning et al. 2016) and in the IGAD region of Eastern Africa (Omay et al. 2023). Consequently, on the one hand, the start of the sowing or seeding period is delayed around 1 to 3 months, and the harvesting period is postponed in the future. Rice crops are more affected than maize crops. To cope with this situation, new rice breeds have been generated called NERICA stands for New Rice for Africa which can tolerate drought, weeds, and pests (Somado et al. 2008). On the other hand, some opportunities have been observed in Central land or Highland and South, especially increasing the sowing or seeding period of around 10 to 20 days for short-cycle crops. Gerardeaux et al. (2012) noticed other opportunities due to temperatures and increasing CO2 for rice crops.

CHAPTER 7 Future perspectives

This chapter covers the improvement that could be implemented and ascertains the thesis findings. Firstly, trust in scientific climate information is mainly dependent on the efficiency of the scientific methods and the quality of the climate dataset. Therefore, our improvement focuses on updating the in-situ dataset period and removing non-climatic factors by applying the state-of-the-art on homogenization. Improving the homogenized dataset of the observational weather and climate data is an important step toward have efficiency and reliability of climate data and information. Climatol has well homogenized Madagascar in-situ datasets, (Guijarro et al. 2023). Then applying different homogenization methods may bring more added values such as geostatistical simulation (Caineta et al. 2015 and Ribeiro et al. 2017).

Furthermore, spatial and temporal assessment between climate model and observational datasets may be improved. The challenges would be to build gridded high-resolution climate datasets from in-situ and climate models. To tackle this issue, bias adjustment and technical downscaling methods may be implemented. For instance, Werner and Cannon (2016) identified seven downscaling methods that could be applied to improve our results. They found that the double bias correction constructed analogs were more accurate as far as climdex indices were concerned. Vogel et al. (2023) applied four downscaling and bias correction methods which were more focused on hydrological application but could be used in another research domain. On the one hand, applying a dynamic downscaling approach would need more computation resources but some Regional Climate Model outputs are freely available such as CORDEX-AFRICA (see https://cordex.org/domains/region-5-africa/). The Global Climate Model outputs may be downscaled by combining machine learning and statistical downscaling methods to obtain excellent results. For instance, Sidhu et al. (2023) ascertained that machine learning performed better than the ordinary least square linear regression when dealing with climate change impact. Moreover, the International Conference on Regional Climate-CORDEX 2023 (see https://cordex.org/icrc-cordex-2023/) held in Italy in September was a great opportunity to exchange with experts on bias correction, machine learning and statistical downscaling, especially with experts from the National Institute of Water and Atmospheric Research (NIWA), Auckland, New Zealand (Rampal et al. 2022) and Toulouse university, Météo France (Doury et al. 2023). Learning by-doing sessions will be held in the future. These efforts will contribute to improving the findings on climate change impact assessment of rainy season characteristics and crop growing seasons. Furthermore, the sub-seasonal and seasonal analysis

for the onset and cessation of rainy seasons and crop growing seasons may be improved by introducing other parameters than precipitation such as solar radiation, wind speed, relative humidity, minimum temperature, and maximum temperature.

Reference

Addi, M, Y Gyasi-Agyei, E Obuobie, and L K Amekudzi. 2022. "Evaluation of Imputation Techniques for Infilling Missing Daily Rainfall Records on River Basins in Ghana." *Hydrological Sciences Journal* 67 (4): 613–27. https://doi.org/10.1080/02626667.2022.2030868.

African Development Bank. 2011. "The Cost of Adaptation to Climate Change in Africa." *African Development Bank*, 21–36.

Afrifa-Yamoah, E., U. A. Mueller, S. M. Taylor, and A. J. Fisher. 2020. "Missing Data Imputation of High-Resolution Temporal Climate Time Series Data." *Meteorological Applications* 27 (1): e1873. https://doi.org/10.1002/MET.1873.

Ait Issad, Hassina, Rachida Aoudjit, and Joel J P C Rodrigues. 2019. "A Comprehensive Review of Data Mining Techniques in Smart Agriculture." *Engineering in Agriculture, Environment and Food* 12 (4): 511–25. https://doi.org/https://doi.org/10.1016/j.eaef.2019.11.003.

Akinseye, F M, S O Agele, P C S Traore, M Adam, and A M Whitbread. 2016. "Evaluation of the Onset and Length of Growing Season to Define Planting Date—'a Case Study for Mali (West Africa).'" *Theoretical and Applied Climatology* 124 (3–4): 973–83. https://doi.org/10.1007/s00704-015-1460-8.

Alexandersson, H. 1986. "A Homogeneity Test Applied to Precipitation Data." *Journal of Climatology* 6 (6): 661–75. https://doi.org/10.1002/joc.3370060607.

ALEXANDERSSON, HANS, and ANDERS MOBERG. 1997. "Homogenization of Swedish Temperature Data. Part I: Homogeneity Test for Linear Trends." *International Journal of Climatology* 17 (1): 25–34. https://doi.org/10.1002/(sici)1097-0088(199701)17:1<25::aid-joc103>3.3.co;2-a.

Andrianarimanana, Mihasina Harinaivo, Pu Yongjian, and Mirindra Finaritra Rabezanahary Tanteliniaina. 2023. "Assessment of the Importance of Climate, Land, and Soil on the Global Supply for Agricultural Products and Global Food Security: Evidence from Madagascar." *Food Policy* 115: 102403. https://doi.org/https://doi.org/10.1016/j.foodpol.2023.102403.

Asafu-Adjaye, John. 2014. "The Economic Impacts of Climate Change on Agriculture in Africa." *Journal of African Economies* 23 (SUPPL.2). https://doi.org/10.1093/jae/eju011.

Ash, Kevin, and Corene Matyas. 2012. “The Influences of ENSO and the Subtropical Indian Ocean Dipole on Tropical Cyclone Trajectories in the South Indian Ocean.” *International Journal of Climatology* 32 (January): 41–56. https://doi.org/10.1002/joc.2249.

Barimalala, R., N. Raholijao, W. Pokam, and C. J.C. Reason. 2021. “Potential Impacts of 1.5 °C, 2 °C Global Warming Levels on Temperature and Rainfall over Madagascar.” *Environmental Research Letters* 16 (4). https://doi.org/10.1088/1748-9326/abeb34.

Battistini, R., and G. Richard-Vindard. 1974. *Biogeography and Ecology in Madagascar*. *The Journal of Animal Ecology*. Vol. 43. https://doi.org/10.2307/3544.

Bindoff, N.L. Stott, P.A. AchutaRao, K.M. Allen, M.R. Gillett, N. Gutzler, D. Hansingo, K. Hegerl, G. Hu, Y. Jain, S. Mokhov, I.I. Overland, J. Perlwitz, J. Sebbari, R. Zhang, X. 2013. “Detection and Attribution of Climate Change: From Global to Regional.” In *Climate Change 2013 the Physical Science Basis: Working Group I Contribution to the Fifth Assessment Report of the Intergovernmental Panel on Climate Change*, 9781107057999:867–952. Cambridge University Press. https://doi.org/10.1017/CBO9781107415324.022.

Busch, J, R Dave, L Hannah, E Ashkenazi, A Cameron, D Fischman, A Rasolohery, and George Schatz. 2012. “Climate Change and the Cost of Conserving Biodiveristy in Madagascar.” *Conservation Biology* 26 (3): 1–48.

Caineta, J, S Ribeiro, A Soares, and A C Costa. 2015. “Workflow for the Homogenisation of Climate Data Using Geostatistical Simulation.” In , 1:921–29. NOVA IMS, Universidade Nova de Lisboa, Portugal: International Multidisciplinary Scientific Geoconference.

Coll, John, Peter Domonkos, José Guijarro, Mary Curley, Elke Rustemeier, Enric Aguilar, Séamus Walsh, and John Sweeney. 2020. “Application of Homogenization Methods for Ireland’s Monthly Precipitation Records: Comparison of Break Detection Results.” *International Journal of Climatology*, no. March: 1–20. https://doi.org/10.1002/joc.6575.

Cornet, Antoine. 1974. “Essai de Cartographie Bioclimatique à Madagascar.” *ORSTOM*, 1974.

Deser, Clara, Adam Phillips, Vincent Bourdette, and Haiyan Teng. 2012. “Uncertainty in Climate Change Projections: The Role of Internal Variability.” *Climate Dynamics* 38 (3): 527–46. https://doi.org/10.1007/s00382-010-0977-x.

Dinku, Tufa. 2019. “Challenges with Availability and Quality of Climate Data in Africa.” In *Extreme Hydrology and Climate Variability*, 71–80. https://doi.org/10.1016/B978-0-12-815998-9.00007-5.

Dinku, Tufa, Rija Faniriantsoa, Shammunul Islam, Gloriose Nsengiyumva, and Amanda Grossi. 2022. “The Climate Data Tool: Enhancing Climate Services Across Africa.” *Frontiers in Climate* 3 (February): 1–16. https://doi.org/10.3389/fclim.2021.787519.

Domonkos, Peter. 2013. “Measuring Performances of Homogenization Methods.” *Idojaras* 117 (1): 91–112.

Domonkos, Peter, and John Coll. 2019. “Impact of Missing Data on the Efficiency of Homogenisation: Experiments with ACMANTv3.” *Theoretical and Applied Climatology* 136 (1–2): 287–99. https://doi.org/10.1007/s00704-018-2488-3.

Domonkos, Peter, Róbert Tóth, and László Nyitrai. 2023. “Chapter 4 - Homogenization Task and Its Principal Approaches.” In *Developments in Weather and Climate Science*, edited by Peter Domonkos, Róbert Tóth, and László B T - Climate Observations Nyitrai, 83–103. Elsevier. https://doi.org/https://doi.org/10.1016/B978-0-323-90487-2.00006-2.

Doury, Antoine, Samuel Somot, Sebastien Gadat, Aurélien Ribes, and Lola Corre. 2023. “Regional Climate Model Emulator Based on Deep Learning: Concept and First Evaluation of a Novel Hybrid Downscaling Approach.” *Climate Dynamics* 60 (5): 1751–79. https://doi.org/10.1007/s00382-022-06343-9.

Ducré-Robitaille, Jean François, Lucie A. Vincent, and Gilles Boulet. 2003. “Comparison of Techniques for Detection of Discontinuities in Temperature Series.” *International Journal of Climatology* 23 (9): 1087–1101. https://doi.org/10.1002/joc.924.

Dunning, Caroline M, Emily C L Black, and Richard P Allan. 2016. “The Onset and Cessation of Seasonal Rainfall over Africa.” *Journal of Geophysical Research: Atmospheres* 121 (19): 11,405-411,424. https://doi.org/https://doi.org/10.1002/2016JD025428.

Easterling, David R, Kenneth E Kunkel, Michael F Wehner, and Liqiang Sun. 2016. “Detection and Attribution of Climate Extremes in the Observed Record.” *Weather and Climate Extremes* 11: 17–27. https://doi.org/https://doi.org/10.1016/j.wace.2016.01.001.

F. Giorgi, B. Hewitson. 1996. “Regional Climate Information - Evaluation and Projections.” In *Climate Change 1995: The Science of Climate Change*, edited by J.T. Houghton, L.G. Meira Filho, B.A. Callander, N. Harris, A. Kattenberg, and K. Maskell. Cambridge: Cambridge University Press, Cambridge, Great Britain, New York, NY, USA and Melbourne, Australia.

Fayad, Dominique. 2023. “Food Insecurity and Climate Shocks in Madagascar.” *Selected Issues Papers* 2023 (037): 1. https://doi.org/10.5089/9798400242601.018.

Fitchett, Jennifer M, and Stefan W Grab. 2014. “A 66-Year Tropical Cyclone Record for South-East Africa: Temporal Trends in a Global Context.” *International Journal of Climatology* 34 (13): 3604–15. https://doi.org/10.1002/joc.3932.

Gerardeaux, E, M Giner, A Ramanantsoanirina, and J Dusserre. 2012. “Positive Effects of Climate Change on Rice in Madagascar.” *Agronomy for Sustainable Development* 32 (3): 619–27. https://doi.org/10.1007/s13593-011-0049-6.

Goodman, Steven M., Aristide Andrianarimisa, Amanda H. Armstrong, Andrew Cooke, Maarten De Wit, Jörg U. Ganzhorn, Laurent Gautier, et al. 2022. *The New Natural History of Madagascar*. *The New Natural History of Madagascar*. Princeton University Press. https://doi.org/10.2307/j.ctv2ks6tbb.

Guijarro, José A. 2013. “Climatological Series Shift Test Comparison on Running Windows.” *Idojaras* 117 (1): 35–45.

Guijarro, Jose A. 2023. “User ’ s Guide of the Climatol R Package (Version 4),” no. version 4: 1–20.

Guijarro, José A., José A. López, Enric Aguilar, Peter Domonkos, Victor K.C. Venema, Javier Sigró, and Manola Brunet. 2023. “Homogenization of Monthly Series of Temperature and Precipitation: Benchmarking Results of the MULTITEST Project.” *International Journal of Climatology* 43 (9): 3994–4012. https://doi.org/10.1002/joc.8069.

Harrington, Luke James, Piotr Wolski, Izidine Pinto, Anzelà Mamiarisoa Ramarosandratana, Rondrotiana Barimalala, Robert Vautard, Sjoukje Philip, et al. 2022. “Limited Role of Climate Change in Extreme Low Rainfall Associated with Southern Madagascar Food Insecurity, 2019–21.” *Environmental Research: Climate* 1 (2): 021003. https://doi.org/10.1088/2752-5295/aca695.

Harvey, Celia A., Zo Lalaina Rakotobe, Nalini S. Rao, Radhika Dave, Hery Razafimahatratra, Rivo Hasinandrianina Rabarijohn, Haingo Rajaofara, and James L. MacKinnon. 2014. “Extreme Vulnerability of Smallholder Farmers to Agricultural Risks and Climate Change in Madagascar.” *Philosophical Transactions of the Royal Society B: Biological Sciences* 369 (1639). https://doi.org/10.1098/rstb.2013.0089.

Hegerl, G C, O Hoegh-Guldberg, G Casassa, M P Hoerling, R S Kovats, C Parmesan, D W Pierce, and P A Stott. 2010a. “Good Practice Guidance Paper on Detection and Attribution Related to Anthropogenic Climate Change.” *Meeting Report of the Intergovernmental Panel on Climate Change Expert Meeting on Detection and Attribution of Anthropogenic Climate Change*, 1–9. http://nova.wh.whoi.edu/palit/Stocker.

Hegerl, Gabriele, and Francis Zwiers. 2011. “Use of Models in Detection and Attribution of Climate Change.” *WILEY INTERDISCIPLINARY REVIEWS-CLIMATE CHANGE* 2 (4): 570–91. https://doi.org/10.1002/wcc.121.

Hegerl, G.C., O. Hoegh-Guldberg, G. Casassa, M.P. Hoerling, R.S. Kovats, C. Parmesan, D.W. Pierce, and P.A. Stott. 2010b. “Good Practice Guidance Paper on Detection and Attribution Related to Anthropogenic Climate Change.” *Meeting Report of the Intergovernmental Panel on Climate Change Expert Meeting on Detection and Attribution of Anthropogenic Climate Change*, 1–9.

Ibrahim, Boubacar, Moussa Waongo, Moussa Sidibe, Safietou Sanfo, and Boubacar Barry. 2022. “Agroclimatological Characteristics of Rainy Seasons in Southwestern Burkina Faso during the 1970-2013 Period.” *Atmospheric and Climate Sciences* 12 (02): 330–57. https://doi.org/10.4236/acs.2022.122021.

Ingram, J. Carter, and Terence P. Dawson. 2005. “Climate Change Impacts and Vegetation Response on the Island of Madagascar.” *Philosophical Transactions of the Royal Society A: Mathematical, Physical and Engineering Sciences* 363 (1826): 55–59. https://doi.org/10.1098/rsta.2004.1476.

Jury, M R, B A Parker, N Raholijao, and A Nassor. 1995. “Variability of Summer Rainfall over Madagascar: Climatic Determinants at Interannual Scales.” *International Journal of Climatology* 15 (12): 1323–32. https://doi.org/10.1002/joc.3370151203.

Jury, M. R., B. Parker, and D. Waliser. 1994. “Evolution and Variability of the ITCZ in the SW Indian Ocean: 1988-90.” *Theoretical and Applied Climatology* 48 (4): 187–94. https://doi.org/10.1007/BF00867048.

Jury, Mark R. 2016. “Summer Climate of Madagascar and Monsoon Pulsing of Its Vortex.” *Meteorology and Atmospheric Physics* 128 (1): 117–29. https://doi.org/10.1007/s00703-015-0401-5.

Lacagnina, Carlo, Francisco Doblas-Reyes, Gilles Larnicol, Carlo Buontempo, André Obregón, Montserrat Costa-Surós, Daniel San-Martín, et al. 2022. “Quality Management Framework for Climate Datasets.” *Data Science Journal* 21 (1). https://doi.org/10.5334/dsj-2022-010.

Li, Yan, Kaiyu Guan, Gary D. Schnitkey, Evan DeLucia, and Bin Peng. 2019. “Excessive Rainfall Leads to Maize Yield Loss of a Comparable Magnitude to Extreme Drought in the United States.” *Global Change Biology* 25 (7): 2325–37. https://doi.org/10.1111/gcb.14628.

Liebmann, Brant, Ileana Bladé, George N. Kiladis, Leila M.V. Carvalho, Gabriel B. Senay, Dave Allured, Stephanie Leroux, and Chris Funk. 2012. "Seasonality of African Precipitation from 1996 to 2009." *Journal of Climate* 25 (12): 4304–22. https://doi.org/10.1175/JCLI-D-11-00157.1.

Ma, Sai, Tianying Wang, Jun Yan, and Xuebin Zhang. 2023. "Optimal Fingerprinting with Estimating Equations." *Journal of Climate* 36 (20): 7109–22. https://doi.org/https://doi.org/10.1175/JCLI-D-22-0681.1.

Massetti, Luciano. 2014. "Analysis and Estimation of the Effects of Missing Values on the Calculation of Monthly Temperature Indices." *Theoretical and Applied Climatology* 117 (3–4): 511–19. https://doi.org/10.1007/s00704-013-1024-8.

Matyas, Corene. 2014. "Tropical Cyclone Formation and Motion in the Mozambique Channel." *International Journal of Climatology* 35 (April). https://doi.org/10.1002/joc.3985.

Mestre, Olivier, Peter Domonkos, Franck Picard, Ingeborg Auer, Stéphane Robin, Emilie Lebarbier, Reinhard Böhm, et al. 2013. "HOMER: A Homogenization Software - Methods and Applications." *Idojaras* 117 (1): 47–67.

Militao, Elias M A, Elsa M Salvador, Olalekan A Uthman, Stig Vinberg, and Gloria Macassa. 2022. "Food Insecurity and Health Outcomes Other than Malnutrition in Southern Africa: A Descriptive Systematic Review." *International Journal of Environmental Research and Public Health*. https://doi.org/10.3390/ijerph19095082.

Müller, Christoph, Wolfgang Cramer, William L Hare, and Hermann Lotze-Campen. 2011. "Climate Change Risks for African Agriculture." *Proceedings of the National Academy of Sciences* 108 (11): 4313–15. https://doi.org/10.1073/pnas.1015078108.

Mutengwa, Charles S, Pearson Mnkeni, and Aleck Kondwakwenda. 2023. "Climate-Smart Agriculture and Food Security in Southern Africa: A Review of the Vulnerability of Smallholder Agriculture and Food Security to Climate Change." *Sustainability*. https://doi.org/10.3390/su15042882.

Myers, Norman, Russell A. Mittermeler, Cristina G. Mittermeler, Gustavo A.B. Da Fonseca, and Jennifer Kent. 2000. "Biodiversity Hotspots for Conservation Priorities." *Nature* 403 (6772): 853–58. https://doi.org/10.1038/35002501.

Nassor, A., and M. R. Jury. 1997. "Intra-Seasonal Climate Variability of Madagascar. Part 2: Evolution of Flood Events." *Meteorology and Atmospheric Physics* 64 (3–4): 243–54. https://doi.org/10.1007/BF01029696.

———. 1998. “Intra-Seasonal Climate Variability of Madagascar. Part 1: Mean Summer Conditions.” *Meteorology and Atmospheric Physics* 65 (1–2): 31–41. https://doi.org/10.1007/BF01030267.

Nguyen, Nguu Van, and Aldo Ferrero. 2006. “Meeting the Challenges of Global Rice Production.” *Paddy and Water Environment* 4 (1): 1–9. https://doi.org/10.1007/s10333-005-0031-5.

Nhamo, L, T Mabhaudhi, and A. T. Modi. 2019. “Preparedness or Repeated Short-Term Relief Aid? Building Drought Resilience through Early Warning in Southern Africa.” *Water SA* 45 (1): 75–85. https://doi.org/10.4314/wsa.v45i1.09.

Nightingale, J, J P D Mittaz, S Douglas, D Dee, J Ryder, M Taylor, C Old, et al. 2019. “Ten Priority Science Gaps in Assessing Climate Data Record Quality.” *Remote Sensing* 11 (8). https://doi.org/10.3390/rs11080897.

Nurse, Leonard A., Roger F. McLean, John Agard, Lino Pascal Briguglio, Virginie Duvat-Magnan, Netatua Pelesikoti, Emma Tompkins, and Arthur Webb. 2015. “Small Islands.” *Climate Change 2014: Impacts, Adaptation and Vulnerability: Part B: Regional Aspects: Working Group II Contribution to the Fifth Assessment Report of the Intergovernmental Panel on Climate Change*, 1613–54. https://doi.org/10.1017/CBO9781107415386.009.

Omay, Paulino Omoj, Nzioka J Muthama, Christopher Oludhe, Josiah M Kinama, Guleid Artan, and Zachary Atheru. 2023. “Changes and Variability in Rainfall Onset, Cessation, and Length of Rainy Season in the IGAD Region of Eastern Africa.” *Theoretical and Applied Climatology* 152 (1): 871–93. https://doi.org/10.1007/s00704-023-04433-0.

Ondrasek, Gabrijel, Zed Rengel, Dragutin Petosic, and Vilim Filipovic. 2014. “Land and Water Management Strategies for the Improvement of Crop Production.” In, edited by Parvaiz Ahmad and Saiema B T - Emerging Technologies and Management of Crop Stress Tolerance Rasool, 291–313. San Diego: Academic Press. https://doi.org/https://doi.org/10.1016/B978-0-12-800875-1.00013-2.

Otto, Friederike E L, Mariam Zachariah, Piotr Wolski, Izidine Pinto, Rondrotiana Barimalala, Bernardino Nhamtumbo, Remy Bonnet, et al. 2022. “Climate Change Increased Rainfall Associated with Tropical Cyclones Hitting Highly Vulnerable Communities in Madagascar, Mozambique & Malawi.” *WWA-MMM-TS-Scientific Report*, no. February.

Paulhus, J L H, and M A Kohler. 1952. “INTERPOLATION OF MISSING PRECIPITATION RECORDS.” *Monthly Weather Review* 80 (8): 129–33. https://doi.org/https://doi.org/10.1175/1520-0493(1952)080<0129:IOMPR>2.0.CO;2.

Prasad, Rajendra, Yashbir Singh Shivay, and Dinesh Kumar. 2017. “Current Status, Challenges, and Opportunities in Rice Production BT - Rice Production Worldwide.” In, edited by Bhagirath S Chauhan, Khawar Jabran, and Gulshan Mahajan, 1–32. Cham: Springer International Publishing. https://doi.org/10.1007/978-3-319-47516-5_1.

Qin, Yun, Guoyu Ren, Panfeng Zhang, Lixiu Wu, and Kangmin Wen. 2021. “An Imputation Method for the Climatic Data with Strong Seasonality and Spatial Correlation.” *Theoretical and Applied Climatology* 144 (1–2): 203–13. https://doi.org/10.1007/s00704-021-03537-9.

Rakotonirina M.D.L., Razafindrazanakolona A.D., Ramanampisoa V.E., Rabesiaka R, Damy T.S., Koto-te-Nyiwa Ngbolua, Robijaona Rahelivololoniaina B., and Muhammad Ridwan. 2023. “Contribution to the Promotion of Innovative and Climate-Smart Agroecology: Application to Agriculture and Livestock in the Haute Matsiatra Region, Madagascar.” *Economic Journal: Scientific Journal of Accountancy, Management and Finance* 3 (2): 99–105. https://doi.org/10.33258/economit.v3i2.874.

Rampal, Neelesh, Peter B Gibson, Abha Sood, Stephen Stuart, Nicolas C Fauchereau, Chris Brandolino, Ben Noll, and Tristan Meyers. 2022. “High-Resolution Downscaling with Interpretable Deep Learning: Rainfall Extremes over New Zealand.” *Weather and Climate Extremes* 38: 100525. https://doi.org/https://doi.org/10.1016/j.wace.2022.100525.

Ribeiro, S, J Caineta, and A C Costa. 2016. “Review and Discussion of Homogenisation Methods for Climate Data.” *Physics and Chemistry of the Earth, Parts A/B/C* 94: 167–79. https://doi.org/https://doi.org/10.1016/j.pce.2015.08.007.

Ribeiro, S, J Caineta, A C Costa, and R Henriques. 2017. “Gsimcli: A Geostatistical Procedure for the Homogenisation of Climatic Time Series.” *International Journal of Climatology* 37 (8): 3452–67. https://doi.org/10.1002/joc.4929.

Rigden, Angela J., Christopher Golden, and Peter Huybers. 2022. “Retrospective Predictions of Rice and Other Crop Production in Madagascar Using Soil Moisture and an NDVI-Based Calendar from 2010–2017.” *Remote Sensing* 14 (5). https://doi.org/10.3390/rs14051223.

Romanovska, Paula, Stephanie Gleixner, and Christoph Gornott. 2023. “Climate Data Uncertainty for Agricultural Impact Assessments in West Africa.” *Theoretical and Applied Climatology* 152 (3): 933–50. https://doi.org/10.1007/s00704-023-04430-3.

Sasson, Albert. 2012. “Food Security for Africa: An Urgent Global Challenge.” *Agriculture and Food Security* 1 (1): 1–16. https://doi.org/10.1186/2048-7010-1-2.

Shannon de Roos. 2021. “Manual For Creating a Weather-Based Crop Calendar.” *WMO AGRICULTURAL METEOROLOGY REPORT SERIES*.

Sidhu, Balsher Singh, Zia Mehrabi, Navin Ramankutty, and Milind Kandlikar. 2023. “How Can Machine Learning Help in Understanding the Impact of Climate Change on Crop Yields?” *Environmental Research Letters* 18 (2): 24008. https://doi.org/10.1088/1748-9326/acb164.

Sivakumar, M V K. 1988. “Predicting Rainy Season Potential from the Onset of Rains in Southern Sahelian and Sudanian Climatic Zones of West Africa.” *Agricultural and Forest Meteorology* 42 (4): 295–305. https://doi.org/https://doi.org/10.1016/0168-1923(88)90039-1.

Skrynyk, Oleg, Vladyslav Sidenko, Enric Aguilar, Jose Guijarro, Olesya Skrynyk, Liudmyla Palamarchuk, Dmytro Oshurok, Valeriy Osypov, and Volodymyr Osadchyi. 2023. “Data Quality Control and Homogenization of Daily Precipitation and Air Temperature (Mean, Max and Min) Time Series of Ukraine.” *International Journal of Climatology* 43 (9): 4166–82. https://doi.org/10.1002/joc.8080.

Somado, E.a., R.G. Guei, and S.O. Keya. 2008. “NERICA : The New Rice for Africa – a Compendium.” *WARDA, Cotonou, Benin*, 210.

Sorrentino, Giancarlo, Gianluca Scaccianoce, Massimo Morale, and Vincenzo Franzitta. 2012. “The Importance of Reliable Climatic Data in the Energy Evaluation.” *Energy* 48 (1): 74–79. https://doi.org/https://doi.org/10.1016/j.energy.2012.04.015.

Stern, R. D., M. D. Dennett, and D. J. Garbutt. 1981. “The Start of the Rains in West Africa.” *Journal of Climatology* 1 (1): 59–68. https://doi.org/10.1002/joc.3370010107.

Stott, Peter, Nikolaos Christidis, Friederike Otto, Ying Sun, Jean-Paul Vanderlinden, Geert Jan van Oldenborgh, Robert Vautard, et al. 2016. “Attribution of Extreme Weather Events in the Context of Climate Change.” *Wiley Interdisciplinary Reviews: Climate Change* 7: 23–41. https://doi.org/⟨10.17226/21852⟩. ⟨hal-01872724⟩.

Tadross, Mark, Luc Randriamarolaza, Zo Rabefitia, and Zheng Ki Yip. 2008. “Climate Change in Madagascar; Recent Past and Future.” *Washington, DC: World Bank*, no. February.

Tan, Mou Leong, Liew Juneng, Fredolin T. Tangang, Jing Xiang Chung, and R. B. Radin Firdaus. 2021. “Changes in Temperature Extremes and Their Relationship with ENSO in Malaysia from 1985 to 2018.” *International Journal of Climatology* 41 (51): E2564–80. https://doi.org/https://doi.org/10.1002/joc.6864.

Tao, Shengcai, Yinlong Xu, Ke Liu, Jie Pan, and Shiwei Gou. 2011. "Research Progress in Agricultural Vulnerability to Climate Change." *Advances in Climate Change Research* 2 (4): 203–10. https://doi.org/https://doi.org/10.3724/SP.J.1248.2011.00203.

T.M.L. Wigley, and T.P. Barnett. 1990. "Detection of the Greenhouse Effect in the Observations." In *Climate Change: The IPCC Scientific Assessment J.T. Houghton, G.J. Jenkins, J.J. Ephraums [Eds]*., 410. Cambridge University Press, Cambridge, Great Britain, New York, NY, USA and Melbourne, Australia.

Trisos, C.H., I.O. Adelekan, E. Totin, A. Ayanlade, J. Efitre, A. Gemeda, K. Kalaba, et al. 2022. "Africa." In *Climate Change 2022: Impacts, Adaptation and Vulnerability. Contribution of Working Group II to the Sixth Assessment Report of the Intergovernmental Panel on Climate Change [H.-O. Pörtner, D.C. Roberts, M. Tignor, E.S. Poloczanska, K. Mintenbeck, A. Alegr*, 1285–1455. Cambridge University Press. https://doi.org/10.1017/9781009325844.011.

Usman, M T, and A AbdulKadir. 2013. "On Determining the 'Real' Onset Date of Seasonal Rains in the Semi-Arid and Sub-Humid Areas of West Africa." *Natural Hazards* 66 (2): 749–58. https://doi.org/10.1007/s11069-012-0514-9.

Vincent, L. A., E. Aguilar, M. Saindou, A. F. Hassane, G. Jumaux, D. Roy, P. Booneeady, et al. 2011. "Observed Trends in Indices of Daily and Extreme Temperature and Precipitation for the Countries of the Western Indian Ocean, 1961-2008." *Journal of Geophysical Research Atmospheres* 116 (10): 1–12. https://doi.org/10.1029/2010JD015303.

Vincent, Lucie A. 1998. "A Technique for the Identification of Inhomogeneities in Canadian Temperature Series." *Journal of Climate* 11 (5): 1094–1104. https://doi.org/https://doi.org/10.1175/1520-0442(1998)011<1094:ATFTIO>2.0.CO;2.

Vogel, Elisabeth, Fiona Johnson, Lucy Marshall, Ulrike Bende-Michl, Louise Wilson, Justin R Peter, Conrad Wasko, et al. 2023. "An Evaluation Framework for Downscaling and Bias Correction in Climate Change Impact Studies." *Journal of Hydrology* 622: 129693. https://doi.org/https://doi.org/10.1016/j.jhydrol.2023.129693.

Wang, Xiaolan L, and Yang Feng. 2010. "RHtests V3 User Manual" 2010 (January): 1–27.

Weiskopf, Sarah R., Janet A. Cushing, Toni Lyn Morelli, and Bonnie J.E. Myers. 2021. "Climate Change Risks and Adaptation Options for Madagascar." *Ecology and Society* 26 (4). https://doi.org/10.5751/ES-12816-260436.

Werner, A T, and A J Cannon. 2016. “Hydrologic Extremes -- an Intercomparison of Multiple Gridded Statistical Downscaling Methods.” *Hydrology and Earth System Sciences* 20 (4): 1483–1508. https://doi.org/10.5194/hess-20-1483-2016.

Willis, Kathy J., and Shonil A. Bhagwat. 2009. “Biodiversity and Climate Change.” *Science*. American Association for the Advancement of Science. https://doi.org/10.1126/science.1178838.